Amruta Agharkar, A guanidine dietary supplement influences pH sensitivity and NSAID activity in acid-sensing ion channels. Doctor of Philosophy (Biomedical Sciences) October 2015, 200 pages, 23 illustrations, 5 tables.

The acid-sensing ion channels (ASICs) are proton sensitive, sodium channels that belong to the epithelial sodium channel/ Degenerin family of ligand-gated ion channels. Activation of the ASIC1a subtype in the central nervous system increases neurodegeneration after ischemic stroke while ASIC3 subtype in the peripheral nervous system is involved in perception of pain. They are emerging targets for ischemic stroke, pain and inflammation. However, we lack selective ligands to target ASICs.

In order to gain a better understanding of the channel and to develop selective ligands we must first determine how ASICs are modulated by synthetic as well as endogenous guanidine compounds. This study investigates whether a guanidine dietary supplement, creatine, modulates ASICs. Creatine has been shown to protect from ischemia and benefits patients suffering from muscular dystrophy, osteoarthritis, and fibromyalgia. Furthermore, pain medications such as non-steroidal anti-inflammatory drugs (NSAIDs) inhibit ASICs. Since supplements and NSAIDs are available over-the-counter, the significant amount of the population would consume them simultaneously.However, the interactions of combination of creatine and NSAIDs on ASICs still remain elusive. Here we sought to determine if creatine would modulate ASIC1a and ASIC3 proton sensitivity and if the combination of creatine and NSAIDs would inhibit ASIC3. Our results indicate that, creatine reduces human ASIC1a (hASIC1a) steady-state desensitization and increases their recovery from desensitization. Creatine also

slows down the open-state desensitization of hASIC1a. The efficacy of hASIC1a is increased by creatine at higher concentrations. This indicates that, creatine increases channel's reactivation from desensitization by stabilizing the closed conformation of hASIC1a.

Creatine's effect on rat ASIC3 (rASIC3) was calcium dependent. Creatine reduced proton sensitivity of rASIC3 in the nominal calcium environment. As previously reported, NSAIDs inhibited steady-state current of rASIC3 which is involved in pain perception. However, creatine reduced NSAIDs efficacy on rASIC3.

To summarize, the creatine's effect depends on the desensitized state of hASIC1a and creatine increases the availability of channels for opening. While in rASIC3, creatine reduces proton sensitivity in nominal Ca^{2+} and antagonizes NSAIDs inhibitory effect. Thus, the use of creatine should be monitored in diseased states and when it is consumed along with NSAIDs.

A GUANIDINE DIETARY SUPPLEMENT INFLUENCES pH SENSITIVITY AND NSAID ACTIVITY IN ACID-SENSING ION CHANNELS

Dissertation

Presented to the Graduate Council of the

Graduate School of Biomedical Sciences

University of North Texas

Health Science Center at Fort Worth

For the Degree of

DOCTOR OF PHILOSOPHY

By

Amruta S. Agharkar, B. Pharm.

Fort Worth, Texas

October, 2015

ACKNOWLEDGMENT

I would like to express my deepest gratitude to my mentor Dr. Eric B. Gonzales, for his exceptional guidance and support throughout the program. Thank you for always being supportive, patient, kind and encouraging. I couldn't have asked for a better lab or a mentor. Thank you for giving me an opportunity of working in your laboratory. This has been a great learning experience for me and without your enthusiasm for teaching, it wouldn't have been possible. Thank you for teaching me experimental techniques, reading through numerous manuscript drafts, writing reference letters for me and listening while I practice my presentations. You helped me to be an independent thinker and researcher. This lab has always been my home away from home.

I thank my committee members Dr. Meharvan Singh, Dr. Robert Ludtke, Dr. Nathalie Sumien and Dr. Peter Raven for their support, valuable time and the guidance they provided throughout my graduate career.

To my lab-mates, Dr. Rachael Smith and Heather Snell for being great friends and for always being encouraging and supportive. We all went through this together and it has been a great journey. I cannot imagine the lab without you guys. I would also like to thank Mandy McBroom, who taught me all the techniques when I joined the lab. Thank you Mandy for your friendship. I miss our endless discussions on culture, food and what not.

My family is my biggest strength. I would like to thank my parents, grandparents and brother for always supporting me in achieving my dreams. Thank you for your moral support, love and encouragement. I wish my grandfather was with us today. I can't move forward without mentioning Ganesh, our African-grey parrot. He was the smartest pet and a great entertainer. I would also like to thank my in-laws for always supporting and encouraging me. It was impossible for me to complete this journey without my best friend and husband, Shreyas. His understanding, encouragement, patience and love means a lot to me. We went through this journey together and he has always been my best critic and a person who listens to my research endlessly. I am very fortunate to have supportive friends here in the USA as well as back in India. I am thankful to all of them.

I thank everyone in the Department of Pharmacology & Neuroscience and University of North Texas Health Science Center for helping me achieve my goals. I will cherish this experience for life.

-Amruta Agharkar

TABLE OF CONTENTS

LIST OF PUBLICATIONS

Agharkar A, Rzadkowolski J, McBroom M, Gonzales EB, *'Detergent screening of the human voltage-gated proton channel (Hv1) using fluorescence-detection size exclusion chromatography'*, Protein Science 2014, 23(8): 1136-1147.

Smith RN, **Agharkar AS** and Gonzales EB. '*A review of creatine supplementation in age-related diseases: more than a supplement for athletes'* [v1; ref status: approved 1, http://f1000r.es/4ak] *F1000Research* 2014, **3**:222 (doi: 10.12688/f1000research.5218.1).

Manuscripts in preparation:

Agharkar AS, Wang WM, Gonzales EB, *Creatine modulates desensitization ans pH sensitivity of human acid-sensing ion channel 1a*' (manuscript in preparation)

Agharkar AS, Gonzales EB, '*Rat acid-sensing ion channel 3 is modulated by creatine alone or in combination with NSAIDs*' (manuscript in Preparation).

LIST OF ILLUSTRATIONS

Chapter Page No.

Chapter 1

Chapter 2

Chapter 3

Chapter 4

LIST OF TABLES

Chapter Page No.

Chapter 2

Chapter 3

LIST OF ABBREVIATIONS

APETx2	Sea Anemone (*Anthopleura elegantissima*) toxin
ASIC	Acid-sensing ion channel
C termini	Carboxyl termini
Ca^{2+}	Calcium
cASIC1a	Chicken acid-sensing ion channel 1a
CHO-K1	Chinese hamster (*Cricetulus griseus)* ovarian cell line
Cl^-	Chloride
CNS	Central nervous system
COX	Cyclooxygenase
Cr	Creatine Kinase
Deg	Degenerin
EGTA	Ethylene glycol tetraacetic acid
ENaC	Epithelial Sodium Channel
fASIC1a	Toadfish acid-sensing ion channel 1a

FMRF-amide	Phenylalanine–Methionine–Arginine–Phenylalanine-amide
GMQ	2-guanidine-4-methylquinazoline
hASIC1a	Human acid-sensing ion channel 1a
HEK293t	Human embryonic kidney cell line
HEPES	4-(2-hydroxyethyl)-1-piperazineethanesulfonic acid
K^+	Potassium
MES	2-(N-morpholino) ethanesulfonic acid
Mg^{2+}	Magnesium
MitTx	Texas Coral Snake (*Micrurus tener tener*) toxin
N termini	Amino termini
Na^+	Sodium
Neuropeptide FF	Phe-Leu-Phe-Gln-Pro-Gln-Arg-Phe-amide
NSAIDs	Non-steroidal antiinflammatory drugs
Pb^{2+}	Lead
PCr	Phosphocreatine
PcTx1	Psalmotoxin-1
pH_{50}	pH associated with half of the maximal response
PNS	Peripheral nervous system
q.d.	One a day
q.i.d.	Four times a day
rASIC3	Rat acid-sensing ion channel 3
RF amide	Arginine-phenylalanine-amide
SSD	Steady-state desensitization

Zn^{2+}	Zinc
τ	Time constant

CHAPTER 1

INTRODUCTION

1.1 Brief history of ion channels & patch-clamp technique

Cell surface receptors are integral membrane proteins that play an important role in transmitting extracellular signals to the intracellular environment[1]. Ion channels are an important part of cell surface receptors which allow the flow of ions across the cell membrane and transmit electrical signals into chemical signals. Hence, they are important in maintaining membrane potential, signal transmission and ionic balance. Ion channels are water filled pores that allow cells to conduct ions across the cell membrane[2]. Hodgkin & Huxley in 1952 gave a mathematical model to describe ion channels quantitatively[3-5]. In this model, an ion channel is explained in terms of an electrical circuit where changes in membrane voltage are due to flow of sodium and potassium ions across the membrane[6]. They described the action potential propagation in squid giant axon with this model[6,7]. The electrochemical gradient of ions across the cell membrane leads to the movement of ions. Later, Erwin Neher and Bert Sakmann first developed the patch-clamp technique in the 1970s, when they recorded currents from the membrane of frog muscle

fiber[8,9]. They measured the current flowing through a single ion channel by isolating a patch of membrane[10,11]. In voltage-clamp experiments, the voltage is kept constant and current flowing through ion channels that is required to maintain the constant voltage is measured[5,7]. The relationship between potential difference (V), conductance (1/R) and current (I) is best described by Ohm's law[12] which states that the current flowing through a conductor between two points is directly proportional to the potential difference **(Figure 1)**[13].

Depending upon the activity, ion channels are categorized as voltage gated or ligand gated ion channels. Voltage-gated ion channels are activated by changes in membrane potential while ligand-gated ion channels open upon the binding of a ligand, which leads to changes in channel conformation, or protein structure. Ligand-gated ion channels are subdivided into subtypes depending on the chemical structure of the ligands that bind to them. The classical ligand-gated ion channel families are the ionotropic glutamate receptors and the cys-loop receptors. Another group is the epithelial sodium channel/ Degenerin (ENaC/DEG) family of ion channels.

1.2 ENaC/DEG family of ion channels

The epithelial sodium channel/ Degenerin family of ion channels includes sodium selective and amiloride sensitive channels **(Figure 2)**. This family includes, constitutively open ENaCs which are expressed on the apical membrane of epithelial cells in the kidney and are involved in maintaining sodium homeostasis[14,15]. The mechanosensitive channels in *Caenorhabditis elegans*[16,17] and Phenylalanine–Methionine–Arginine–Phenylalanine (FMRF) amide (peptide) gated channel in snail *Helix Aspersa*[18] also belong to the ENaC/DEG family. Another member of this channel family is activated by extracellular protons and is called the

acid-sensing ion channels[19-22]. The subfamilies in ENaC/DEG superfamily have about 15-20% amino acid sequence similarity[23].

1.3 The acid-sensing ion channels (ASICs)

The acid-sensing ion channels are proton sensitive Na^+ channels[22] and were first observed in 1981 as sodium (Na^+) currents generated in response to changes in pH[24,25]. Later, these channels were further studied and cloned from human and rat brain[26-28]. The ASIC1a[22], ASIC2a[27,28], ASIC2b[29], ASIC3[20,21,30] subytpes were cloned. The ASIC1a channel is expressed throughout the brain and induces cationic current with more permeability for Na^+ ions ($Na^+ > Ca^{2+} > K^+$)[22]. The hASIC3 channel with biphasic response to lower pH was cloned[20,29,30] which showed that along with expression in sensory neurons it is also expressed in the lungs, testis and plays an important role in human physiology[30]. The crystal structure of chicken ASIC1 (cASIC1) shows that functional ASIC is a trimer **(Figure 3)** formed by 3 subunits consisting of the large extracellular domain, two transmembrane domains with amino (N-termini) and carboxyl termini (C-termini) present on the intracellular side of the plasmamembrane[31-34]. The transmembrane domain (TM2) forms the lining of the pore of the channel. The three ASIC subunits that form a functional channel can be homomeric or heteromeric. The crystal structure describes the channel as a hand holding a ball with palm, thumb, knuckles, finger and β ball form the different domains of the channel[31,32]. The Na^+ ions can pass through the channel by hydration[32]. The selectivity filter for ASICs is formed by G-A-S (Glycine-Alanine-Serine) which is conserved in all subtypes[33].

1.3.1 ASIC subtypes

Currently known ASIC subtypes include ASICs 1,2,3, 4 and 5 which are encoded by five different genes[23,35,36]. Further, ASIC1 and ASIC2 have splice variants, ASIC1a, ASIC1b, ASIC2a and ASIC2b[37] **(Figure 4)**. The ASIC subtypes share 45-60% sequence similarity amongst them[23]. The ASIC human and rat orthologs are about 100% identical for ASIC1, ASIC2 and ASIC4 and approximately 83% identical for ASIC3[23]. Except for ASIC2b and ASIC4, all ASIC subtypes can form functional homomers. ASIC2b can assemble with other ASIC subunits to form heteromeric channels[38]. This feature of being homomeric or heteromeric channels, modulates these channel's sensitivity towards pH. The ASIC sensitivity to pH ranges from pH 5.0 to 7.0 is dependent on the type and distribution of channel in an organism. For example, ASICs found in neurons of the amygdala are sensitive to pH of 7.2[39] while homomeric ASIC2a are less sensitive to protons and have a pH_{50} of 4.4[27,29]. The homomeric ASIC1a has a pH_{50} of about 6.2[22] while homomeric ASIC3 has a higher sensitivity to protons with pH_{50} of 6.7[40]. Though Na^+ is the primary cation that is conducted through ASICs, homomeric ASIC1a is permeable to Ca^{2+} ions[41,42], with a permeability ratio of 18:1[37].

The ASIC subtypes demonstrate different activation and desensitization properties. Repeated activation of homomeric ASIC1a with a ligand results in attenuation of current due tachyphylaxis[43]. This phenomenon takes place because of the long-lived inactive state produced by protons binding to ASIC1a[44]. Tachyphylaxis has been shown to be dependent on pH and extracellular Ca^{2+} concentration. The hill coefficients of steady-state desensitization of ASIC1a is high, indicating that more protons are bound in desensitized conformation[45]. Similarly, pH less than physiological pH of 7.4, induces desensitization in ASICs and residues that are involved in

activation and desensitization overlap[45]. The desensitization of ASICs particularly renders it inactive and is said to play an important role in preventing damage after ischemic stroke[42].

The ASICs activity is tightly regulated by calcium[46]. The Ca^{2+} allosterically modulates the channel and removal of just extracellular Ca^{2+} leads to channel opening[46-48]. Reduction in pH or extracellular calcium, increases the number of open channels along with an increase in the rate of channel opening[46,48]. The spermine in low Ca^{2+} potentiates ASIC1a currents[49]. The ASIC3 response to acidification has two components which include transient peak current and sustained current[21,40]. The transmembrane domain 1 (TM1) and amino terminal (N-terminal) play an important role in generating sustained current evoked at low pH solutions[50] while TM2 domain and C-terminal negatively regulates it[50]. At the pH range close to physiological pH, ASIC3 exhibits sustained current which is important in causing persistent pain, since this current is non-desensitizing and it is also non selective to Na^{+} ions[51]. Reduction in extracellular Ca^{2+} concentration and a reduction in pH, leads to protonation of the Ca^{2+} binding site which opens ASIC3 channel producing non-desensitizing current. This current persists, until the Ca^{2+} concentrations are returned to normal[46,47]. The lactic acid produced due to anaerobic metabolism has been shown to activate ASIC3 by chelating Ca^{2+} [47]. The rASIC3 ligands like GMQ can activate ASICs at physiological pH. Similarly, inflammatory mediators have been shown to modulate ASIC3 and influence pain perception

1.3.2 Physiological importance of ASICs in ischemic stroke and pain:

The ASICs are expressed in central nervous system (CNS) in the cortex, hippocampus and amygdala[52-56]. They are also expressed in sensory neurons of peripheral nervous system which includes dorsal root ganglion[53,56]. In the CNS, ASIC1a plays an important role in synaptic

plasticity[55,57]. A study by Wemmie et al., suggested that ASIC1a is necessary for fear conditioning[56]. ASIC1a null mice showed decreased fear conditioning. ASIC1a expressed in CNS plays an important role in tissue damage after ischemic stroke by increasing influx of Na^+ and Ca^{2+} ions[42]. Ischemia is characterized by acidosis, an increase in intracellular calcium, and the formation of reactive oxygen species[58]. The findings from Yang et al., indicated that pharmacological blocking of ASIC1a by Psalmotoxin-1 reduces the infarct size after ischemic injury in piglets[59]. ASIC1a also mediates hypersensitivity to pain following thermal and mechanical stimuli[60]. The role of ASIC1a in hypersensitivity to pain is further evident from the fact that blocking of ASIC1a by Psalmotoxin-1 (PcTx-1) reduces the pain hypersensitivity[61].

Pain is a perception of discomfort and in most cases, one of the very first symptoms of a disease. The factors causing pain include noxious peripheral stimuli like heat and cold or chemicals[62]. ASIC3 are primarily expressed in sensory neurons[20,21,30,50] and mediates acidic and primary inflammatory pain[63,64]. ASIC3 blockade by APET-x2, a sea Anemone peptide, reduces the pain sensitivity to heat induced hyperalgesia[65,66]. ASICs sense the changes in the extracellular environment in pain pathologies[67]. The GMQ and agmatine can activate ASICs and cause pain[68-70]. Thus, ASICs can be selectively targeted and inhibited to prevent ischemic damage and to alleviate pain.

1.3.3. The acid-sensing ion channel ligands:

ASICs have multiple binding sites, and a variety of ligands can interact with ASICs[49,61,68-74]. The ASIC crystal structure describes different domains in the channel which are important in ligand binding. Various endogenous molecules, toxins and synthetic compounds can modulate the ASIC activity.

Protons & Amiloride

Protons are the main activators of ASICs[22,29]. Recently, protons have been termed as neurotransmitters with ASICs as their postsynaptic receptor that leads to influx of Na^+ and Ca^{2+} ions[55]. This indicates their role in synaptic plasticity. The finger and thumb domain of ASICs containing acidic amino acid residue pairs (aspartate and glutamate) was particularly found to be important in proton binding[75]. The concentration of protons at physiological pH is 40 nM[45]. The constant exposure to protons desensitizes ASICs which become non responsive to further stimuli[40,45,76].

The classical, non-selective blocker of ENaC/DEG family of ion channels is amiloride. Amiloride is a potent, non-selective, and reversible pore blocker of ASICs[26,27]. It is a potassium sparing diuretic that is used in hypertension and congestive heart failure. Along with ASICs amiloride can also block Na^+/H^+ exchangers[77] and Na^+/Ca^{2+} exchangers[78]. Hence it limits the use of amiloride as a potential drug for targeting ASICs.The IC_{50} of amiloride for ASICs is in the range of 10-100 μM and varies depending on the ASIC subtype[23]. Amiloride block is voltage-dependent (δ of 0.5)[79-82] and it can also bind in the extracellular domain with high affinity to stimulate the channel[72]. This explains the multiple interactions of amiloride with ASICs. Another ligand, the non-amiloride blocker A-317567, has also been shown to inhibit ASICs to prevent pain response[83].

Divalent Cations

The divalent cations like $Ca^{2+,}$ Mg^{2+}, and Zn^{2+} inhibit ASICs[46,48,84]. Both Pb^{2+} and Cu^{2+} ions have been shown to inhibit ASIC1a channels in cultured neurons[85,86]. Ca^{2+} is widely studied and is an important cation which regulates ASICs. The reduction in extracellular Ca^{2+}

concentration potentiates ASIC current by removal of calcium block[46-48]. In reduced Ca^{2+} conditions, ASIC response to extracellular acidity dramatically increases. In toadfish ASIC1, reducing pH or increase in Ca^{2+} concentration was shown to increase the frequency of channel opening[48]. The protons compete for high affinity Ca^{2+} binding. This depicts that extracellular Ca^{2+} regulates ASICs allosterically[48]. However, it has been also shown that, in ASIC1a, the region in extracellular domain involved in mediating proton sensitivity and Ca^{2+} dependent activation is different[76]. Furthermore hASIC1a is also sensitive to extracellular Ca^{2+} and the activity of compounds that modulate desensitization and proton sensitivity of hASIC1a, is dependent on extracellular Ca^{2+}[49,87].

Natural Venom Toxins

The toxin isolated from *Psalmopoeus cambridgei*,- tarantula venom psalmotoxin1 (PcTx1), has been shown to block homomeric ASIC1a channels[88]. It has been shown to act as an analgesic in rodents[60,61]. The psalmotoxin-1 bound chicken ASIC1 structure at low pH shows that toxin binds at the subunit interface[34]. The PcTx1 binding to ASIC1a and ASIC1b differs and is dependent on conformational state[87]. It shifts steady-state desensitization (SSD) to more alkaline pH and reduces proton sensitivity[87]. The APETx2 toxin from the sea anemone *Anthopleura elegantissima*, inhibits homomeric ASIC3 channels[89]. Also, it has been shown that APETx2 produces analgesic effects in rats when applied peripherally[63]. Recently, a study proposed a rASIC3 model which describes the two possible binding sites for APETx2 in rASIC3[90]. According to the model, one site is located in the upper palm region away from the central vestibule and the other site is just above the wrist region which can modulate the pore opening. Another toxin called MiTx from Texas coral snake *Micrurus tener tener*, has been

shown to activate ASIC1a[91]. The toxin mambalgin-1 from black mamba *Dendroaspis polylepis polylepis*, inhibits currents mediated by ASIC1a[92]. These are examples of interesting sources for ASIC ligands.

Peptides, dynorphins and polyamines

The inflammatory mediators like polypeptide molecules Phe-Leu-Phe-Gln-Pro-Gln-Arg-Phe amide (neuropeptide FF)), and Phe-Met-Arg-Phe amide (FMRF-amide) stimulate current elicited by homomeric ASIC1a and ASIC3 channels primarily by slowing down the desensitization[73,74]. In inflammatory conditions, expression of neuropeptide FF increases, which can modulate currents in rat DRG neurons. The arginine-phenylalanine-amide (RF-amide) related peptides alter SSD profile of hASIC1a indicating the importance of ASICs in pain and ischemia[73]. Also, dynorphins reduce steady-state desensitization of ASIC1a and thus potentiate the currents, leading to reduced neuroprotection[93,94]. The polyamine spermine, which is a metabollite in the arginine degradation pathway, increases ASIC1a activity by reducing steady-state desensitization and increasing activation from desensitization[49]. Also, spermine stimulates ASIC1a currents in reduced Ca^{2+} concentrations and is found to increase neuronal injury after ischemic stroke.

NSAIDs

The nonsteroidal anti-inflammatory drugs (NSAIDs) are the established medications for treating pain and inflammation. Their primary mechanism of action is to inhibit the cyclooxygenase (COX) enzyme involved in prostaglandin synthesis. The NSAIDs also inhibit ASICs at therapeutic concentrations[95]. Ibuprofen, aspirin and diclofenac have been shown to

inhibit ASIC1a and ASIC3 currents in sensory neurons as well as heterologously expressed channels[95]. They also reduce the expression of ASIC transcripts in sensory neurons during inflammation[95,96]. Diclofenac and aspirin inhibit steady-state current of rASIC3 and have no effect on peak current. The IC_{50} for diclofenac in heterologously expressed cells is about 92 µM[95] but in hippocampal neurons it is about 622 µM[96]. Diclofenac along with the effect on peak current, also shifted the SSD curve of ASICs to a more alkaline pH and reduced recovery from desensitization but aspirin didn't have any effect on the SSD curve of ASICs. This indicated that diclofenac might stabilize the desensitized state of the channel[96].

Guanidinium compounds

The new class of compounds with a guanidinium group act on ASIC1a and ASIC3 at the non-proton ligand sensing domain[68-70,97]. This site is different from a proton binding site, and ligands that bind here can modulate pH sensitivity of the channel or can activate channels at physiological pH. These include synthetic compounds such as 2-guanidine-4-methylquinazoline (GMQ) and the endogenous arginine metabolites, agmatine and arcaine[69,70]. Amiloride, which is a guanidine compund can also bind to the non proton ligand sensing domain and potentiate ASICs[72]. These compounds can activate rASIC3 at neutral pH. GMQ modulates the pH dependence of ASIC3 by shifting the activation and SSD curves of ASIC3 to produce window current. Window current is a pH range where ASIC3 can activate but do not desensitize. Similarly, GMQ produces pain after paw injection in rats[70]. Recently, our lab showed that, cASIC1 is sensitive to GMQ and it shifts the proton dependence of cASIC1[97]. GMQ stimulates cASIC1 when it is in a persistent-desensitized state after PcTx-1 application[97]. A variety of drugs in the market are guanidine compounds which include antihypertensives, antihistaminics,

antiinflammatory and, antiviral drugs. Similarly, large group of dietary supplements like creatine, arginine and, guanidinopropionic acid are guanidine compounds. The arginine amino acid in these ligands contain positively charged guanidine group that can interact with negatively charged residues in the channel. Figure 5 shows the structural similarity of creatine with other ASIC guanidinium ligands.The modulation by guanidine ligands provides a novel mechanism by which ASICs can be stimulated.

This suggests that ASICs can be modulated by a vast number of ligands through potentially multiple binding sites.

1.4 Creatine- dietary Supplement

Creatine is a guanidine compound and is produced in the body, particularly by the liver and kidneys from the amino acids glycine, arginine and methionine[98]. It can also be obtained in the diet through fish and meat. Creatine is a common dietary supplement that is available at many supermarkets or pharmacies and is used primarily by the fitness community to increase lean body mass. It is considered as very safe due to less side effects. Ninety-five percent (95%) of the body's creatine is stored in skeletal muscles, with the rest in the liver, kidneys, brain and heart. Creatine is transported in the brain and skeletal muscles via the creatine transporter (CrT)[99]. In the muscles, creatine combines with ATP to form phosphocreatine (pCr) and ADP. The pCr is polar and thus keeps the creatine in muscles[100]. To generate energy, pCr acts as an intermediate by donating a phosphate molecule to ADP to form ATP[101]. Creatine kinase (CK) is an important enzyme in the brain and skeletal muscles, which regulates energetics[102]. Creatine metabolizes to creatinine, which is completely eliminated from the body. Creatine monohydrate is the most commonly available form of creatine which is used as a dietary supplement. It is

usually taken in a dose of 20 g/day (5g q.i.d.{4 times a day}, loading dose) for five days followed by 5 g/day (5 q.d. {Once a day} maintenance dose)[103,104]. Creatine intake, though generally safe, should be monitored by persons with impaired kidney function.

1.4.1 Creatine in neuroprotection and pain pathologies

The pathophysiological conditions in which creatine has a beneficial effect includes ischemic stroke, osteoarthritis, and muscular disorders which involve perception of pain[105-107]. Creatine has been shown to be protective in ischemic damage in mice[108]. Creatine-phosphocreatine improves the anoxic damage in rat hippocampal slices[109].Total brain creatine is found to be reduced in patients suffering from acute ischemic stroke than normal volunteers[110]. Creatine has been beneficial in improving symptoms of muscular disorders and osteoarthritis. The creatine supplementation improves the muscle strength in patients suffering from muscular dystrophy[111]. Also, children suffering from muscular dystrophy showed improved hand grip strength after creatine supplementation[112]. Creatine supplementation in women with osteoarthritis reduced knee stiffness and pain[107]. Creatine improved muscle function in patients suffering from fibromyalgia[113]. Also, oral creatine supplementation improved headache, dizziness, and fatigue in patients suffering from traumatic brain injury[114]. With all these beneficial effects the mechanism by which creatine acts in stroke, osteoarthritis, and muscular dystrophy is not known.

In this proposal, we will study the effect of a guanidinium compound, creatine, on human ASIC1a (hASIC1a) and rat ASIC3 (rASIC3) channel subtypes and determine if creatine combination with NSAIDs can modulate the rASIC3 channel.

1.5 Specific Aims:

The neuroprotective effect of creatine has been previously reported where prophylactic oral supplementation of creatine reduces infarct size in a mouse model of ischemic stroke[108]. Studies have also reported usefulness of creatine supplementation for patients suffering from osteoarthritis and muscular pain in turn improving their muscle strength and reducing the pain[107,111,115]. Though it is known that creatine improves cellular energetics, the exact mechanism by which it is beneficial in ischemic stroke and muscular disorders is not clear.

In ischemic events and pain associated with inflammation, the extracellular pH decreases. Acid-sensing ion channels (ASICs), which are proton sensitive channels, can sense this reduced pH causing influx of Na^+ and Ca^{2+} ions. They are expressed in the central and peripheral nervous systems. The ASIC1a subtype in the CNS is involved in acidity induced neuronal death and inhibition of ASIC1a channel has been found to be neuroprotective. The ASIC3 subtype in the periphery senses drop in extracellular pH and is known to mediate an inflammatory pain via pain pathway. The NSAIDs, which inhibit cyclooxygenase enzyme, have been shown to inhibit ASICs. The ligands like amiloride, agmatine, arcaine and GMQ, which are known to modulate ASICs, are guanidinium compounds. Hence, we speculated that creatine, since it is a guanidine compound, exerts its beneficial effects via ASICs.

We hypothesized that creatine reduces ASIC 1a and 3 proton sensitivity and increases NSAIDs potency on rASIC3.

The overall goal of this project is to characterize the creatine activity on acid-sensing ion channel and to determine the mechanism of ASIC modulation by creatine. We have tested the hypothesis with the following specific aims.

(1) To characterize the effect of creatine on human acid-sensing ion channel 1a (hASIC1a). **(2)** To characterize the effect of creatine on rat acid-sensing ion channel 3 (rASIC3) and to assess the effect of creatine and NSAIDs combination on ASIC3.

1.6 Significance

This study will focus on the effect of creatine alone on ASIC1a and ASIC3 and in combination with NSAIDs on ASIC3, the knowledge of which can be used to identify novel ligands that can modulate ASICs to have beneficial effects. We anticipate that, successful completion of this project will provide an insight into the action of creatine on ASICs and open the door to the use of dietary supplements, based on the rational hypothesis driven research, as for the use in neuroprotective and nociceptive treatments

In the United States, stroke is the fourth leading cause of death and 1 out of 19 deaths is due to stroke[116]. The available treatments for stroke include the use of tissue plasminogen activator (tPA) and/or surgical treatments. The tPA has to be given to the patient within 3 hours after an ischemic attack. Hence it is critical to find novel therapeutic agents for ischemic stroke. According to the American Academy of Pain Medicine, more Americans suffer from pain than they do from heart disease, diabetes and cancer combined[117-120]. The currently available treatments for pain include non-steroidal anti-inflammatory drugs (NSAIDs) and opioid analgesics. In patients suffering from chronic pain, NSAIDs can have serious side effects if taken for a long period of time. Thus, there is a need of agents which can enhance the effect of NSAIDs with least side effects.

ASICs have been identified to play a critical role in mediating damage after ischemia and musculoskeletal pain. However, there are very few ligands available which can antagonize these

channels. The natural venoms which antagonize ASICs are expensive and amiloride is non-selective for ASIC subtypes and can also inhibit ENaCs . The large extracellular domain of ASICs offers several ligand binding sites apart from protons[31-33]. This study will determine the action of a guanidinium compound, creatine, which is a dietary supplement, on ASICst. The effect of creatine on ASICs will be determined alone and in combination with established pain medications like NSAIDs. Determining the mechanism by which creatine can modulate ASICs, will help in understanding its use as a prophylactic in reducing the risk of stroke in patients suffered from transient ischemic attack (TIA) and to alleviate pain. This will also explain the mechanism of ASIC modulation by creatine and its use in diseased conditions and in combination with NSAIDs. Creatine is easily available and is proven to be clinically safe. Thus, establishing the effect of creatine on acid-sensing ion channels will provide a new avenue for the use of creatine.

Figures and Legends

Fig. 1 Schematic of ion channels in the form of an electrical circuit (Adapted from Hille B. 1997) (a) Transmembrane ion channel depicted as an electrical circuit. **(b)** An electrical circuit showing resistance; R, Capacitor; C, Resting potential; Vrest.

(a)

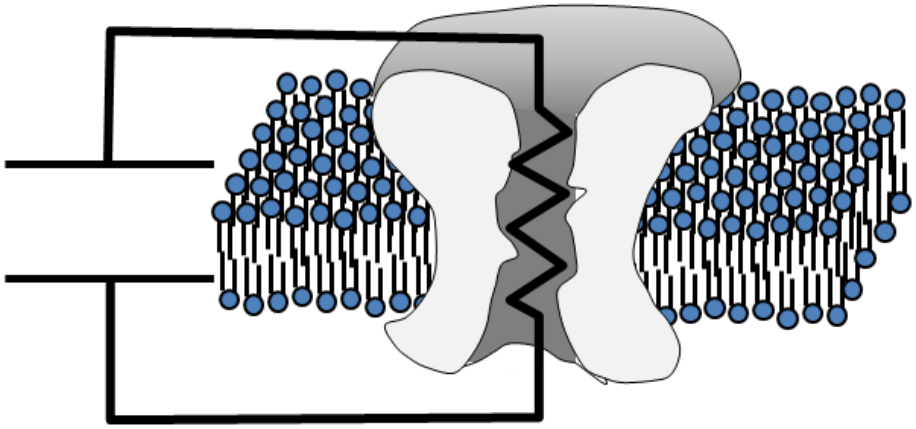

(b)

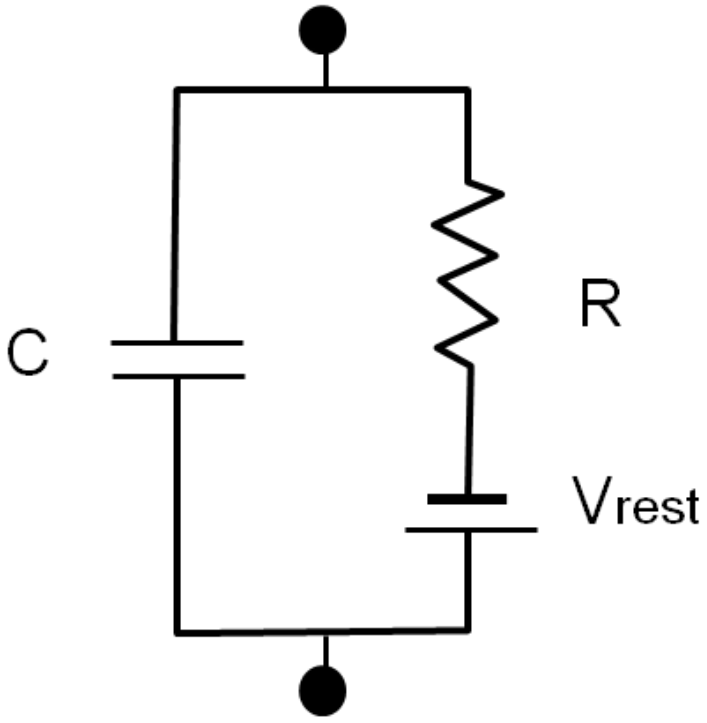

Fig. 2 Phylogenetic tree of the epithelial sodium channel (ENaC)/Degenerin (DEG) family of ion channels (Adapted from Kellenberger S.and Schild L. 2002). ENaC- Epithelial sodium channel. DEG-Degenerin; ASIC- acid-sensing ion channel; FaNaCh- FMRF- amide gated channel; BLiNaC- Brain liver and intestine sodium channel.

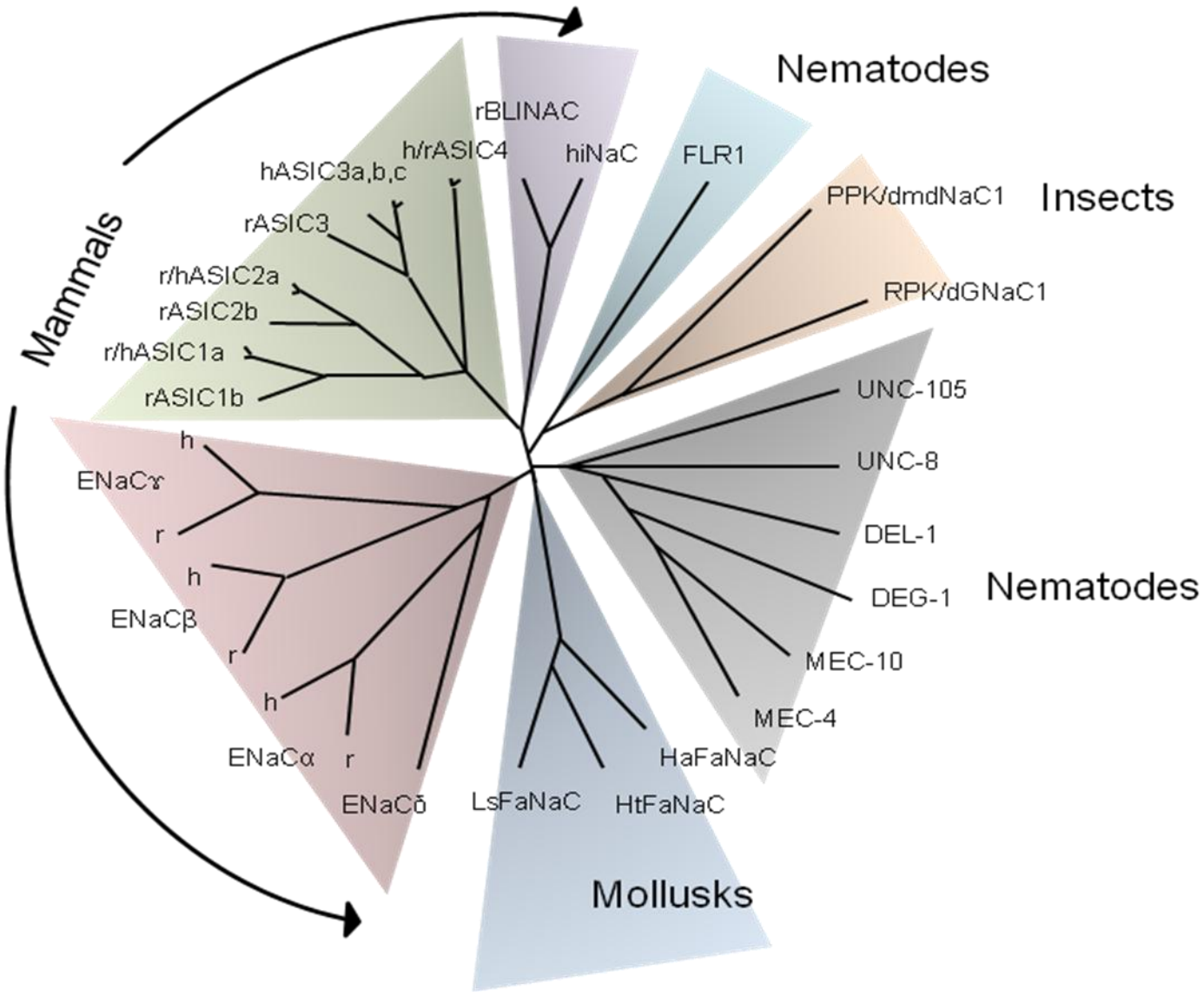
Nematodes
rBLINAC
h/rASIC4
hiNaC
FLR1
hASIC3a,b,c
PPK/dmdNaC1
Insects
rASIC3
RPK/dGNaC1
r/hASIC2a
rASIC2b
r/hASIC1a
rASIC1b
Mammals
UNC-105
UNC-8
h
ENaCγ
DEL-1
r
h
DEG-1
Nematodes
ENaCβ
MEC-10
r
h
MEC-4
ENaCα
r
HaFaNaC
ENaCδ
LsFaNaC
HtFaNaC
Mollusks

Fig. 3 The acid-sensing ion channel crystal structure. Chicken acid-sensing ion channel 1 (cASIC1) trimer crystal structure. Each subunit is represented by different colors and has two transmembrane domains with intracellular amino and carboxyl termini. PDB code 4NYK (PDB code from Baconguis and Gouaux 2014).

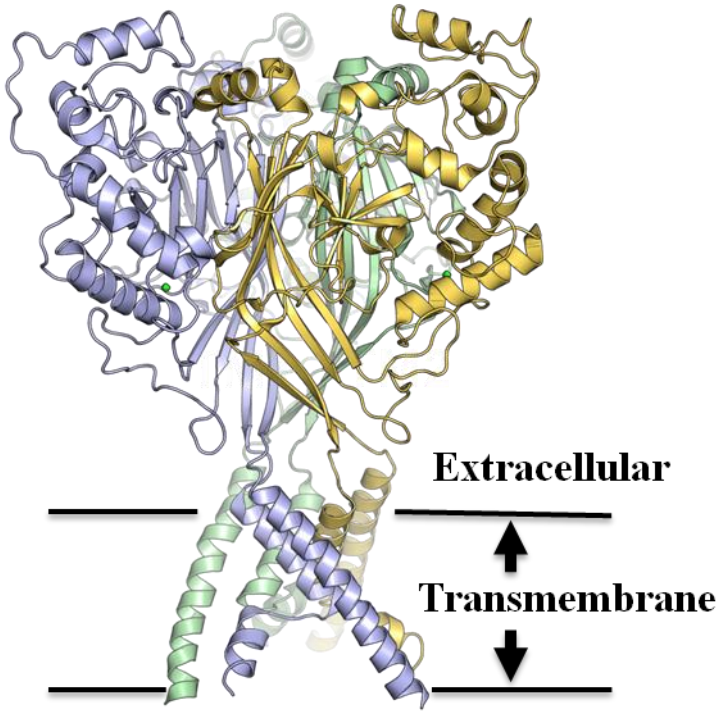
Extracellular
Transmembrane

Fig. 4 ASIC subunits and activation profiles. (a) Topology of ASIC1a protein. **(b)** Homomeric ASIC1a current profiles in heterologous cells (Cos-7 cells) **(c)** Proton-evoked currents from (i) DRG neurons, (ii) Heteromeric ASICs, (iii) ASIC3-/- DRG neurons, (iv) heteromeric ASIC1a/ASIC2a, and **(d)** ASIC1a currents are primaruly found in neurons (Welsh M.J. et al. 2002, Wemmie, J.A. et al. 2006).

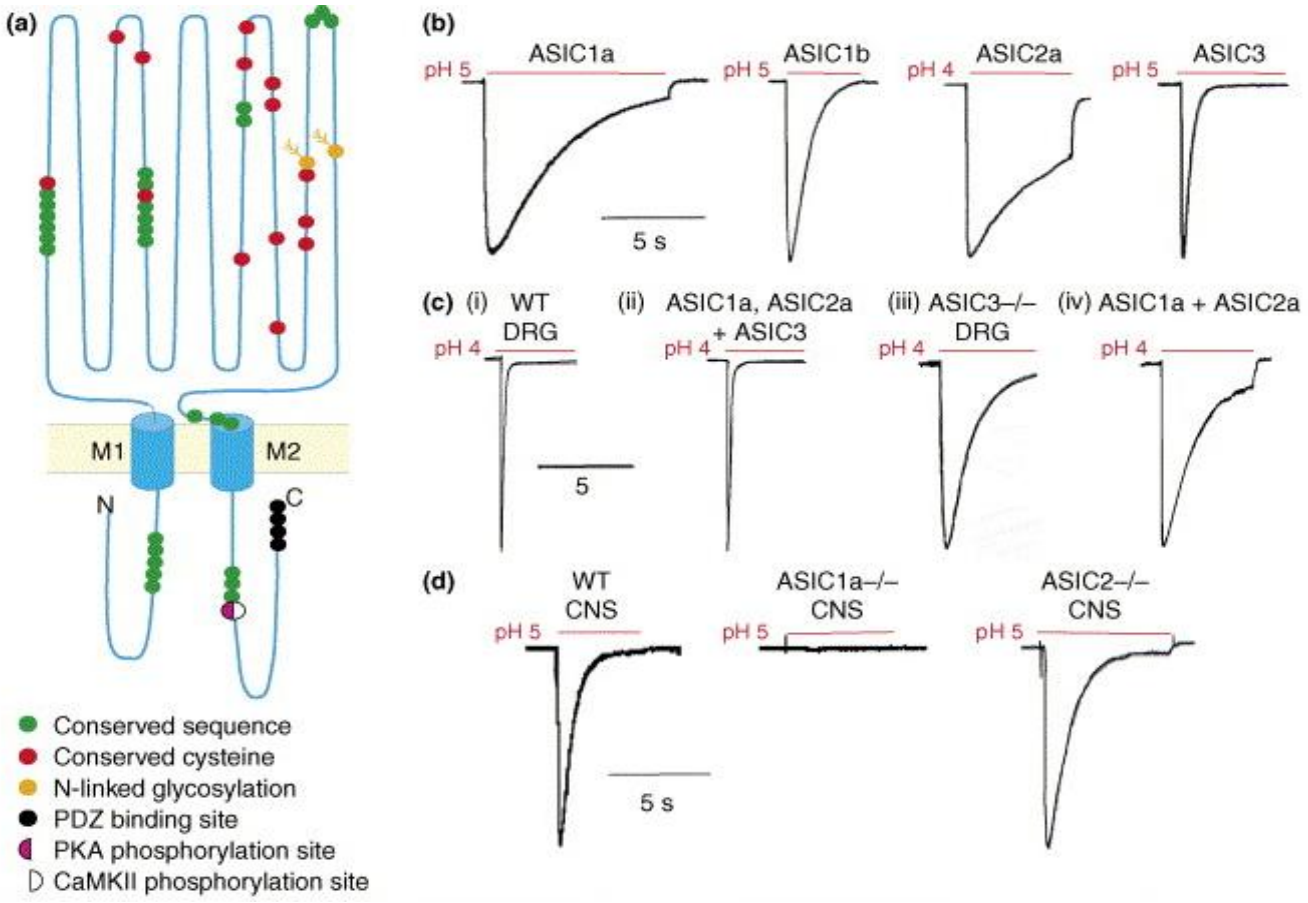
(a)
M1
M2
N
C
Conserved sequence
Conserved cysteine
N-linked glycosylation
PDZ binding site
PKA phosphorylation site
CaMKII phosphorylation site
(b)
ASIC1a
pH 5
5 s
ASIC1b
pH 5
ASIC2a
pH 4
ASIC3
pH 5
(c) (i) WT DRG
pH 4
5
(ii) ASIC1a, ASIC2a + ASIC3
pH 4
(iii) ASIC3–/– DRG
pH 4
(iv) ASIC1a + ASIC2a
pH 4
(d)
WT CNS
pH 5
5 s
ASIC1a–/– CNS
pH 5
ASIC2–/– CNS
pH 5

Fig. 5 Chemical structure comparison of acid sensing ion channel ligands (guanidine compounds and NSAIDs) and creatine. Red box represents guanidine group in the structure.

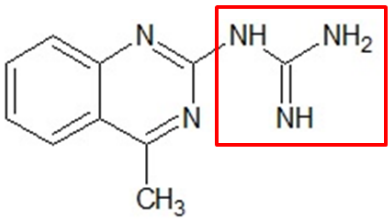

2-guanidine-4-methylquinazoline (GMQ)

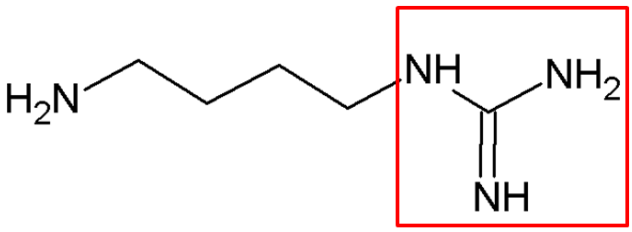

Agmatine

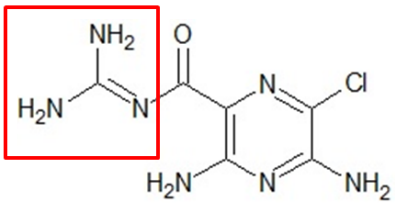

Amiloride

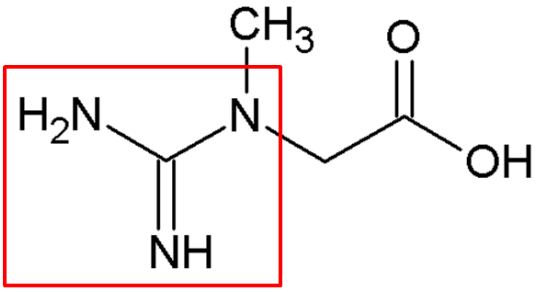

Creatine

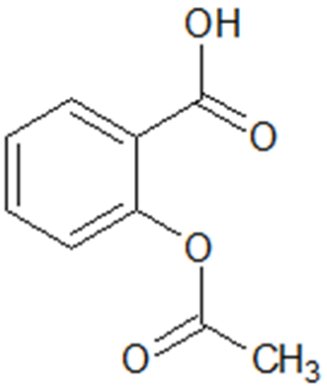

Aspirin

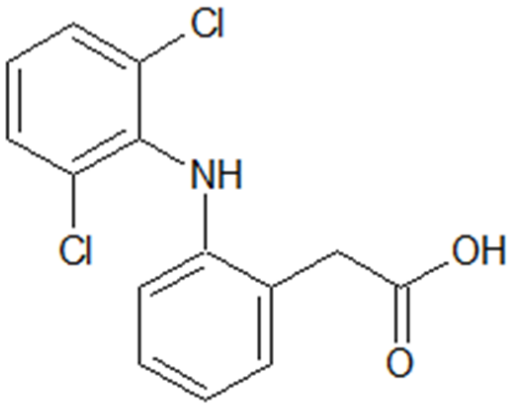

Diclofenac

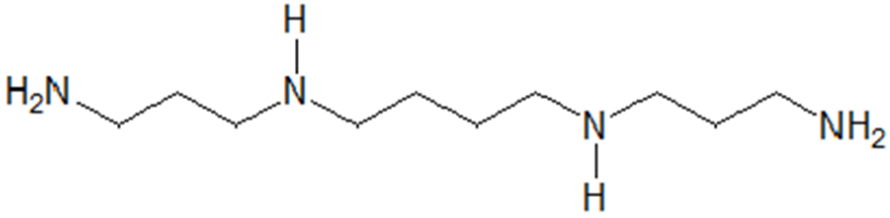

Spermine

1.8 References

1. Cuatrecasas P. Membrane receptors. *Annu Rev Biochem*. 1974;43(0):169-214. doi: 10.1146/annurev.bi.43.070174.001125 [doi].

2. Hille B, Armstrong CM, MacKinnon R. Ion channels: From idea to reality. *Nat Med*. 1999;5(10):1105-1109. doi: 10.1038/13415 [doi].

3. HODGKIN AL, KATZ B. The effect of temperature on the electrical activity of the giant axon of the squid. *J Physiol*. 1949;109(1-2):240-249.

4. HODGKIN AL, KATZ B. The effect of sodium ions on the electrical activity of giant axon of the squid. *J Physiol*. 1949;108(1):37-77.

5. HODGKIN AL, HUXLEY AF, KATZ B. Measurement of current-voltage relations in the membrane of the giant axon of loligo. *J Physiol*. 1952;116(4):424-448.

6. HODGKIN AL, HUXLEY AF. A quantitative description of membrane current and its application to conduction and excitation in nerve. *J Physiol*. 1952;117(4):500-544.

7. COLE KS. Some physical aspects of bioelectric phenomena. *Proc Natl Acad Sci U S A*. 1949;35(10):558-566.

8. Neher E, Sakmann B. Single-channel currents recorded from membrane of denervated frog muscle fibres. *Nature*. 1976;260(5554):799-802.

9. Neher E, Sakmann B. Noise analysis of drug induced voltage clamp currents in denervated frog muscle fibres. *J Physiol*. 1976;258(3):705-729.

10. Neher E, Sakmann B, Steinbach JH. The extracellular patch clamp: A method for resolving currents through individual open channels in biological membranes. *Pflugers Arch*. 1978;375(2):219-228.

11. Hamill OP, Marty A, Neher E, Sakmann B, Sigworth FJ. Improved patch-clamp techniques for high-resolution current recording from cells and cell-free membrane patches. *Pflugers Arch*. 1981;391(2):85-100.

12. Sherman-Gold R. *The axon guide for electrophysiology and biophysics laboratory techniques*. Foster City, CA.: Axon Instruments; 1993.

13. Hille B. *Ionic channels of excitable membranes.* Sunderland, Massachusetts: Sinauer Associates; 1992.

14. Palmer LG, Frindt G. Amiloride-sensitive na channels from the apical membrane of the rat cortical collecting tubule. *Proc Natl Acad Sci U S A*. 1986;83(8):2767-2770.

15. Palmer LG. Epithelial na channels: Function and diversity. *Annu Rev Physiol*. 1992;54:51-66. doi: 10.1146/annurev.ph.54.030192.000411 [doi].

16. Chalfie M, Sulston J. Developmental genetics of the mechanosensory neurons of caenorhabditis elegans. *Dev Biol*. 1981;82(2):358-370. doi: 0012-1606(81)90459-0 [pii].

17. Driscoll M, Chalfie M. The mec-4 gene is a member of a family of caenorhabditis elegans genes that can mutate to induce neuronal degeneration. *Nature*. 1991;349(6310):588-593. doi: 10.1038/349588a0 [doi].

18. Lingueglia E, Champigny G, Lazdunski M, Barbry P. Cloning of the amiloride-sensitive FMRFamide peptide-gated sodium channel. *Nature*. 1995;378(6558):730-733. doi: 10.1038/378730a0 [doi].

19. Waldmann R, Champigny G, Lingueglia E, De Weille JR, Heurteaux C, Lazdunski M. H(+)-gated cation channels. *Ann N Y Acad Sci*. 1999;868:67-76.

20. de Weille JR, Bassilana F, Lazdunski M, Waldmann R. Identification, functional expression and chromosomal localisation of a sustained human proton-gated cation channel. *FEBS Lett*. 1998;433(3):257-260. doi: S0014-5793(98)00916-8 [pii].

21. Waldmann R, Bassilana F, de Weille J, Champigny G, Heurteaux C, Lazdunski M. Molecular cloning of a non-inactivating proton-gated na+ channel specific for sensory neurons. *J Biol Chem*. 1997;272(34):20975-20978.

22. Waldmann R, Champigny G, Bassilana F, Heurteaux C, Lazdunski M. A proton-gated cation channel involved in acid-sensing. *Nature*. 1997;386(6621):173-177. doi: 10.1038/386173a0 [doi].

23. Kellenberger S, Schild L. Epithelial sodium channel/degenerin family of ion channels: A variety of functions for a shared structure. *Physiol Rev*. 2002;82(3):735-767. doi: 10.1152/physrev.00007.2002 [doi].

24. Krishtal OA, Pidoplichko VI. Receptor for protons in the membrane of sensory neurons. *Brain Res*. 1981;214(1):150-154. doi: 0006-8993(81)90446-7 [pii].

25. Krishtal OA, Pidoplichko VI. A "receptor" for protons in small neurons of trigeminal ganglia: Possible role in nociception. *Neurosci Lett*. 1981;24(3):243-246.

26. Waldmann R, Bassilana F, Voilley N, Lazdunski M, Mattei M. Assignment of the human amiloride-sensitive na+ channel delta isoform to chromosome 1p36.3-p36.2. *Genomics*. 1996;34(2):262-263. doi: S0888754396902827 [pii].

27. Waldmann R, Champigny G, Voilley N, Lauritzen I, Lazdunski M. The mammalian degenerin MDEG, an amiloride-sensitive cation channel activated by mutations causing neurodegeneration in caenorhabditis elegans. *J Biol Chem*. 1996;271(18):10433-10436.

28. Price MP, Snyder PM, Welsh MJ. Cloning and expression of a novel human brain na+ channel. *J Biol Chem*. 1996;271(14):7879-7882.

29. Lingueglia E, de Weille JR, Bassilana F, et al. A modulatory subunit of acid sensing ion channels in brain and dorsal root ganglion cells. *J Biol Chem*. 1997;272(47):29778-29783.

30. Babinski K, Le KT, Seguela P. Molecular cloning and regional distribution of a human proton receptor subunit with biphasic functional properties. *J Neurochem*. 1999;72(1):51-57.

31. Jasti J, Furukawa H, Gonzales EB, Gouaux E. Structure of acid-sensing ion channel 1 at 1.9 A resolution and low pH. *Nature*. 2007;449(7160):316-323. doi: nature06163 [pii].

32. Gonzales EB, Kawate T, Gouaux E. Pore architecture and ion sites in acid-sensing ion channels and P2X receptors. *Nature*. 2009;460(7255):599-604. doi: 10.1038/nature08218 [doi].

33. Baconguis I, Bohlen CJ, Goehring A, Julius D, Gouaux E. X-ray structure of acid-sensing ion channel 1-snake toxin complex reveals open state of a na(+)-selective channel. *Cell*. 2014;156(4):717-729. doi: 10.1016/j.cell.2014.01.011 [doi].

34. Dawson RJ, Benz J, Stohler P, et al. Structure of the acid-sensing ion channel 1 in complex with the gating modifier psalmotoxin 1. *Nat Commun*. 2012;3:936. doi: 10.1038/ncomms1917 [doi].

35. Sakai H, Lingueglia E, Champigny G, Mattei MG, Lazdunski M. Cloning and functional expression of a novel degenerin-like na+ channel gene in mammals. *J Physiol*. 1999;519 Pt 2:323-333. doi: PHY_9480 [pii].

36. Boiko N, Kucher V, Wang B, Stockand JD. Restrictive expression of acid-sensing ion channel 5 (asic5) in unipolar brush cells of the vestibulocerebellum. *PLoS One*. 2014;9(3):e91326. doi: 10.1371/journal.pone.0091326 [doi].

37. Bassler EL, Ngo-Anh TJ, Geisler HS, Ruppersberg JP, Grunder S. Molecular and functional characterization of acid-sensing ion channel (ASIC) 1b. *J Biol Chem*. 2001;276(36):33782-33787. doi: 10.1074/jbc.M104030200 [doi].

38. Noel J, Salinas M, Baron A, Diochot S, Deval E, Lingueglia E. Current perspectives on acid-sensing ion channels: New advances and therapeutic implications. *Expert Rev Clin Pharmacol*. 2010;3(3):331-346. doi: 10.1586/ecp.10.13 [doi].

39. Ziemann AE, Allen JE, Dahdaleh NS, et al. The amygdala is a chemosensor that detects carbon dioxide and acidosis to elicit fear behavior. *Cell*. 2009;139(5):1012-1021. doi: 10.1016/j.cell.2009.10.029 [doi].

40. Sutherland SP, Benson CJ, Adelman JP, McCleskey EW. Acid-sensing ion channel 3 matches the acid-gated current in cardiac ischemia-sensing neurons. *Proc Natl Acad Sci U S A*. 2001;98(2):711-716. doi: 10.1073/pnas.011404498 [doi].

41. Yermolaieva O, Leonard AS, Schnizler MK, Abboud FM, Welsh MJ. Extracellular acidosis increases neuronal cell calcium by activating acid-sensing ion channel 1a. *Proc Natl Acad Sci U S A*. 2004;101(17):6752-6757. doi: 10.1073/pnas.0308636100 [doi].

42. Xiong ZG, Zhu XM, Chu XP, et al. Neuroprotection in ischemia: Blocking calcium-permeable acid-sensing ion channels. *Cell*. 2004;118(6):687-698. doi: 10.1016/j.cell.2004.08.026 [doi].

43. Neaga E, Amuzescu B, Dinu C, Macri B, Pena F, Flonta ML. Extracellular trypsin increases ASIC1a selectivity for monovalent versus divalent cations. *J Neurosci Methods*. 2005;144(2):241-248. doi: S0165-0270(04)00400-5 [pii].

44. Chen X, Grunder S. Permeating protons contribute to tachyphylaxis of the acid-sensing ion channel (ASIC) 1a. *J Physiol*. 2007;579(Pt 3):657-670. doi: jphysiol.2006.120733 [pii].

45. Babini E, Paukert M, Geisler HS, Grunder S. Alternative splicing and interaction with di- and polyvalent cations control the dynamic range of acid-sensing ion channel 1 (ASIC1). *J Biol Chem*. 2002;277(44):41597-41603. doi: 10.1074/jbc.M205877200 [doi].

46. Immke DC, McCleskey EW. Protons open acid-sensing ion channels by catalyzing relief of Ca2+ blockade. *Neuron*. 2003;37(1):75-84. doi: S0896627302011303 [pii].

47. Immke DC, McCleskey EW. Lactate enhances the acid-sensing na+ channel on ischemia-sensing neurons. *Nat Neurosci*. 2001;4(9):869-870. doi: 10.1038/nn0901-869 [doi].

48. Zhang P, Sigworth FJ, Canessa CM. Gating of acid-sensitive ion channel-1: Release of Ca2+ block vs. allosteric mechanism. *J Gen Physiol*. 2006;127(2):109-117. doi: jgp.200509396 [pii].

49. Duan B, Wang YZ, Yang T, et al. Extracellular spermine exacerbates ischemic neuronal injury through sensitization of ASIC1a channels to extracellular acidosis. *J Neurosci*. 2011;31(6):2101-2112. doi: 10.1523/JNEUROSCI.4351-10.2011 [doi].

50. Salinas M, Lazdunski M, Lingueglia E. Structural elements for the generation of sustained currents by the acid pain sensor ASIC3. *J Biol Chem*. 2009;284(46):31851-31859. doi: 10.1074/jbc.M109.043984 [doi].

51. Yagi J, Wenk HN, Naves LA, McCleskey EW. Sustained currents through ASIC3 ion channels at the modest pH changes that occur during myocardial ischemia. *Circ Res*. 2006;99(5):501-509. doi: 01.RES.0000238388.79295.4c [pii].

52. Wu H, Wang C, Liu B, et al. Altered expression pattern of acid-sensing ion channel isoforms in piriform cortex after seizures. *Mol Neurobiol*. 2015. doi: 10.1007/s12035-015-9130-5 [doi].

53. Alvarez de la Rosa D, Krueger SR, Kolar A, Shao D, Fitzsimonds RM, Canessa CM. Distribution, subcellular localization and ontogeny of ASIC1 in the mammalian central nervous system. *J Physiol*. 2003;546(Pt 1):77-87. doi: PHY_030692 [pii].

54. Weng XC, Zheng JQ, Gai XD, Li J, Xiao WB. Two types of acid-sensing ion channel currents in rat hippocampal neurons. *Neurosci Res*. 2004;50(4):493-499. doi: S0168-0102(04)00230-5 [pii].

55. Du J, Reznikov LR, Price MP, et al. Protons are a neurotransmitter that regulates synaptic plasticity in the lateral amygdala. *Proc Natl Acad Sci U S A*. 2014;111(24):8961-8966. doi: 10.1073/pnas.1407018111 [doi].

56. Wemmie JA, Askwith CC, Lamani E, Cassell MD, Freeman JH,Jr, Welsh MJ. Acid-sensing ion channel 1 is localized in brain regions with high synaptic density and contributes to fear conditioning. *J Neurosci*. 2003;23(13):5496-5502. doi: 23/13/5496 [pii].

57. Huang Y, Jiang N, Li J, Ji YH, Xiong ZG, Zha XM. Two aspects of ASIC function: Synaptic plasticity and neuronal injury. *Neuropharmacology*. 2015;94:42-48. doi: 10.1016/j.neuropharm.2014.12.010 [doi].

58. Warner DS, Sheng H, Batinic-Haberle I. Oxidants, antioxidants and the ischemic brain. *J Exp Biol*. 2004;207(Pt 18):3221-3231. doi: 10.1242/jeb.01022 [doi].

59. Yang ZJ, Ni X, Carter EL, Kibler K, Martin LJ, Koehler RC. Neuroprotective effect of acid-sensing ion channel inhibitor psalmotoxin-1 after hypoxia-ischemia in newborn piglet striatum. *Neurobiol Dis*. 2011;43(2):446-454. doi: 10.1016/j.nbd.2011.04.018 [doi].

60. Duan B, Wu LJ, Yu YQ, et al. Upregulation of acid-sensing ion channel ASIC1a in spinal dorsal horn neurons contributes to inflammatory pain hypersensitivity. *J Neurosci*. 2007;27(41):11139-11148. doi: 27/41/11139 [pii].

61. Mazzuca M, Heurteaux C, Alloui A, et al. A tarantula peptide against pain via ASIC1a channels and opioid mechanisms. *Nat Neurosci*. 2007;10(8):943-945. doi: nn1940 [pii].

62. Basbaum AI, Bautista DM, Scherrer G, Julius D. Cellular and molecular mechanisms of pain. *Cell*. 2009;139(2):267-284. doi: 10.1016/j.cell.2009.09.028 [doi].

63. Deval E, Noel J, Lay N, et al. ASIC3, a sensor of acidic and primary inflammatory pain. *EMBO J*. 2008;27(22):3047-3055. doi: 10.1038/emboj.2008.213 [doi].

64. Li WG, Xu TL. ASIC3 channels in multimodal sensory perception. *ACS Chem Neurosci*. 2011;2(1):26-37. doi: 10.1021/cn100094b [doi].

65. Sluka KA, Price MP, Breese NM, Stucky CL, Wemmie JA, Welsh MJ. Chronic hyperalgesia induced by repeated acid injections in muscle is abolished by the loss of ASIC3, but not ASIC1. *Pain*. 2003;106(3):229-239. doi: S0304395903002690 [pii].

66. Ikeuchi M, Kolker SJ, Burnes LA, Walder RY, Sluka KA. Role of ASIC3 in the primary and secondary hyperalgesia produced by joint inflammation in mice. *Pain*. 2008;137(3):662-669. doi: 10.1016/j.pain.2008.01.020 [doi].

67. Woolf CJ, American College of Physicians, American Physiological Society. Pain: Moving from symptom control toward mechanism-specific pharmacologic management. *Ann Intern Med*. 2004;140(6):441-451. doi: 140/6/441 [pii].

68. Alijevic O, Kellenberger S. Subtype-specific modulation of acid-sensing ion channel (ASIC) function by 2-guanidine-4-methylquinazoline. *J Biol Chem*. 2012;287(43):36059-36070. doi: 10.1074/jbc.M112.360487 [doi].

69. Li WG, Yu Y, Zhang ZD, Cao H, Xu TL. ASIC3 channels integrate agmatine and multiple inflammatory signals through the nonproton ligand sensing domain. *Mol Pain*. 2010;6:88-8069-6-88. doi: 10.1186/1744-8069-6-88 [doi].

70. Yu Y, Chen Z, Li WG, et al. A nonproton ligand sensor in the acid-sensing ion channel. *Neuron*. 2010;68(1):61-72. doi: 10.1016/j.neuron.2010.09.001 [doi].

71. Kusama N, Harding AM, Benson CJ. Extracellular chloride modulates the desensitization kinetics of acid-sensing ion channel 1a (ASIC1a). *J Biol Chem*. 2010;285(23):17425-17431. doi: 10.1074/jbc.M109.091561 [doi].

72. Adams CM, Snyder PM, Welsh MJ. Paradoxical stimulation of a DEG/ENaC channel by amiloride. *J Biol Chem*. 1999;274(22):15500-15504.

73. Askwith CC, Cheng C, Ikuma M, Benson C, Price MP, Welsh MJ. Neuropeptide FF and FMRFamide potentiate acid-evoked currents from sensory neurons and proton-gated DEG/ENaC channels. *Neuron*. 2000;26(1):133-141. doi: S0896-6273(00)81144-7 [pii].

74. Sherwood TW, Askwith CC. Endogenous arginine-phenylalanine-amide-related peptides alter steady-state desensitization of ASIC1a. *J Biol Chem*. 2008;283(4):1818-1830. doi: M705118200 [pii].

75. Ishikita H. Proton-binding sites of acid-sensing ion channel 1. *PLoS One*. 2011;6(2):e16920. doi: 10.1371/journal.pone.0016920 [doi].

76. Sherwood T, Franke R, Conneely S, Joyner J, Arumugan P, Askwith C. Identification of protein domains that control proton and calcium sensitivity of ASIC1a. *J Biol Chem*. 2009;284(41):27899-27907. doi: 10.1074/jbc.M109.029009 [doi].

77. Masereel B, Pochet L, Laeckmann D. An overview of inhibitors of na(+)/H(+) exchanger. *Eur J Med Chem*. 2003;38(6):547-554. doi: S0223523403001004 [pii].

78. Siegl PK, Cragoe EJ,Jr, Trumble MJ, Kaczorowski GJ. Inhibition of Na+/Ca2+ exchange in membrane vesicle and papillary muscle preparations from guinea pig heart by analogs of amiloride. *Proc Natl Acad Sci U S A*. 1984;81(10):3238-3242.

79. Woodhull AM. Ionic blockage of sodium channels in nerve. *J Gen Physiol*. 1973;61(6):687-708.

80. Warncke J, Lindemann B. Voltage dependence of na channel blockage by amiloride: Relaxation effects in admittance spectra. *J Membr Biol*. 1985;86(3):255-265.

81. Warncke J, Lindemann B. Voltage dependence of the blocking rate constants of amiloride at apical na channels. *Pflugers Arch*. 1985;405 Suppl 1:S89-94.

82. Kashlan OB, Sheng S, Kleyman TR. On the interaction between amiloride and its putative alpha-subunit epithelial na+ channel binding site. *J Biol Chem*. 2005;280(28):26206-26215. doi: M503500200 [pii].

83. Dube GR, Lehto SG, Breese NM, et al. Electrophysiological and in vivo characterization of A-317567, a novel blocker of acid sensing ion channels. *Pain*. 2005;117(1-2):88-96. doi: S0304-3959(05)00255-1 [pii].

84. Baron A, Schaefer L, Lingueglia E, Champigny G, Lazdunski M. Zn2+ and H+ are coactivators of acid-sensing ion channels. *J Biol Chem*. 2001;276(38):35361-35367. doi: 10.1074/jbc.M105208200 [doi].

85. Wang W, Duan B, Xu H, Xu L, Xu TL. Calcium-permeable acid-sensing ion channel is a molecular target of the neurotoxic metal ion lead. *J Biol Chem*. 2006;281(5):2497-2505. doi: M507123200 [pii].

86. Wang W, Yu Y, Xu TL. Modulation of acid-sensing ion channels by cu(2+) in cultured hypothalamic neurons of the rat. *Neuroscience*. 2007;145(2):631-641. doi: S0306-4522(06)01686-1 [pii].

87. Chen X, Kalbacher H, Grunder S. Interaction of acid-sensing ion channel (ASIC) 1 with the tarantula toxin psalmotoxin 1 is state dependent. *J Gen Physiol*. 2006;127(3):267-276. doi: jgp.200509409 [pii].

88. Escoubas P, De Weille JR, Lecoq A, et al. Isolation of a tarantula toxin specific for a class of proton-gated na+ channels. *J Biol Chem*. 2000;275(33):25116-25121. doi: 10.1074/jbc.M003643200 [doi].

89. Diochot S, Baron A, Rash LD, et al. A new sea anemone peptide, APETx2, inhibits ASIC3, a major acid-sensitive channel in sensory neurons. *EMBO J*. 2004;23(7):1516-1525. doi: 10.1038/sj.emboj.7600177 [doi].

90. Rahman T, Smith ES. In silico assessment of interaction of sea anemone toxin APETx2 and acid sensing ion channel 3. *Biochem Biophys Res Commun*. 2014. doi: S0006-291X(14)01019-5 [pii].

91. Bohlen CJ, Chesler AT, Sharif-Naeini R, et al. A heteromeric texas coral snake toxin targets acid-sensing ion channels to produce pain. *Nature*. 2011;479(7373):410-414. doi: 10.1038/nature10607 [doi].

92. Diochot S, Baron A, Salinas M, et al. Black mamba venom peptides target acid-sensing ion channels to abolish pain. *Nature*. 2012;490(7421):552-555. doi: 10.1038/nature11494 [doi].

93. Sherwood TW, Askwith CC. Dynorphin opioid peptides enhance acid-sensing ion channel 1a activity and acidosis-induced neuronal death. *J Neurosci*. 2009;29(45):14371-14380. doi: 10.1523/JNEUROSCI.2186-09.2009 [doi].

94. Vick JS, Askwith CC. ASICs and neuropeptides. *Neuropharmacology*. 2015;94:36-41. doi: 10.1016/j.neuropharm.2014.12.012 [doi].

95. Voilley N, de Weille J, Mamet J, Lazdunski M. Nonsteroid anti-inflammatory drugs inhibit both the activity and the inflammation-induced expression of acid-sensing ion channels in nociceptors. *J Neurosci*. 2001;21(20):8026-8033. doi: 21/20/8026 [pii].

96. Dorofeeva NA, Barygin OI, Staruschenko A, Bolshakov KV, Magazanik LG. Mechanisms of non-steroid anti-inflammatory drugs action on ASICs expressed in hippocampal interneurons. *J Neurochem*. 2008;106(1):429-441. doi: 10.1111/j.1471-4159.2008.05412.x [doi].

97. Smith RN, Gonzales EB. Protons and psalmotoxin-1 reveal nonproton ligand stimulatory sites in chicken acid-sensing ion channel: Implication for simultaneous modulation in ASICs. *Channels (Austin)*. 2014;8(1):49-61. doi: 10.4161/chan.26978 [doi].

98. Walker JB. Creatine: Biosynthesis, regulation, and function. *Adv Enzymol Relat Areas Mol Biol*. 1979;50:177-242.

99. Guimbal C, Kilimann MW. A na(+)-dependent creatine transporter in rabbit brain, muscle, heart, and kidney. cDNA cloning and functional expression. *J Biol Chem*. 1993;268(12):8418-8421.

100. Greenhaff PL, Casey A, Short AH, Harris R, Soderlund K, Hultman E. Influence of oral creatine supplementation of muscle torque during repeated bouts of maximal voluntary exercise in man. *Clin Sci (Lond)*. 1993;84(5):565-571.

101. Clark JF. Creatine: A review of its nutritional applications in sport. *Nutrition*. 1998;14(3):322-324. doi: S0899900797004826 [pii].

102. Hemmer W, Wallimann T. Functional aspects of creatine kinase in brain. *Dev Neurosci*. 1993;15(3-5):249-260.

103. Persky AM, Brazeau GA. Clinical pharmacology of the dietary supplement creatine monohydrate. *Pharmacol Rev*. 2001;53(2):161-176.

104. Persky AM, Muller M, Derendorf H, Grant M, Brazeau GA, Hochhaus G. Single- and multiple-dose pharmacokinetics of oral creatine. *J Clin Pharmacol*. 2003;43(1):29-37.

105. Wilken B, Ramirez JM, Probst I, Richter DW, Hanefeld F. Anoxic ATP depletion in neonatal mice brainstem is prevented by creatine supplementation. *Arch Dis Child Fetal Neonatal Ed*. 2000;82(3):F224-7.

106. Nabuurs CI, Choe CU, Veltien A, et al. Disturbed energy metabolism and muscular dystrophy caused by pure creatine deficiency are reversible by creatine intake. *J Physiol*. 2013;591(Pt 2):571-592. doi: 10.1113/jphysiol.2012.241760 [doi].

107. Neves M,Jr, Gualano B, Roschel H, et al. Beneficial effect of creatine supplementation in knee osteoarthritis. *Med Sci Sports Exerc*. 2011;43(8):1538-1543. doi: 10.1249/MSS.0b013e3182118592 [doi].

108. Zhu S, Li M, Figueroa BE, et al. Prophylactic creatine administration mediates neuroprotection in cerebral ischemia in mice. *J Neurosci*. 2004;24(26):5909-5912. doi: 10.1523/JNEUROSCI.1278-04.2004 [doi].

109. Carter AJ, Muller RE, Pschorn U, Stransky W. Preincubation with creatine enhances levels of creatine phosphate and prevents anoxic damage in rat hippocampal slices. *J Neurochem*. 1995;64(6):2691-2699.

110. Gideon P, Henriksen O, Sperling B, et al. Early time course of N-acetylaspartate, creatine and phosphocreatine, and compounds containing choline in the brain after acute stroke. A proton magnetic resonance spectroscopy study. *Stroke*. 1992;23(11):1566-1572.

111. Banerjee B, Sharma U, Balasubramanian K, Kalaivani M, Kalra V, Jagannathan NR. Effect of creatine monohydrate in improving cellular energetics and muscle strength in ambulatory duchenne muscular dystrophy patients: A randomized, placebo-controlled 31P MRS study. *Magn Reson Imaging*. 2010;28(5):698-707. doi: 10.1016/j.mri.2010.03.008 [doi].

112. Tarnopolsky MA, Mahoney DJ, Vajsar J, et al. Creatine monohydrate enhances strength and body composition in duchenne muscular dystrophy. *Neurology*. 2004;62(10):1771-1777.

113. Alves CR, Santiago BM, Lima FR, et al. Creatine supplementation in fibromyalgia: A randomized, double-blind, placebo-controlled trial. *Arthritis Care Res (Hoboken)*. 2013;65(9):1449-1459. doi: 10.1002/acr.22020 [doi].

114. Sakellaris G, Nasis G, Kotsiou M, Tamiolaki M, Charissis G, Evangeliou A. Prevention of traumatic headache, dizziness and fatigue with creatine administration. A pilot study. *Acta Paediatr*. 2008;97(1):31-34. doi: APA529 [pii].

115. Santos RV, Bassit RA, Caperuto EC, Costa Rosa LF. The effect of creatine supplementation upon inflammatory and muscle soreness markers after a 30km race. *Life Sci*. 2004;75(16):1917-1924. doi: 10.1016/j.lfs.2003.11.036 [doi].

116. Kochanek KD, Xu J, Murphy SL, Minino AM, Kung HC. Deaths: Final data for 2009. *Natl Vital Stat Rep*. 2011;60(3):1-116.

117. *Relieving Pain in America, A blueprint for transforming prevention, care, education and research.* Washington D.C.: The National Academies Press; 2011.

118. Heart disease and stroke statistics- 2011 update: A report from the American Heart Association. *Circulation*. 2011:123:e18-e209, Page 20.

119. American diabetes association. http://www.diabetes.org/diabetes-basics/statistics/. Updated 2015.

120. Cancer prevalence: How many people have cancer? http://www.cancer.org/cancer/cancerbasics/cancer-prevalence. Updated 2014.

CHAPTER 2

Creatine modulates desensitization and pH sensitivity of human acid-sensing ion channel 1a

Amruta S. Agharkar[1], Wen Mai Wong[2], Eric B. Gonzales[1]

[1]Center for Neuroscience Discovery, University of North Texas Health Science Center, Fort Worth, Texas, USA 76107

[2]St. Mary's University, San Antonio, Texas, USA 78228

Abbreviated title: Dietary supplement modulation of hASIC1a

This work was supported by grants from the American Heart Association (12BGIA8820001), Welch Foundation (BK-1736), Doctoral student bridge grant, and UNTHSC Internal Seed Grants and startup funds.

*Corresponding Author:

Eric B. Gonzales, Ph.D.

Assistant Professor

Center for Neuroscience Discovery

University of North Texas Health Science Center

3500 Camp Bowie Blvd.

Fort Worth, TX 76107

Email: eric.b.gonzales@unthsc.edu

Phone: 817-735-2755

Fax: 817-735-0408

2.1 ABSTRACT

Acid-sensing ion channels (ASICs) are proton sensitive sodium channels that open in response to lowered extracellular pH and are expressed in the central and peripheral nervous systems. Human ASIC1a (hASIC1a) has been associated with pathologies, including neurodegeneration following ischemic stroke, and pain. A growing number of ligands that contain a guanidine group have shown efficacy in modulating ASIC activity. Furthermore, many of the available over-the-counter dietary supplements are guanidine-containing ligands. These ligands have been proposed to supplement established treatments for pain and neurological diseases. We considered that an over-the-counter dietary supplement creatine, may be efficacious at hASIC1a. Here, we show that hASIC1a is sensitive to creatine, a guanidine dietary supplement. In the presence of creatine, the hASIC1a pH sensitivity was reduced. However, 10 mM creatine reduced desensitization of hASIC1a, by influencing the steady-state pH desensitization profile, resulting in more channels in the closed state that could be activated by low pH, while at the same concentration reduced the activation pH sensitivity of hASIC1a. When controlled for desensitization, creatine at higher concentration also increased the efficacy of hASIC1a channels by about 40%, indicating that creatine increases recovery from desensitization. Creatine also increased hASIC1a recovery after desensitization at conditioning pH 7.2 and slowed down the open-state desensitization. Our data, taken in the context of neuroprotection following stroke, suggests that creatine's actions via ASIC1a neurodegeneration is best administered as a prophylactic rather than a therapeutic.

2.2 INTRODUCTION

An emerging target for limiting neurodegeneration following ischemia and possibly neuroprotection are the acid-sensing ion channels (ASICs)[1-4]. ASICs are proton sensitive channels that sense changes in extracellular acidity leading to the influx of Na^+ and Ca^{2+} ions[5,6]. Of the multiple ASIC subtypes, ASIC1a is robustly expressed in the central nervous system and mediates low pH-driven neuronal death through the resulting influx of calcium[7]. Inhibiting the activity of neuronal ASIC1a has been shown to reduce neuronal cell death following ischemia[5,8] suggesting that inhibiting ASIC1a can be neuroprotective[9]. The interest in ASIC has been further solidified with the resolution of the ASIC three-dimensional structure[10-12]. Furthermore, the large ASIC extracellular domain may house additional ligand-binding sites. The ASIC ligand amiloride, a guanidine group containing antagonist is both potent and inhibits all ASIC subtypes[13]. Along with amiloride, other guanidine compounds such as 2-guanidine-4-methylquinazoline[14-16], agmatine[15,17]and, the other closely related polyamines and peptides[6,18,19] have efficacy on acid-sensing ion channels.

A preventative dietary supplement that could minimize neurodegeneration would be of significant clinical importance in the prevention of stroke-induced neuronal death. One such dietary supplement that has demonstrated efficacy in neuroprotection is creatine, an over-the-counter guanidine-containing compound. Creatine is a commonly used nutraceutical/dietary supplement available through a variety of formulations. Endogenously, creatine is produced from glycine, arginine, and methionine[20]. Additionally, creatine has been the subject of peer-reviewed research and clinical trials to assess the beneficial effects of this dietary supplement in age-associated diseases[21]. Furthermore, studies have shown that prophylactic creatine oral supplementation reduces infarct size in a mouse model of stroke[22]. Creatine restored the energy defi-

ciency in an anoxic model in neonatal mice, demonstrating creatine's neuroprotection[23]. Furthermore, total brain creatine is reduced in patients suffering from acute ischemic stroke than normal volunteers[24]. The possible mechanism of creatine's neuroprotective effects and if there are other pathways to elicit these neuroprotective effects remains unclear.

Due to creatine's possession of a guanidine group like other ASIC ligands, we hypothesized that creatine inhibits the activity of human ASIC1a (hASIC1a). We sought to assess the creatine efficacy on hASIC1a using whole-cell patch clamp electrophysiology and the endogenously expressed hASIC1a found in human embryonic kidney (HEK293t) cells. We observed a reduction in the proton sensitivity of hASIC1 in the presence of 5 and 10 mM creatine. Furthermore, we saw a shift in the hASIC1a steady-state desensitization curve to acidic pH values with 10 mM creatine, indicating that creatine increases recovery after desensitization. Additionally, creatine reduces open-state desensitization at 5 and 10 mM. Also, the typical desensitization observed with repeated stimulation of hASIC1a at pH 6.0 is reversed as the conditioning pH decreases. This suggests that creatine's modulatory effects occur when the channel is in a desensitized state. Our results suggest that hASIC1a is influenced by the creatine and it changes the proton sensitivity and desensitization of ASIC1a possibly by stabilizing the closed state of the channel. The observed reversal of ASIC desensitization at high concentrations of creatine suggest that the dietary supplement may be more suited as a prevention and higher concentration after an ischemic event could be detrimental.

2.3 MATERIALS AND METHODS

2.3.1 Cell culture: Human embryonic kidney cells constitutively expressing simian virus 40 (SV40) large T-antigen (HEK293t) were obtained from (American Type Culture Collection, USA). They endogenously express hASIC1a subtype[25]. HEK293t cells were cultured in Dulbecco's Modified Eagle Medium (DMEM) (Life Technologies, New York, USA) with 10% fetal bovine serum (Denville Scientific Inc., New Jersey, USA) and 1% penicillin-streptomycin (Cellgro, Virginia, USA) in a CO_2 (5%) incubator at a temperature of 37 °C. HEK293t cells were plated (cell confluency, 200,000 cells/ml) in a 35-mm tissue culture dish and were allowed to adhere to square glass coverslips for 24 hours prior to electrophysiology recording.

2.3.2 Chemicals: Creatine monohydrate was obtained from Sigma-Aldrich (#C-3630). Creatine test solutions were prepared fresh on the day of recording. The pH and osmolarity of all test solutions was adjusted using N-methyl D-gluconate (NMDG) and sucrose solution, respectively.

2.3.3 External and internal (pipette) solutions:

The extracellular solution used for recording consisted of (in mM): NaCl (150), KCl (5), HEPES (5), MES (5). The $CaCl_2$ (1 mM) was added to extracellular solution on the day of recording. The internal (pipette) solution consisted of (in mM): KCl (100), $MgCl_2$ (5), EGTA (10), HEPES (40), NaCl (5) buffered to pH 7.4. N-methyl D-glucamine and HCl were used to adjust the pH of recording solutions.

2.3.4 Whole-cell patch-clamp electrophysiology: External and internal (pipette) solutions used in this study were described previously. Patch pipettes were pulled from borosilicate glass capillary tubes (Sutter Instruments P97 brown filament puller) and were fire polished to 3-10 MΩ re-

sistance. Patch-clamp recording was performed on an inverted microscope with a computer driven pinch-valve array of perpendicular capillary tubes using an Axopatch 200B amplifier and pCLAMP10 data acquisition and analysis software (Molecular Devices), filtered and sampled at 5 and 10 kHz, respectively. All recordings were performed at room temperature and at a holding potential of -70 mV. Data are presented and analyzed using OriginLab 8.0 and GraphPad Prism 6.

For direct activation, patched cells were activated with pH 6.0 (Control) solution followed by pH 8.0 and 7.4 solution contaning 5 mM creatine (Fig.1). Cells plated on coverslips were placed in an external solution and test solution (pH 5.5, 7.0, 6.75, 6.5, 6.25, 6.0) in the absence and presence of creatine were applied for 5 seconds with a washout period of one minute between exposures to generate a hASIC1a activation pH-response profile while being normalized to pH 5.5 (Fig.2). Each pH-response profile was generated with exposure to control followed by exposures from high pH to low pH. For 10 mM creatine, the maximal peak current amplitude was obtained using pH 5.0 and creatine. For the hASIC1a steady-state pH-activation profile, patched cells were exposed to pH 8.0, 7.75, 7.4, 7.25, 7.0, and 6.75 in the presence and absence of creatine for 1 minute prior to exposure to pH 5.5 in the absence of creatine(Fig.3). The responding low pH mediated current was normalized to the response observed at pH 8.0. To assess the effect of channel desensitization on creatine efficacy, we exposed patch-clamped cells to pH 5.0, followed by the test solution, and finally an additional exposure to pH 5.0 solution. The test peak current amplitude was normalized to the average of flanking currents (Fig.4). The data was plotted for 5 and 10 mM creatine. The open-state desensitization was assessed in hASIC1a by exposing patch-clamped cells to pH 6.0 at conditioning pH of 8.0 followed by pH 6.0 solution containing 5 or 10 mM creatine at 1 minute intervals (Fig.5). The currents were scaled for comparison and overlayed to determine the difference in desensitization in the absence and presence of creatine. The

hASIC1a channel was repeatedly activated with pH 6.0 to determine the desensitization from a conditioning pH 8.0, 7.4 or 7.2. A control response was obtained using pH 6.0 in the absence of creatine and were followed by pH 6.0 with 5 or 10 mM creatine (Fig.6). A one-minute washout separated each recording. Where applicable, each open-state desensitization profile was fit with a monoexponential function to compare changes in desensitization in the presence and absence of creatine.

2.3.5 Data analysis: Data was analyzed using GraphPad Prism6 and OriginLab 8.0 software. The current elicited in the absence and presence of creatine at test pH was normalized to the maximum peak current amplitude observed with their respective pH solution controls. Two groups were analyzed using the unpaired student t test. The concentration-response profiles were compared using sum-of-square F-test in prism 6 (GraphPad). The kinetics of desensitization at different conditioning pHs in the presence and absence of creatine were fitted to the exponential equation (One phase decay). The time constants (τ) are reported. The desensitization kinetics data was analyzed by one way ANOVA followed by Tukey's multiple comparison test. Data are the mean ± SEM.

2.4 RESULTS

2.4.1 Creatine failed to activate hASIC1a channel.

Nonproton ligands, which contain a guanidine group, have been shown to directly activate acid-sensing ion channels, specifically ASIC3[14-16]. Although there has been no reported evidence that these guanidine compounds activate hASIC1a, we applied 5 mM creatine to hASIC1a at conditioning pH 8.0 and 7.4. At both conditioning pH values, we failed to observe creatine mediated direct activation of hASIC1a (Fig.1). Hence we sought to determine its effect on the proton sensitivity of the channel.

2.4.2 Creatine reduced hASIC1a pH sensitivity.

We performed pH activation and steady-state desensitization experiments to determine creatine's influence on the proton sensitivity of the channel. We exposed patched HEK293t cells that express hASIC1a to lower pH values to generate an activation profile. A rapid reduction of pH from alkaline conditioning solution (pH 8.0) resulted in a transient inward current (Fig.2a). The peak current amplitude of endogenous hASIC1a increased as the pH was decreased (Fig.2e). The hASIC1a half-maximal value of activation (activation pH_{50}) was 6.52 ± 0.02 with a Hill coefficient of 2.13 ± 0.17. After establishing a control response for hASIC1a, we sought to determine the effects of creatine on the activation profile of this acid-sensing ion channel. Addition of 3mM creatine did not affect the pH sensitivity of the channel and a pH_{50} was 6.39 ± 0.03 ($n \geq 4$, $p = 0.520$) with a Hill coefficient of 1.89 ± 0.23 ($p = 0.61$) (Fig.2b,2e). Additions of 5mM creatine to the test solutions were used to assess the effect of creatine on the channel's proton sensitivity (Fig.2b, 2e). At this concentration, creatine reduced proton sensitivity in the hASIC1a to a determined pH_{50} of 6.26 ± 0.03 ($n \geq 4$, $p < 0.0001$ compared to the control) with a Hill coefficient of

1.65 ± 0.17 (n≥4, p=0.032 compared to control). Furthermore, the inclusion of 10 mM creatine further reduced the activation pH_{50}, a value of 6.11 ± 0.06 (n≥4, p<0.0001 compared to control) and Hill coefficient of 0.98 ± 0.11 (n≥4, p<0.0001 compared to control) (Fig.2c, 2e). These values are summarized in Table 1.

2.4.3 Creatine at 10mM shifts hASIC1a SSD profile to lower pH values.

After determining the effect of creatine on an activation profile of hASIC1a, we sought to determine its effect on the steady-state desensitization (SSD) profile of hASIC1a. This is critical, unlike other ligand-gated ion channels, as protons are always present in solution and influence the activity of acid-sensing ion channels. Thus, a steady-state desensitization profile provides an estimate of the number of channels available for opening after exposure to increasing acidic test solutions as insults. The SSD profile of hASIC1a was obtained by exposing patched cells to different conditioning pH (for 1 minute) prior to activating with pH 5.5. The currents measured were normalized to the maximum peak current amplitude observed at pH 5.5. The control response to conditioning pH resulted in an hASIC1a SSD pH_{50} value of 7.32 ± 0.01 with an associated Hill coefficient of 6.91 ± 1.13 (Fig.3a, 3e). Near physiological pH (~ pH 7.35), about 30% of the hASIC1a protein was found in the desensitized state and unresponsive to exposures of low pH. We sought to determine if creatine influenced steady-state desensitization of hASIC1a. With 3 mM creatine, the hASIC1a SSD pH_{50} was 7.30 ± 0.02 (n≥4, p = 0.1235) and a Hill coefficient of 2.69 ± 0.35 (p = 0.044) (Fig. 3b, 3e). With conditioning pH and 5 mM creatine, the hASIC1 SSD pH_{50} was not significantly different than the control. At 5 mM creatine, the hASIC1a SSD pH_{50} was 7.36 ± 0.02 (p = 0.1217) with a Hill coefficient of 9.86 ± 3.75 (p = 0.3685) in at least four distinct cells (Fig.3b, 3e). In the presence of 10 mM creatine, there was an observed increase

in availability of channels to be opened by acidity (Fig.3c,3e). The hASIC1a SSD pH_{50} with 10 mM creatine in the conditioning solution was 7.21 ± 0.02 ($p = 0.0007$, compared to the control) with a Hill coefficient of 5.38 ± 1.08 ($p = 0.3944$, compared to control), reflective of a significant reduction of hASIC1a SSD pH_{50} by creatine.

2.4.4 Creatine increases efficacy of hASIC1a at 10 mM

Our coapplication of low pH and creatine to assess changes in pH potency may introduce a confounding influence of channel desensitization. To control for desensitization in hASIC1a channel, we exposed patched cells to test solutions by flanking with pH 5.0 as a control. The response to test pH solutions with or without 5 or 10 mM creatine was normalized to the response obtained by average of pre and post exposure to pH 5.0 solution. Creatine activation curve at 5 mM did not increase the efficacy of the channel. With 10 mM creatine, we observed an increase in efficacy of hASIC1a by about 40% which was significantly different compared to control ($p = 0.0076$) (Fig.4). We could not determine the pH_{50} values for efficacy. The traces for control, 5 mM and, 10 mM creatine efficacy in supplementary Fig. 1,2, and 3 show the effect of creatine on efficacy of hASIC1a. We observed the differences in steady-state currents elicited by control pH 5.0 in efficacy experiment. The graph of percentage of steady-state current [(Iss/Ipeak)*100] vs first and last (9th) application of pH 5.0 solution for control and test was plotted. The intermediate applications with increasing pH solutions contained, no creatine (Black square), 5 mM creatine (Red circles) or 10 mM creatine (Blue traingle), represented in supplementary figs 1,2 and 3. When intermediate applications contained 10 mM creatine, steady-state current for last pulse was significantly increased from 12% (control) to 56% (10 mM creatine) ($p = 0.0125$) (supplementary Fig.4). Data represented as mean ± SEM ($n \geq 4$).

2.4.5 Creatine delays open-state desensitization of hASIC1a.

During our studies, we observed striking differences in channel kinetics in the current generated in the presence of creatine (Fig.5a, 5c). The hASIC1a steady-state currents observed while in the presence of low pH 6.0 and creatine at 5 and 10 mM creatine were distinct from their respective control and washout currents. To assess the changes in desensitization during the course of hASIC1a exposure to creatine, we measured the percent desensitization (%Des) following the peak current amplitude at 0.5, 1, and 3 seconds (Fig.5, Table 2). The overlay of current profiles shows the difference in desensitization profiles observed after application of 5 and 10 mM creatine (Fig.5a, 5c). The bar graph represents percent desensitization calculated after 5 mM (Fig.5b) and 10 mM (Fig.5d) creatine application. The influence of creatine on the percent desensitization at 0.5 seconds ($\%Des_{0.5}$) was not significantly different from the control in the presence of 5 or 10 mM creatine. The measured %Des at 1 second for 5 mM creatine and 10 mM creatine was not significantly different compared to the control. The 10 mM creatine %Des for control at 3 sec (83.96 ± 1.14, n=4, p= 0.0013) was significantly different than the control %Des for 10 mM creatine at 3 seconds (91.26±0.60). These values are summarized in Table 2. The overall, the observed differences in %Des values in the presence of creatine suggest that the creatine slows down the hASIC1a open-state desensitization at 10 mM.

2.4.6 Creatine increases recovery after desensitization at conditioning pH 7.2.

One limitation with hASIC1a is that it undergoes desensitization with repeated exposure to low pH solutions[26]. The creatine effect on hASIC1a desensitization has not been studied before. After an initial exposure of patched HEK293t cells to pH 6.0, we repeated applications of

pH 6.0 with the dietary supplement for 5 seconds with a recovery period of 1 minute between exposures (Fig.6). The conditioning pH values of 8.0, 7.4 and 7.2 were used.

Because of channel desensitization, the hASIC1a peak current amplitude diminished over time from the initial pH 6.0 peak current amplitude in the control, 5 mM, and 10 mM creatine recordings at conditioning PH 8.0 (Fig.6a). The control peak current amplitude appeared to plateau to approximately 50% of the initial peak current amplitude. In the corresponding recording applications with creatine present, the pH 6.0 peak current amplitudes at 5 mM and 10 mM creatine concentrations diminished as well, indicating desensitization. However, these peak current amplitudes were not significantly different compared to the control. The one way ANOVA to compare the means for exponential decay suggest that, means of + 5mM creatine and + 10 mM creatine are not significantly different from control at conditioning pH 8.0. The time constants (τ) for exponential decay are summarized in Table 3.

At a conditioning pH of 7.4, hASIC1a peak current amplitude diminished with higher magnitude compared to conditioning pH 8.0 (Fig. 6b). For a 7.4 conditioning pH, the control peak current amplitude diminishes to approximately 30% of the initial peak current amplitude. The repeated applications of creatine (5 mM and 10 mM) in the presence of low pH exhibited desensitization. However, only the initial response to pH 6.0 and 5 mM creatine fractional open value was 0.89 ±0.02 of the initial pH 6.0 peak current amplitude and was significantly different than desensitization observed in the absence of creatine at the equivalent application, a 0.80 ± 0.03 fraction of the respective pH 6.0 peak current amplitude ($p = 0.045$). The one way ANOVA to compare the means for exponential decay suggest that, the means of + 5mM creatine and + 10 mM creatine are not significantly different from control. The time constants (τ) for exponential decay are summarized in Table 3.

At conditioning pH of 7.2, the peak current amplitude with pH 6.0 diminished to about 47% of the initial peak current amplitude (Fig 6c). At conditioning pH 7.2, most of the hASIC1a channels are desensitized. However, 5 mM and 10 mM creatine increase recovery from desensitization significantly at conditioning pH of 7.2 and the current diminished to about 65% of the initial peak current for 5 and 10 mM creatine. The one way ANOVA to compare the means for exponential decay suggest that, means of + 5mM creatine ($p= 0.032$) and + 10 mM creatine ($p= 0.030$) are significantly different from control. For conditioning pH 7.2, we were unable to fit the test data (5 and 10 mM creatine) to one phase decay equation. This suggests that creatine altered desensitization that differs from exponential decay. The time constants for exponential decay for control, 5 mM creatine and 10 mM creatine at varying conditioning pHs are listed in the Table 3.

2.5 DISCUSSION

We have demonstrated that the creatine reduces the proton sensitivity of hASIC1a at 5 and 10 mM (Fig.2) but also shifts steady-state desensitization curve to lower pH values at 10 mM (Fig.3). When controlled for desensitization, creatine at 10 mM concentration increases hASIC1a efficacy by about 50% (Fig.4), suggesting that creatine is able to recover channels from desensitization. ASIC1a open-state desensitization kinetics is also influenced by creatine (Fig.5), as creatine slowed the open-state desensitization. Also, at acidic conditioning pH, when most of the channels are in the desensitized state, creatine increases recovery from desensitization (Fig.6). These effects of creatine were similar to the effects observed with spermine on hASIC1a channel[18]. Spermine, an endogenous polyamine, has been shown to activate hASIC1a channel and modulates channel desensitization to increase the channel's recovery. Similarly, Alijevic and Kellenberger show that 2-guanidine-4-methylquinazoline (GMQ) (1 mM) shifts the hASIC1a activation curve and steady-state desensitization curve to more acidic pH values, suggesting that GMQ binding site is accessible in desensitized state of the hASIC1a channel[16]. Also, peptides like RF-amide and dynorphins were shown to shift steady-state desensitization profile of hASIC1a to acidic pH values[6,19]. But other polyamines putrescine and spermidine don't affect hASIC1a significantly[18]. We observed that the shifts in hASIC1a pH sensitivity and effects on desensitization occurred at high creatine concentrations (5 and 10 mM).

Creatine is an endogenous guanidine compound[27] that is a commonly used dietary supplement[28]. Typically, the suggested supplementation of an over-the-counter creatine consists of two phases: a loading phase and a maintenance phase. In the loading phase, creatine intake regimen is 20 grams/day for 5 days. This is typically followed by a maintenance phase consisting of a daily dose of 5 grams of creatine[29,30]. Within the loading phase of creatine, the serum levels of

creatine are 2.17 ± 0.66 mM[31]. Although the measured serum levels of creatine are lower than our experimental concentrations, the concentrations used support that the studied creatine concentrations are physiologically relevant and that the observed effects in our report may occur at *in vivo* acid-sensing ion channels. Furthermore, 5 mM creatine has been shown to exert neuroprotective effect in a hippocampal cell culture model of neuronal degeneration[32]. Thus, the concentrations we have selected are similar to clinically relevant serum creatine concentrations and could be achieved by individuals that ingest this dietary supplement.

The local concentration of creatine where ASIC1a is found is not known. Human ASIC1a is found in the central nervous system at synapses, where local concentrations of ligands and neurotransmitters would be the most robust. One published report found evidence to suggest that creatine was released in response to excitatory action potentials[33]. The authors observed that removing calcium attenuated the resulting creatine release providing evidence to support that creatine may be released in a manner similar to conventional neurotransmitters. However, the quantity of creatine released into the synapse correlates with these concentrations to modulate the acid-sensing ion channel remains unclear. One possibility is that the creatine concentration following excitatory stimulation is high, similar to the proton concentration fluctuations following an action potential. Li et al.[34] estimate that within a sufficiently small region in the brain, pH fluctuates to hASIC1a activating values (pH 6.5) with the addition of a few proton ions. Perhaps creatine supplementation further increases the amount of the guanidine dietary supplement in the synapse in addition to the released creatine.

One aspect of hASIC1a activity that should be taken into account is the sensitivity of the channel to high concentrations of creatine. The creatine concentration studied here, 10 mM, is higher than what is observed in patients or athletes who ingest creatine as a supplement. In the

steady-state desensitization studies, the hASIC1a SSD pH_{50} value is decreased, significantly, from 7.32 to 7.2. At pH 7.32, hASIC1a has 50% of the channels in the protonated-desensitized state, while 10 mM creatine hASIC1a had fewer than 20% of the channels in the desensitized state. Similarly, when desensitization was introduced in the channel, creatine at 10 mM concentration, increased hASIC1a efficacy by about 40%. We also observed a significant increase in steady-state current from first application to last (9th) application of control 5.0 solution in 10 mM cretine efficacy curve. The steady-state current in ASICs is a non-desensitizing current which mediates damage after ischemic stroke and pain. This, under physiological conditions, suggests that high levels of creatine may not be as beneficial as lower (5 mM) creatine concentrations. This is the opposite of what was observed for hASIC1 in the presence of 5 mM creatine. There was no significant change in the SSD pH_{50} when hASIC1a was exposed to 5 mM creatine compared to the control. If a novel therapeutic were to be used that targets hASIC1a by modulating the steady-state desensitization properties of the channel, the compound should increase the percentage of channels that are in the desensitized state. However, creatine may act to increase the number of ASICs in the closed state. This would explain both reduced pH_{50} of steady-state desensitization and reduced number of the channels in the desensitized state while in the presence of the dietary supplement.

In case of ischemic stroke, local brain pH is reduced. Creatine reduced hASIC1a proton sensitivity, which suggested that the dietary supplement has potential as a neuroprotective agent. However, the mechanism of creatine's suggested loading/maintenance dosing regimens suggest that creatine may not be efficacious following an ischemic event. Administration of creatine to reach this concentration may be difficult to achieve and not safe for a patient following a stroke. Creatine may have maximal efficacy as a prophylactic, preventative treatment for ischemia and

stroke. Studies have shown that creatine is neuroprotective in cases of ischemic stroke[22,23,35] and other age-related diseases [21]. *In vitro,* creatine has been shown to protect cells from excitotoxicity and creatine concentrations as high as 10 mM do not affect the cells adversely[32]. However, the mechanism by which creatine mediates this neuroprotection has not been clear. Some have attributed the neuroprotective effect of creatine to its role in supporting brain energy or metabolism[23]. To regenerate the energy stores in neurons, time is a factor. Our results suggest that creatine modulation of hASIC1a occurred rapidly. A non-ion channel mechanism would require time for creatine to be transported and converted to ATP. If creatine had only an effect on the cell energy, the short duration of our recording protocols would fail to observe these effects.

Furthermore, the effects of creatine on hASIC1a desensitization are of interest. Specifically, the ASIC1a subtypes of these proton-sensitive ion channels undergoes desensitization and tachyphylaxis, which is the reduction of peak current amplitude following repeated exposures to lower pH (increased protons)[26]. Proton tachyphylaxis had been observed early in the history of the acid-sensing ion channel[36] and has become a fundamental property of the ASIC1a subtype. Expressed hASIC1a in HEK293t cells show desensitization at conditioning pH values pH 8.0, the physiologically relevant pH 7.4 and pH 7.2 (Fig.6). The desensitization of hASIC1a was more striking at pH 7.2. Furthermore, it was at this pH that we observed creatine's recovery from desensitization. One possible explanation for this is that creatine prevents additional hASIC1a proteins from entering a desensitized state[26]. From a pH 8.0 conditioning pH, exposures to a low pH environment in the absence and presence of creatine showed similar profiles. At conditioning pH 7.4, desensitization profile in presence of creatine began to diverge from the control and at 7.2 conditioning pH creatine significantly reduced desensitization. Thus, creatine may prevent channel desensitization by shifting the acid-sensing ion channel to a closed state that can be acti-

vated by low pH. Finally, at conditioning pH 7.2, creatine reduces the extent of tachyphylaxis. This prevention of tachyphylaxis, if encountered in vivo, would counteract the neuroprotective effects that creatine may accomplish by resetting ASIC1a for further activation.

In conclusion, creatine modulates endogenous hASIC1a by reducing the pH sensitivity of activation and modulating the desensitization of the channel. The reduction in pH_{50} of steady-state desensitization, increase in efficacy at 10 mM and recovery from desensitization from low conditioning pH suggests that creatine can result in ASIC1a channels available for activation after persistent acidification. Furthermore, it is reasonable to consider that creatine may exacerbate the effects of ischemia, similar to the polyamine spermine if administered following the ischemic event. Creatine's utility as a neuroprotective agent may be before the insult occurs, limiting the dietary supplement's efficacy to that of a preventative measure. Thus, under strict adherence to suggested use, creatine may be a simple dietary supplement that may have an effect through ASIC-mediated pathway. Additional characterization of creatine's activity on other ASIC subtypes will be required to assess the overall role of creatine in the ischemic stroke and possibly other ASIC-mediated disorders.

Table 1. Summary of hASIC1a activation pH_{50} and Hill coefficients in the presence and absence of creatine. Creatine was present in the activating pH test solutions (**Activation**) or the conditioning pH (**Steady-state desensitization**). *Italics* indicate significance.

	Activation				**Steady-state Desensitization**			
	pH_{50}	**P value**	**Hill, *n***	**P value**	**pH_{50}**	**P value**	**Hill, *n***	**P value**
Control	6.53 ± 0.02	-	2.13 ± 0.17	-	7.32 ± 0.01	-	6.91 ± 1.13	-
Creatine								
+ 3 mM	6.39 ± 0.03	0.520	1.89 ± 0.23	0.61	7.30 ± 0.02	0.1235	2.69 ± 0.35	*0.044**
+ 5 mM	*6.26 ± 0.03****	<0.0001	*1.65 ± 0.17**	0.0317	7.36 ± 0.02	0.1217	9.86 ± 3.75	0.3685
+ 10 mM	*6.11 ± 0.06****	<0.0001	*0.99 ± 0.11****	<0.001	*7.21 ± 0.02****	0.0007	5.38 ± 1.08	0.3944

*, p<0.05
**, p<0.01
***, p<0.001 Compared to control.

Table 2. Summary of hASIC1a percent desensitization in the presence and absence of creatine at 0.5, 1 and 3 sec after peak current. *Italics* indicate significance.

	5 mM Creatine			10 mM Creatine		
Time	**%Des, control**	**%Des, creatine**	**P value**	**%Des, control**	**%Des, creatine**	**P value**
0.5 sec	19.82 ± 1.76	20.42 ± 4.63	0.9094	21.55 ± 4.59	19.33 ± 2.52	0.6864
1 sec	50.64 ± 2.91	40.82 ± 4.12	0.1234	52.13 ± 5.39	39.50 ± 3.59	0.0990
3 sec	87.73 ± 1.70	83.24 ± 1.63	0.1239	91.26 ± 0.60	*83.9 6± 1.14***	0.0013

**, $p<0.01$ Compared to control

Table 3. Summary of time constant tau (τ) for hASIC1a desensitization at conditioning pH 8.0, 7.4 and 7.2.

τ value for desensitization					
Condition	**8.0**	**P value**	**7.4**	**P value**	**7.2**
Control	3.53±1.41		3.64±1.54		2.44±1.0
+ 5 mM Creatine	5.4±1.8	0.4447	6.05±2.21	0.4054	ND
+ 10 mM Creatine	4.52±1.0	0.5876	4.0±1.3	0.8604	ND

2.6 FIGURES AND LEGENDS

Fig. 1. Creatine failed to activate hASIC1a at conditioning pH of 8.0 and 7.4. Patched HEK293t cells were exposed to a Control (pH 6.0, conditioning pH 8.0) and 5 mM creatine (red) at activation pH of 8.0 and 7.4 (conditioning pH 8.0) to determine the direct activity of creatine on hASIC1a.

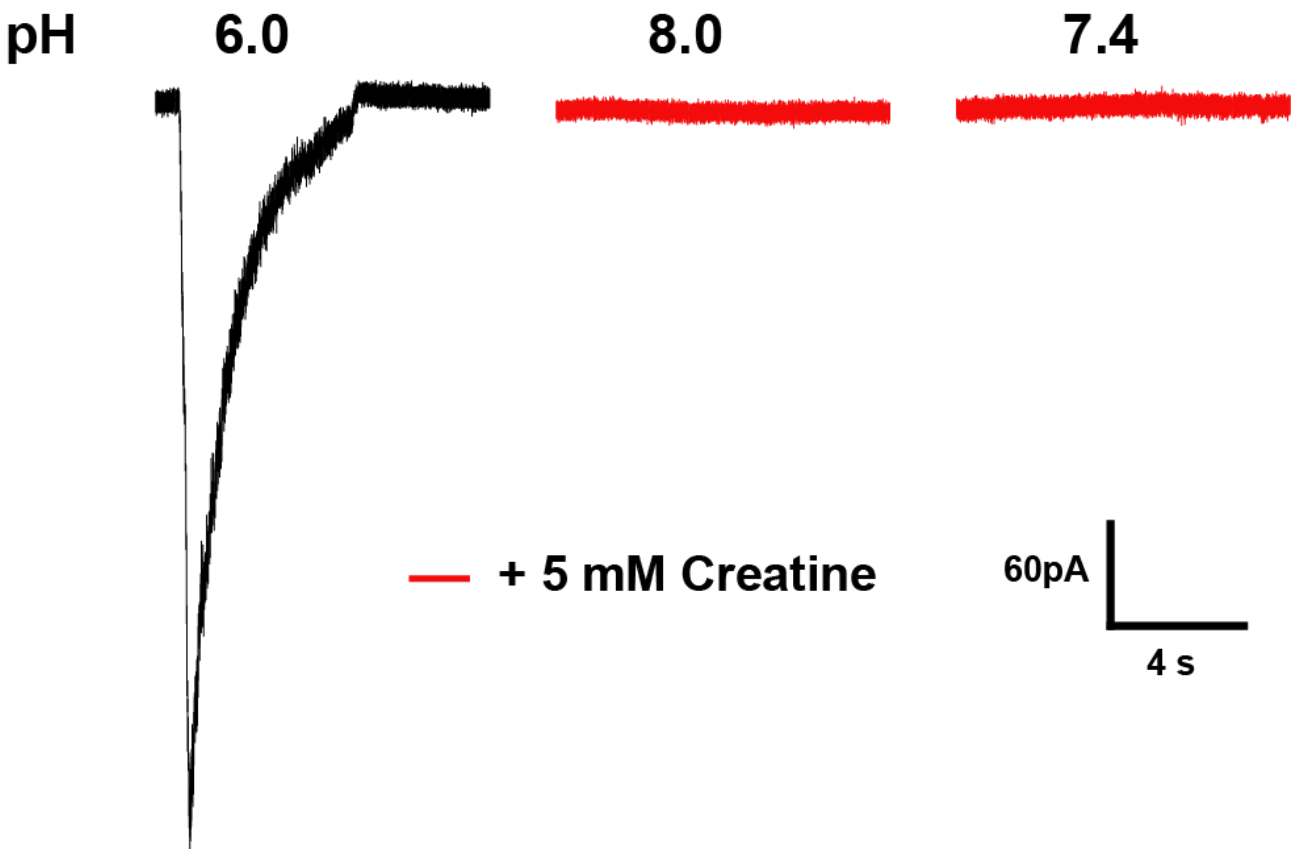
pH
6.0
8.0
7.4
+ 5 mM Creatine
60pA
4 s

Fig.2. Creatine reduced hASIC1a proton sensitivity (a) Control, **(b) +** 3 mM creatine, **(c)** +5 mM creatine, and **(d)** + 10 mM creatine, represents whole-cell patch-clamp recording current for hASIC1a activation. **(e)** Summary of activation profiles of endogenous hASIC1a recorded in HEK293t cells. Switching from conditioning pH 8.0 to increasingly acidic test solutions generated the hASIC1a pH activation profiles. The hASIC1a pH-response profiles for control (black square) had a calculated pH_{50} value of 6.53 ± 0.02 with a Hill coefficient of 2.13 ± 0.17, + 3 mM creatine (green star) had a calculated pH_{50} value 6.39 ± 0.03 and Hill coefficient of 1.89 ± 0.23,+ 5 mM creatine (red circle) had a calculated pH_{50} value of 6.26 ± 0.03 and Hill coefficient of 1.65 ± 0.17, and +10 mM creatine (blue triangle) had a calculated pH_{50} value of 6.11 ± 0.06 with a Hill coefficient of 0.99 ± 0.11. Data represented as mean ± SEM of at least four individual cells per data point. Vertical and horizontal scale bars are in picoAmperes and seconds, respectively.

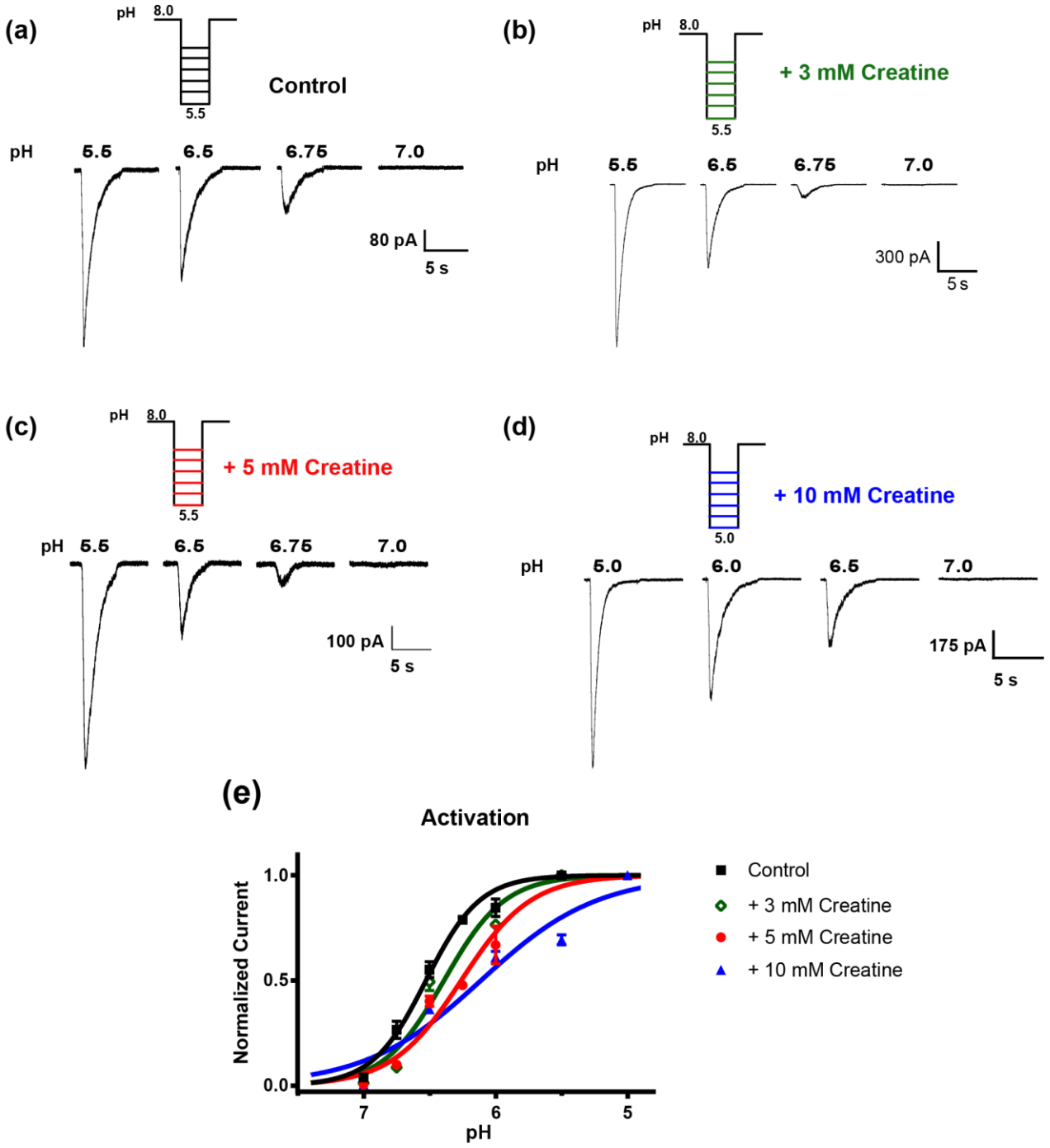
(a)
pH 8.0
5.5
Control
pH 5.5 6.5 6.75 7.0
80 pA
5 s
(b)
pH 8.0
5.5
+ 3 mM Creatine
pH 5.5 6.5 6.75 7.0
300 pA
5 s
(c)
pH 8.0
5.5
+ 5 mM Creatine
pH 5.5 6.5 6.75 7.0
100 pA
5 s
(d)
pH 8.0
5.0
+ 10 mM Creatine
pH 5.0 6.0 6.5 7.0
175 pA
5 s
(e)
Activation
Normalized Current
1.0
0.5
0.0
7
6
5
pH
Control
+ 3 mM Creatine
+ 5 mM Creatine
+ 10 mM Creatine

Fig.3. Creatine at 10 min shifts steady-state desensitization curve to more acidic pH (a) Control, **(b)** +5 mM creatine, and **(c)** + 10 mM creatine, represents whole-cell patch-clamp current recordings for hASIC1a steady-state desensitization. **(d)** Summary of steady-state desensitization (SSD) profiles of endogenous hASIC1a recorded in HEK293t cells. Exposing patched cells to varying conditioning pH values before applying a pH 5.5 solution generated steady state desensitization curve. The SSD profiles of control (black square) had an SSD pH_{50} value of 7.32 ± 0.01 with a Hill coefficient of 6.91±1.13, + 3 mM creatine (green star) had an SSD pH_{50} value of 7.30 ± 0.02 with a Hill coefficient of 2.69 ± 0.35, + 5 mM creatine (red circle) had an SSD pH_{50} value of 7.36 ± 0.02 with a Hill coefficient of 9.86 ± 3.75, and + 10 mM creatine (blue triangle) had an SSD pH_{50} value of 7.21 ± 0.02 with a Hill coefficient of 5.38 ± 1.08. Data represented as mean ± SEM ($n \geq 4$). Vertical and horizontal scale bars are in picoAmperes and seconds, respectively.

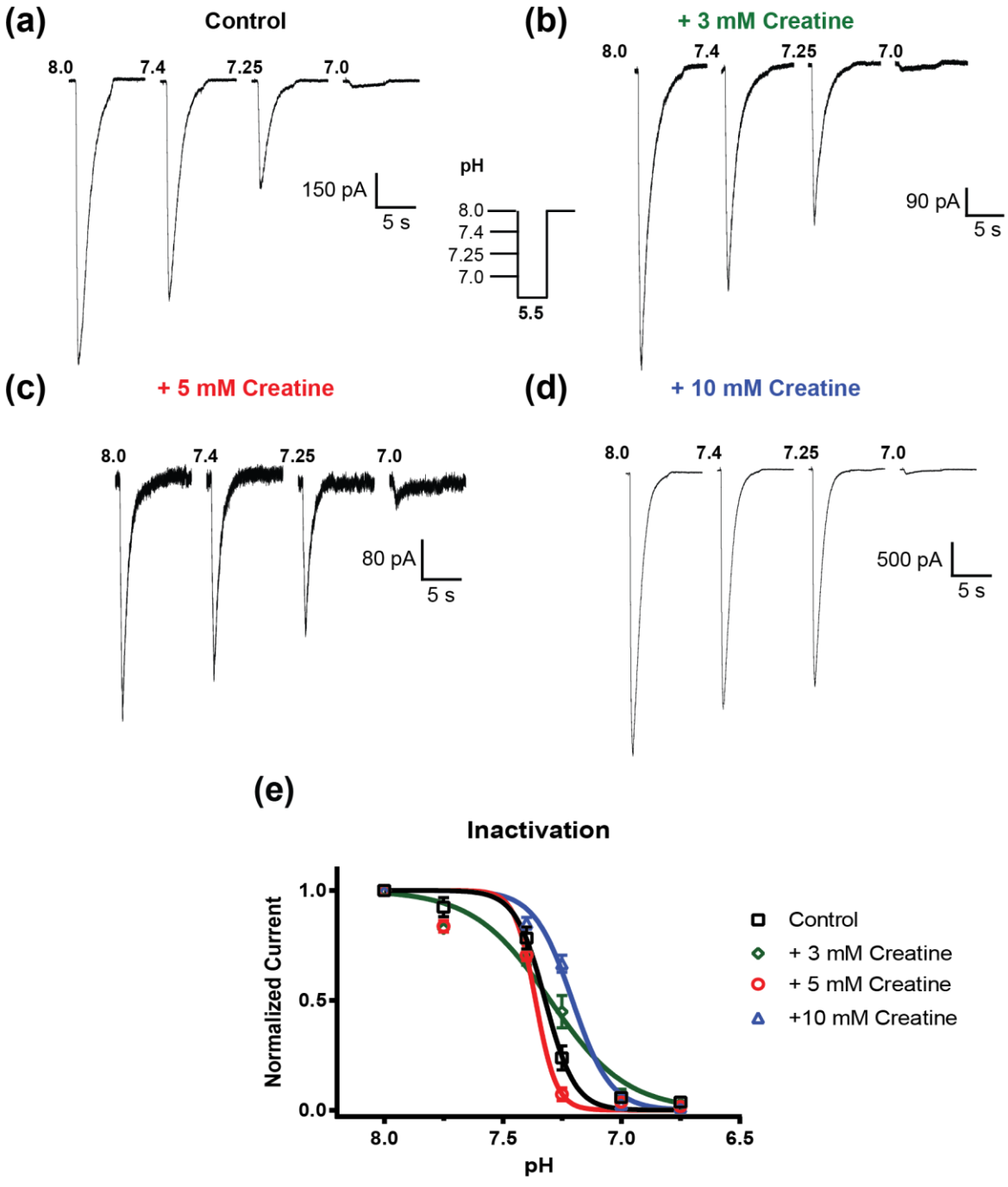
(a)
Control
8.0
7.4
7.25
7.0
150 pA
5 s
pH
8.0
7.4
7.25
7.0
5.5
(b)
+ 3 mM Creatine
8.0
7.4
7.25
7.0
90 pA
5 s
(c)
+ 5 mM Creatine
8.0
7.4
7.25
7.0
80 pA
5 s
(d)
+ 10 mM Creatine
8.0
7.4
7.25
7.0
500 pA
5 s
(e)
Inactivation
Normalized Current
1.0
0.5
0.0
8.0
7.5
7.0
6.5
pH
Control
+ 3 mM Creatine
+ 5 mM Creatine
+10 mM Creatine

Fig. 4. Creatine increases efficacy of hASIC1a at 10 mM

Summary of efficacy profiles of endogenous hASIC1a recorded in HEK293t cells in the absence and presence of creatine. Recordings were generated by switching between conditioning pH 8.0 to increasingly acidic test solutions, which were flanked with exposures to pH 5.0. Responses in the presence of 5 mM creatine (red circles) had maximal response of 89.31 ± 7.8% compared to control. In the presence of 10 mM creatine (blue triangles) the response increased significantly to 140.7 ± 11.3% of the control (91.44 ± 4.15%) ($p= 0.0076$). Data represented as mean ± SEM of at least four individual cells per data point, with the percent peak current compared to an average of the pre- and post- pH 5.0 peak current amplitudes (see Supplementary Figs. 1, 2, and 3).

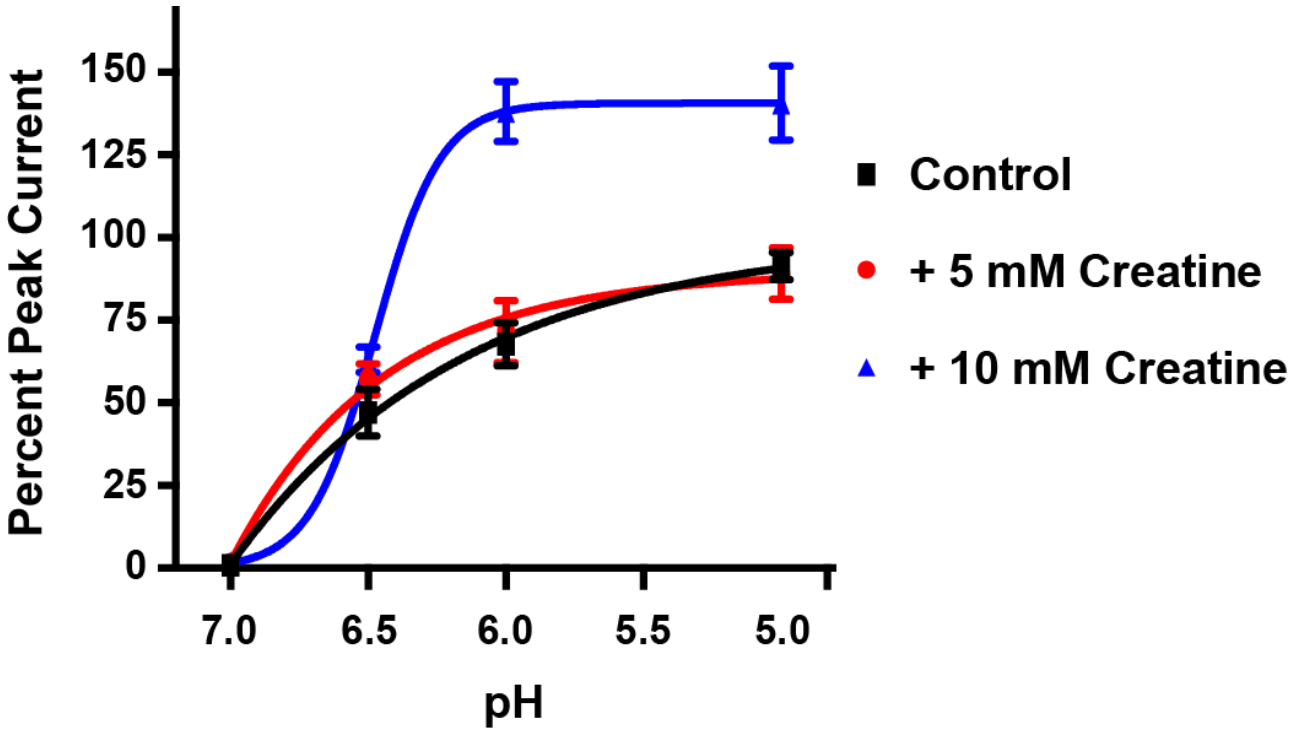
Percent Peak Current
150
125
100
75
50
25
0
7.0
6.5
6.0
5.5
5.0
pH
Control
+ 5 mM Creatine
+ 10 mM Creatine

Fig.5. Creatine slows the open-state desensitization of hASIC1a (a) Overlay of control and + 5 mM creatine traces obtained after activation with pH 6.0 solution. **(b)** Bar graph indicating % desensitization of hASIC1a at 0.5 sec, 1 sec and 3 sec after peak current amplitude. The percent desensitization (%Des) at 0.5,1, and 3 sec after 5mM creatine application was not significantly different compared to control (50.64 ± 2.9%). **(c)** Overlay of control and + 10 mM creatine traces obtained after activation with pH 6.0 solution. **(d)** Bar graph indicating percent desensitization of hASIC1a at 0.5 sec, 1 sec and 3 sec after peak current amplitude. The %Des value, at 3 sec of the 10mM creatine exposure at pH 6.0 value was 83.96 ± 1.14 ($p = 0.0013$) was significantly different when compared to %Des of the control (91.26 ±0.60%) (**$p < 0.01$).

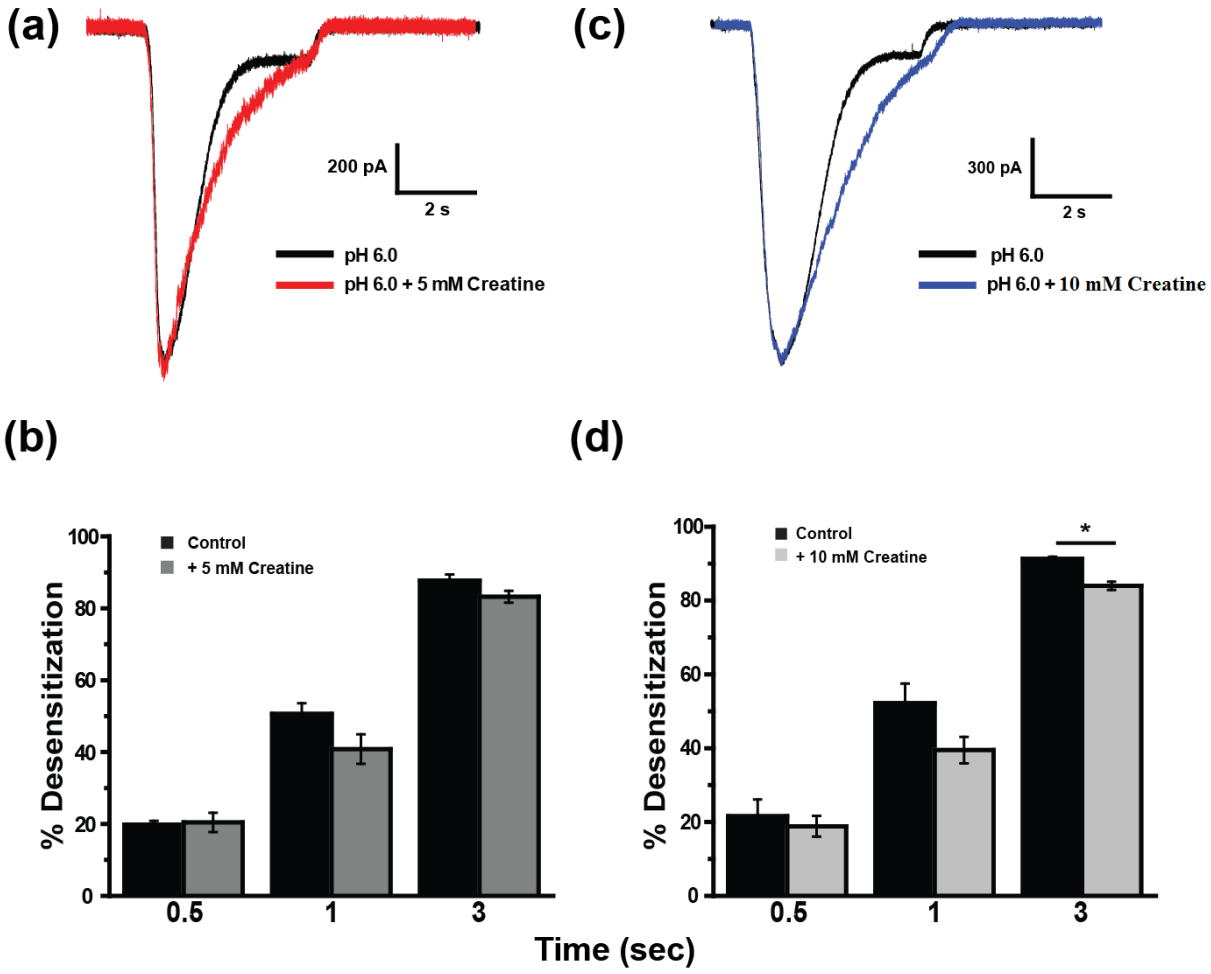
(a)
200 pA
2 s
pH 6.0
pH 6.0 + 5 mM Creatine
(c)
300 pA
2 s
pH 6.0
pH 6.0 + 10 mM Creatine
(b)
(d)
Control
+ 5 mM Creatine
Control
+ 10 mM Creatine
*
% Desensitization
% Desensitization
0
20
40
60
80
100
0.5
1
3
Time (sec)

Fig.6. Creatine recovers endogenous hASIC1a from desensitization in conditioning pH of 7.2. Summary of repeated activation of hASIC1a is shown along with a reduction in peak current amplitude at pH 6.0 (control), and in the presence of either 5 or 10 mM creatine from a conditioning pH 8.0 (a). Summary of normalized peak current amplitude to the control (pH 6.0 peak current amplitude) along with pH 6.0 and 5 or 10 mM creatine conditioning pH 7.4 (b). Only the initial application of 5 mM creatine in the presence of low pH was determined to be statistically significant when compared to the equivalent point in the absence of creatine (desensitization at the second exposure: 0.80 ± 0.03; desensitization in the presence of 5 mM creatine at the second exposure: 0.89 ± 0.03, $p = 0.045$). Summary presentation of repeated activation of hASIC1a wth pH 6.0 in the absence (control) or presence (5 or 10 mM creatine) at conditioning pH 7.2 (c). A one-way ANOVA used to compare the means between control, with 5 mM ($p = 0.032$) and 10 mM ($p = 0.030$) creatine being significantly different than the control. A τ_{des} was not determined for pH 6.0 with 5 or 10 mM creatine from a conditioning pH 7.2 as these data deviated from monoexponential decay. All peak current amplitudes were normalized to the first control pulse in the absence of creatine. Only one repeated application protocol was performed per individual cell ($n \geq 4$). Data are shown as the mean ± SEM.

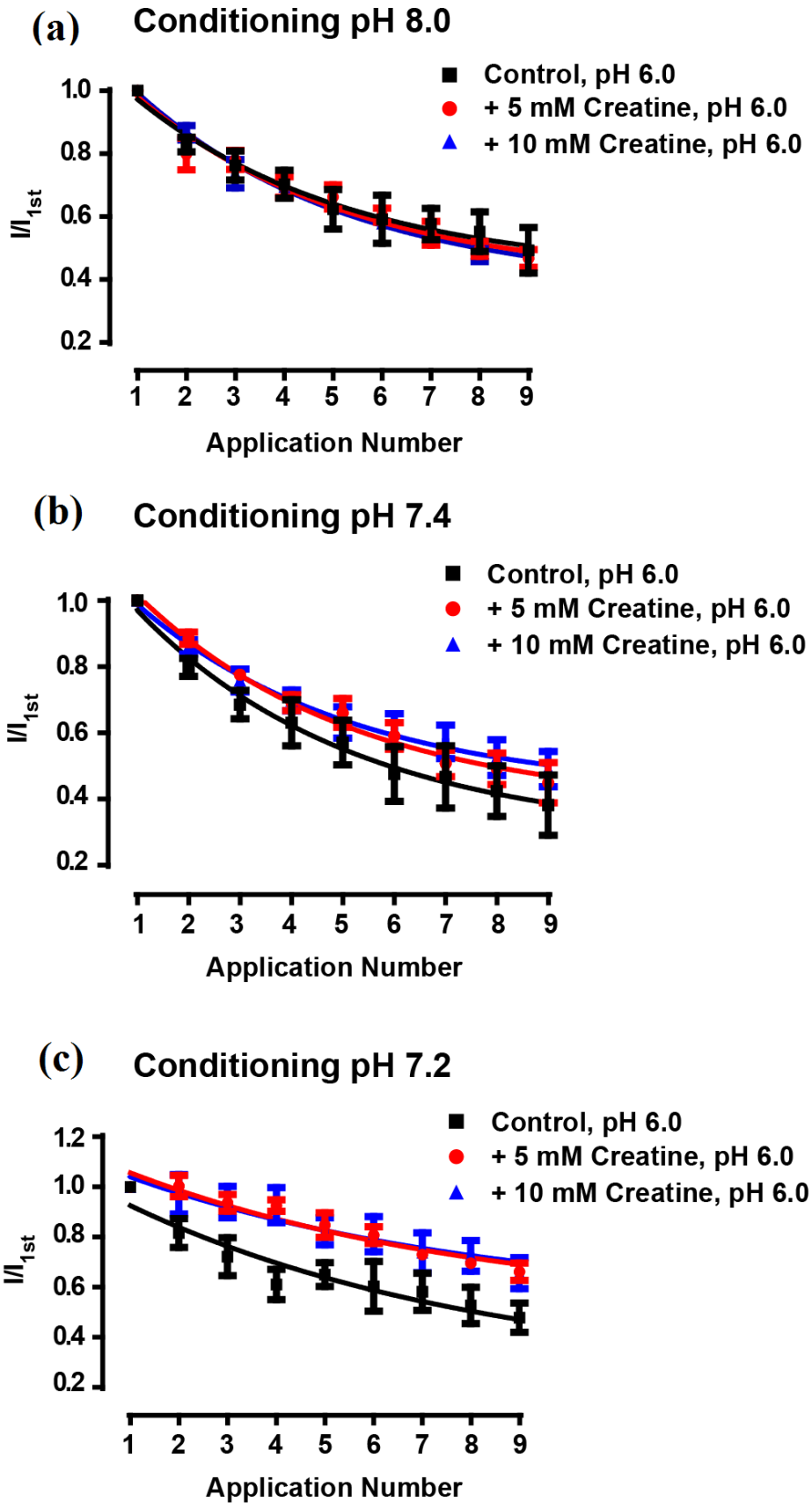
(a)
Conditioning pH 8.0
Control, pH 6.0
+ 5 mM Creatine, pH 6.0
+ 10 mM Creatine, pH 6.0
I/I1st
1.0
0.8
0.6
0.4
0.2
1 2 3 4 5 6 7 8 9
Application Number
(b)
Conditioning pH 7.4
Control, pH 6.0
+ 5 mM Creatine, pH 6.0
+ 10 mM Creatine, pH 6.0
I/I1st
1.0
0.8
0.6
0.4
0.2
1 2 3 4 5 6 7 8 9
Application Number
(c)
Conditioning pH 7.2
Control, pH 6.0
+ 5 mM Creatine, pH 6.0
+ 10 mM Creatine, pH 6.0
I/I1st
1.2
1.0
0.8
0.6
0.4
0.2
1 2 3 4 5 6 7 8 9
Application Number

Supplementary Fig. 1. Control whole-cell patch-clamp recording of creatine efficacy on the hASIC1a efficacy assessment to account for the effects of channel tachyphylaxis. Observed responses to pH from an individual cell expressing hASIC1a in the absence of creatine. The traces show test pH responses to reducing pH solutions in between exposures to the control (pH 5.0).

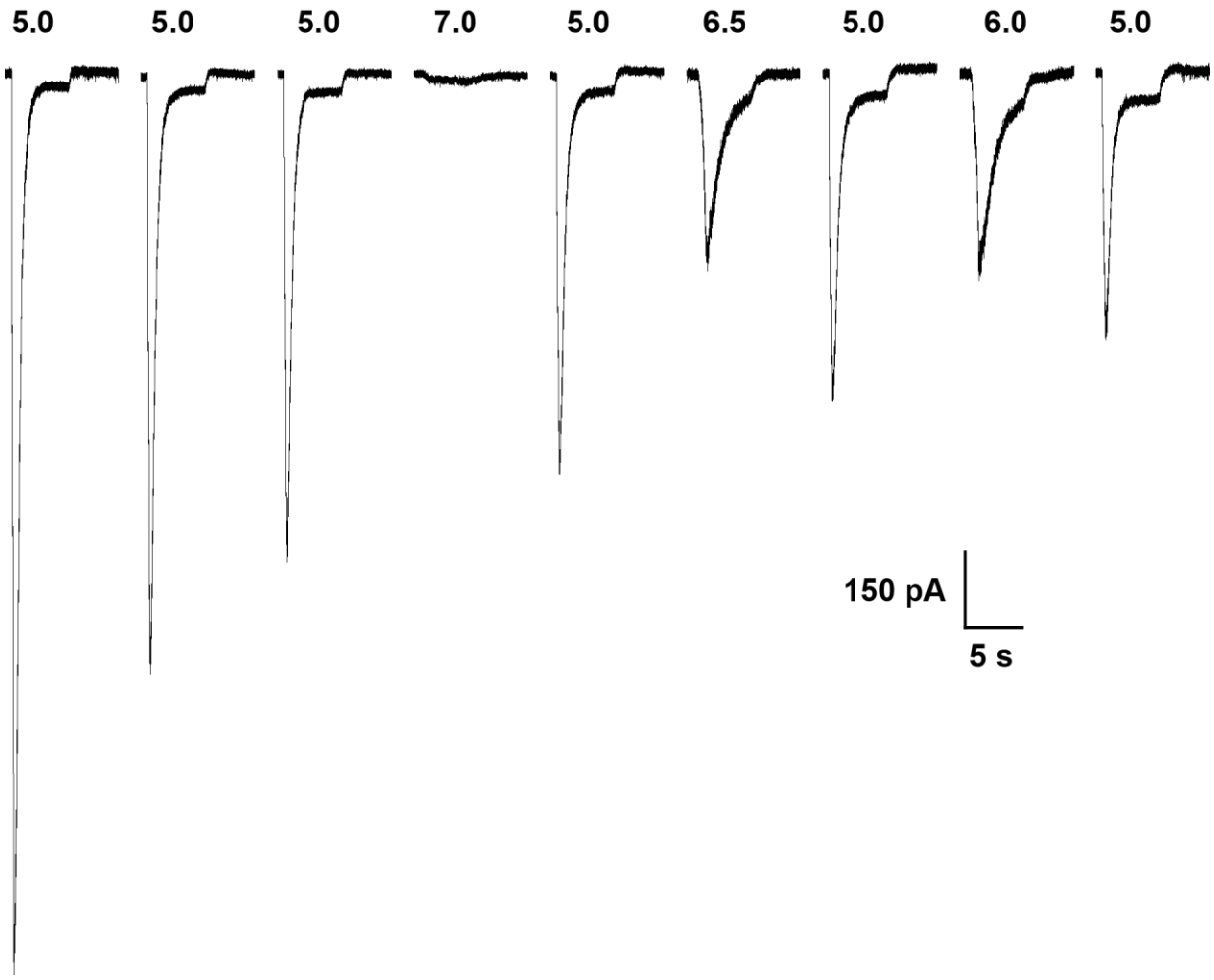
5.0
5.0
5.0
7.0
5.0
6.5
5.0
6.0
5.0
150 pA
5 s

Supplementary Fig. 2. Whole-cell patch-clamp recordings of hASIC1a in the presence of 5 mM creatine to account for the effects of channel tachyphylaxis. Observed responses to pH from an individual cell expressing hASIC1a in the presence of 5 mM creatine (red), which are found between exposures to the control

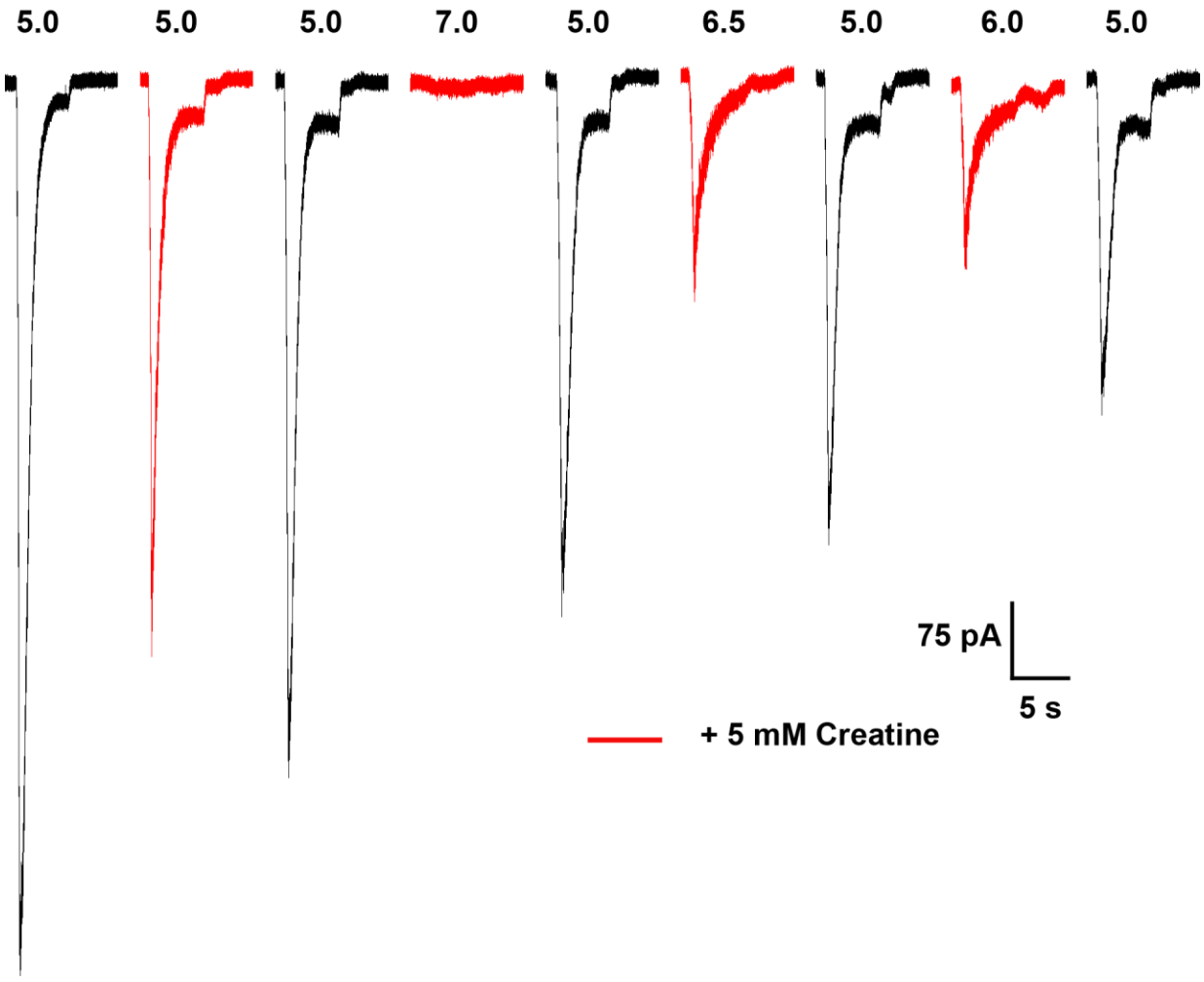
5.0
5.0
5.0
7.0
5.0
6.5
5.0
6.0
5.0
75 pA
5 s
+ 5 mM Creatine

Supplementary Fig. 3. Whole-cell patch-clamp recordings of hASIC1a in the presence of 10 mM creatine to account for the effects of channel tachyphylaxis. Observed responses to pH from an individual cell expressing hASIC1a in the presence of 10 mM creatine (blue), which are found between exposures to the control.

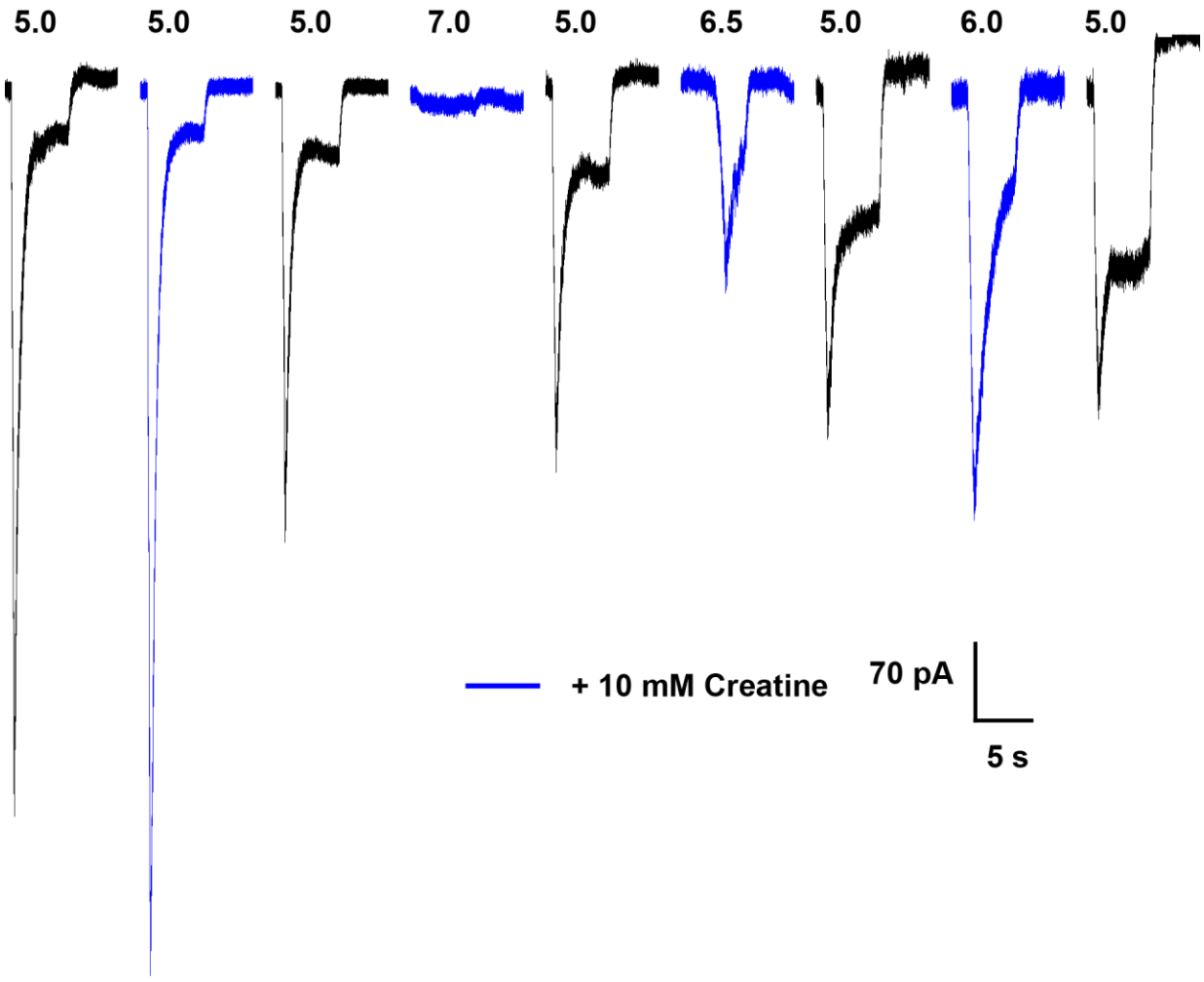
5.0
5.0
5.0
7.0
5.0
6.5
5.0
6.0
5.0
+ 10 mM Creatine
70 pA
5 s

Supplementary Fig. 4. The hASIC1a steady-state current is more robust with 10 mM creatine. Summary of the percentage of steady-state current observed after the initial and last application of control pH 5.0 is shown. Data were pooled and analyzed from experiments shown in Supplementary Fig. 1, 2, and 3 for control (black square), in the presence of 5 mM creatine (red triangle), and in the presence of 10 mM creatine (blue triangle). The initial steady state current amplitude for the control (black square) was 2.49 ± 0.95%, in the presence of 5 mM creatine (red circles) was 7.70 ± 4.43%, and in the presence of 10 mM creatine (blue triangles) was 11.2 ± 3.53%. The mean current amplitude for the pH 5.0 at the end of the recording protocol are 15.60 ± 9.60% for the control, 22.23± 6.20% when in the presence of 5 mM creatine, and 57.94 ± 8.40% when in the presence of 10 mM creatine. The measured hASIC1a steady-state current amplitude for 10 mM was statistically significant compared to the control ($p = 0.0125$). Data are presented as the mean ± SEM from four or more individual cells (*$p < 0.05$). SS, steady-state.

SS = steady-state current

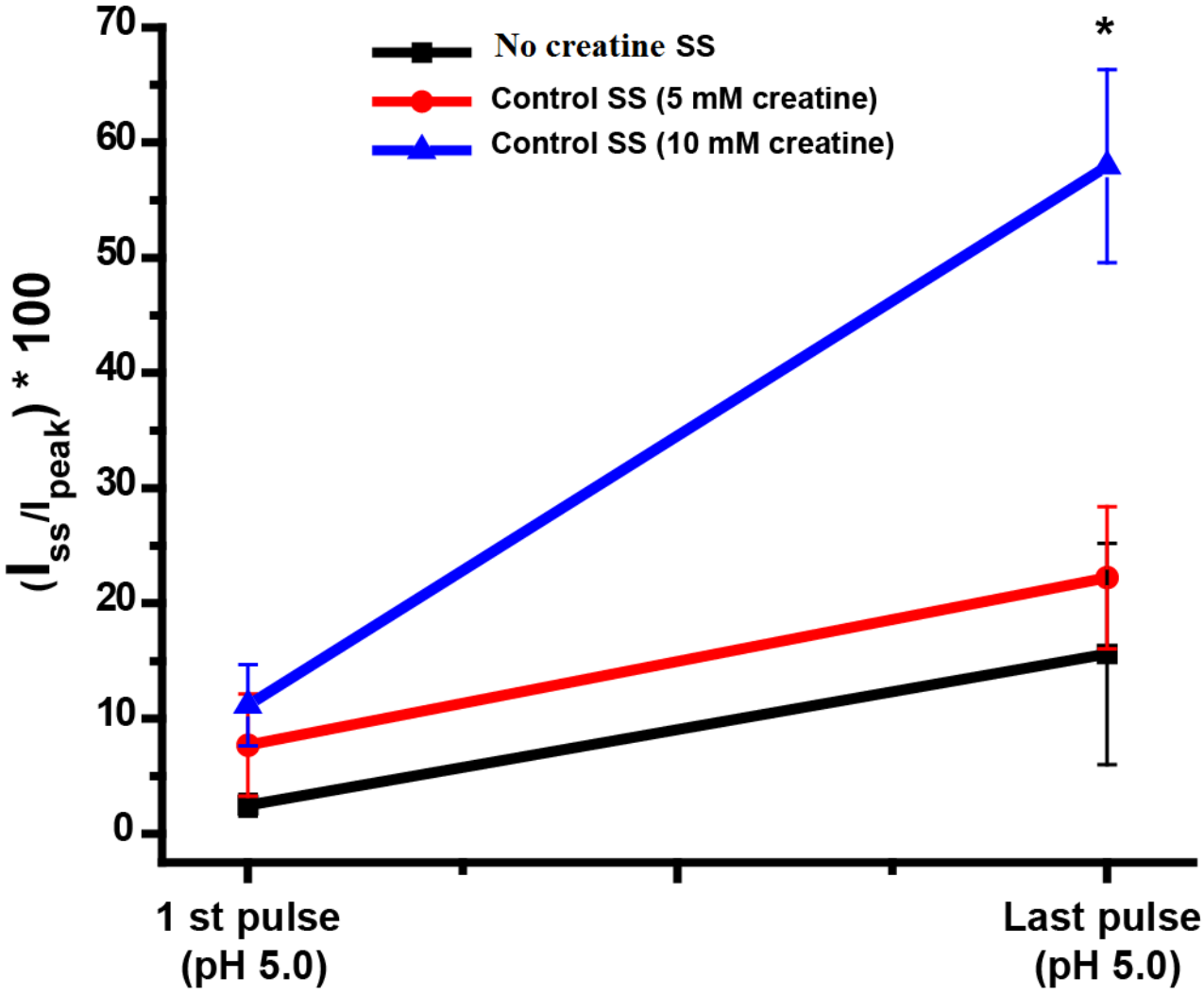

2.7 References:

1. Waldmann R, Champigny G, Bassilana F, Heurteaux C, Lazdunski M. A proton-gated cation channel involved in acid-sensing. *Nature*. 1997;386(6621):173-177. doi: 10.1038/386173a0 [doi].

2. Krishtal OA, Pidoplichko VI. A "receptor" for protons in small neurons of trigeminal ganglia: Possible role in nociception. *Neurosci Lett*. 1981;24(3):243-246.

3. Krishtal OA, Pidoplichko VI. Receptor for protons in the membrane of sensory neurons. *Brain Res*. 1981;214(1):150-154. doi: 0006-8993(81)90446-7 [pii].

4. Krishtal OA, Pidoplichko VI. A receptor for protons in the membrane of sensory neurons may participate in nociception. *Neuroscience*. 1981;6(12):2599-2601. doi: 0306-4522(81)90105-6 [pii].

5. Xiong ZG, Zhu XM, Chu XP, et al. Neuroprotection in ischemia: Blocking calcium-permeable acid-sensing ion channels. *Cell*. 2004;118(6):687-698. doi: 10.1016/j.cell.2004.08.026 [doi].

6. Sherwood TW, Askwith CC. Dynorphin opioid peptides enhance acid-sensing ion channel 1a activity and acidosis-induced neuronal death. *J Neurosci*. 2009;29(45):14371-14380. doi: 10.1523/JNEUROSCI.2186-09.2009 [doi].

7. Yermolaieva O, Leonard AS, Schnizler MK, Abboud FM, Welsh MJ. Extracellular acidosis increases neuronal cell calcium by activating acid-sensing ion channel 1a. *Proc Natl Acad Sci U S A*. 2004;101(17):6752-6757. doi: 10.1073/pnas.0308636100 [doi].

8. Yang ZJ, Ni X, Carter EL, Kibler K, Martin LJ, Koehler RC. Neuroprotective effect of acid-sensing ion channel inhibitor psalmotoxin-1 after hypoxia-ischemia in newborn piglet striatum. *Neurobiol Dis*. 2011;43(2):446-454. doi: 10.1016/j.nbd.2011.04.018 [doi].

9. Pignataro G, Simon RP, Xiong ZG. Prolonged activation of ASIC1a and the time window for neuroprotection in cerebral ischaemia. *Brain*. 2007;130(Pt 1):151-158. doi: awl325 [pii].

10. Jasti J, Furukawa H, Gonzales EB, Gouaux E. Structure of acid-sensing ion channel 1 at 1.9 A resolution and low pH. *Nature*. 2007;449(7160):316-323. doi: nature06163 [pii].

11. Gonzales EB, Kawate T, Gouaux E. Pore architecture and ion sites in acid-sensing ion channels and P2X receptors. *Nature*. 2009;460(7255):599-604. doi: 10.1038/nature08218 [doi].

12. Baconguis I, Bohlen CJ, Goehring A, Julius D, Gouaux E. X-ray structure of acid-sensing ion channel 1-snake toxin complex reveals open state of a na(+)-selective channel. *Cell*. 2014;156(4):717-729. doi: 10.1016/j.cell.2014.01.011 [doi].

13. Waldmann R, Champigny G, Voilley N, Lauritzen I, Lazdunski M. The mammalian degenerin MDEG, an amiloride-sensitive cation channel activated by mutations causing neurodegeneration in caenorhabditis elegans. *J Biol Chem*. 1996;271(18):10433-10436.

14. Yu Y, Chen Z, Li WG, et al. A nonproton ligand sensor in the acid-sensing ion channel. *Neuron*. 2010;68(1):61-72. doi: 10.1016/j.neuron.2010.09.001 [doi].

15. Li WG, Yu Y, Zhang ZD, Cao H, Xu TL. ASIC3 channels integrate agmatine and multiple inflammatory signals through the nonproton ligand sensing domain. *Mol Pain*. 2010;6:88-8069-6-88. doi: 10.1186/1744-8069-6-88 [doi].

16. Alijevic O, Kellenberger S. Subtype-specific modulation of acid-sensing ion channel (ASIC) function by 2-guanidine-4-methylquinazoline. *J Biol Chem*. 2012;287(43):36059-36070. doi: 10.1074/jbc.M112.360487 [doi].

17. Li WG, Xu TL. ASIC3 channels in multimodal sensory perception. *ACS Chem Neurosci*. 2011;2(1):26-37. doi: 10.1021/cn100094b [doi].

18. Duan B, Wang YZ, Yang T, et al. Extracellular spermine exacerbates ischemic neuronal injury through sensitization of ASIC1a channels to extracellular acidosis. *J Neurosci*. 2011;31(6):2101-2112. doi: 10.1523/JNEUROSCI.4351-10.2011 [doi].

19. Sherwood TW, Askwith CC. Endogenous arginine-phenylalanine-amide-related peptides alter steady-state desensitization of ASIC1a. *J Biol Chem*. 2008;283(4):1818-1830. doi: M705118200 [pii].

20. Walker JB. Creatine: Biosynthesis, regulation, and function. *Adv Enzymol Relat Areas Mol Biol*. 1979;50:177-242.

21. Smith RN, Agharkar AS, Gonzales EB. A review of creatine supplementation in age-related diseases: More than a supplement for athletes. *F1000Res*. 2014;3:222. doi: 10.12688/f1000research.5218.1 [doi].

22. Zhu S, Li M, Figueroa BE, et al. Prophylactic creatine administration mediates neuroprotection in cerebral ischemia in mice. *J Neurosci*. 2004;24(26):5909-5912. doi: 10.1523/JNEUROSCI.1278-04.2004 [doi].

23. Wilken B, Ramirez JM, Probst I, Richter DW, Hanefeld F. Anoxic ATP depletion in neonatal mice brainstem is prevented by creatine supplementation. *Arch Dis Child Fetal Neonatal Ed*. 2000;82(3):F224-7.

24. Gideon P, Henriksen O, Sperling B, et al. Early time course of N-acetylaspartate, creatine and phosphocreatine, and compounds containing choline in the brain after acute stroke. A proton magnetic resonance spectroscopy study. *Stroke*. 1992;23(11):1566-1572.

25. Gunthorpe MJ, Smith GD, Davis JB, Randall AD. Characterisation of a human acid-sensing ion channel (hASIC1a) endogenously expressed in HEK293 cells. *Pflugers Arch*. 2001;442(5):668-674.

26. Chen X, Grunder S. Permeating protons contribute to tachyphylaxis of the acid-sensing ion channel (ASIC) 1a. *J Physiol*. 2007;579(Pt 3):657-670. doi: jphysiol.2006.120733 [pii].

27. Wyss M, Kaddurah-Daouk R. Creatine and creatinine metabolism. *Physiol Rev*. 2000;80(3):1107-1213.

28. Clark JF. Creatine: A review of its nutritional applications in sport. *Nutrition*. 1998;14(3):322-324. doi: S0899900797004826 [pii].

29. Greenhaff PL, Bodin K, Soderlund K, Hultman E. Effect of oral creatine supplementation on skeletal muscle phosphocreatine resynthesis. *Am J Physiol*. 1994;266(5 Pt 1):E725-30.

30. Persky AM, Brazeau GA. Clinical pharmacology of the dietary supplement creatine monohydrate. *Pharmacol Rev*. 2001;53(2):161-176.

31. Schedel JM, Tanaka H, Kiyonaga A, Shindo M, Schutz Y. Acute creatine ingestion in human: Consequences on serum creatine and creatinine concentrations. *Life Sci*. 1999;65(23):2463-2470. doi: S0024320599005123 [pii].

32. Genius J, Geiger J, Bender A, Moller HJ, Klopstock T, Rujescu D. Creatine protects against excitoxicity in an in vitro model of neurodegeneration. *PLoS One*. 2012;7(2):e30554. doi: 10.1371/journal.pone.0030554 [doi].

33. Almeida LS, Salomons GS, Hogenboom F, Jakobs C, Schoffelmeer ANM. Exocytotic release of creatine in rat brain. *Synapse*. 2006;60:118-123.

34. Li T, Yang Y, Canessa CM. Impact of recovery from desensitization on acid-sensing ion channel-1a (ASIC1a) current and response to high frequency stimulation. *J Biol Chem*. 2012;287(48):40680-40689. doi: M112.418400 [pii].

35. Carter AJ, Muller RE, Pschorn U, Stransky W. Preincubation with creatine enhances levels of creatine phosphate and prevents anoxic damage in rat hippocampal slices. *J Neurochem*. 1995;64(6):2691-2699.

36. Sontheimer H, Perouansky M, Hoppe D, Lux HD, Grantyn R, Kettenmann H. Glial cells of the oligodendrocyte lineage express proton-activated na+ channels. *J Neurosci Res*. 1989;24(4):496-500. doi: 10.1002/jnr.490240406 [doi].

CHAPTER 3

Rat Acid-sensing ion channel 3 is modulated by creatine alone or in combination with NSAIDs

Amruta S. Agharkar[1], Rachel N. Smith[1], Eric B. Gonzales[1]

[1] Center for Neuroscience Discovery, UNT Health Science Center, Fort Worth, TX- 76107

Abbreviated Title: Dietary supplement and NSAID modulation of rASIC3

This work was supported by grants from the American Heart Association (12BGIA8820001), Welch Foundation (BK-1736), UNTHSC Doctoral Bridge Grant, UNTHSC Internal Seed Grants, and startups funds.

*Corresponding Author:

Eric B. Gonzales, Ph.D.

Assistant Professor

Center for Neuroscience Discovery

UNT Health Science Center

3500 Camp Bowie Blvd.

Fort Worth, TX 76107

Email: eric.b.gonzales@unthsc.edu

Phone: 817-735-2755

Fax: 817-735-0408

3.1 ABSTRACT:

Acid-sensing ion channels (ASICs) are sodium channels which are sensitive to extracellular protons. They are expressed in the central and peripheral nervous system. The ASIC3 subtype has been involved in pathophysiological conditions such as pain and epilepsy. A variety of synthetic and endogenous ligands modulate ASIC3 subtype. Most of these ligands have been observed to contain a guanidinium moiety. We tested the effect of a dietary supplement, creatine on rat ASIC3 (rASIC3). Creatine is available over the counter and is used primarily by the fitness community to build lean body mass. Creatine supplementation has also shown beneficial effects in patients suffering from muscular dystrophy, osteoarthritis and fibromyalgia. We hypothesized that creatine will modulate ASIC3. We observed that creatine reduced rASIC3 proton sensitivity in the nominal calcium environment, but didn't alter rASIC3 pH dependence in the presence of calcium. Also, we determined the modulation of rASIC3 by creatine in the presence of established pain medications like NSAIDs. NSAIDs inhibit rASIC3 steady-state current. We observed that 5 mM creatine reduced NSAIDs inhibition of rASIC3. Our data suggests that rASIC3 is modulated by creatine and the simultaneous use of creatine and over the counter medications like NSAIDs should be monitored considering the ASIC3 mediated effects.

3.2 INTRODUCTION:

Acid-sensing ion channels (ASICs) are proton-gated channel which are expressed in brain as well as dorsal root ganglia (DRG)[1-3]. They belong to the epithelial sodium channel/ Degenerin (ENac/DEG) family of ion channels[4] with four different ASIC genes (ASIC1-4) that encode six subunits[1] and not much is known about ASIC5[5-7]. The crystal structure of ASICs shows that the functional channel is a trimer with a large extracellular domain, two transmembrane domains with intracellular amino and carboxyl termini[8-11]. The large extracellular domain of ASICs offers multiple ligand binding sites apart from protons.

ASIC3, also known as DRASIC, is expressed in DRG sensory neurons and is involved in pain perception. It has been shown to play a significant role in acidic and inflammatory pain[12-15]. In inflammatory conditions, reduction in pH causes activation of ASICs[12,13,16]. Under hypoxic conditions, cells produce lactic acid due to anaerobic respiration. The lactic acid chelates extracellular Ca^{2+} and potentiates ASIC3 currents[17]. Previously it has been reported that ASIC3 can be activated by guanidine group containing synthetic ligand 2-guanidine-4-methylquinazoline (GMQ), endogenous agmatine and arcaine[13,18,19]. The residues E79 and E423 in the palm domain have been shown to play an important role in binding of a non proton ligand[18].

Creatine, an endogenous compound containing a guanidine moiety, plays an important role in building muscle mass and is extensively used as a dietary supplement[20]. Creatine has been shown to be beneficial for patients suffering from muscular dystrophy, osteoarthritis and fibromyalgia[21-26]. It improve muscle strength and overall health of patients. Creatine's exact mechanism of action is not known, but it is thought to exert these beneficial effects by improving

energy balance of cell and acting as an instant source of energy in the form of phosphocreatine[22,23,27-29].

Due to these beneficial effects of creatine and ASIC3 involvement in pathologies as well as creatine's structural similarity to other ASIC ligands, we hypothesized that creatine would modulate rASIC3. Furthermore, the commonly used antiinflammatory medicines called as non-steroidal antiinflammatory drugs (NSAIDs) have also been shown to inhibit sustained component of rASIC3 current[30,31]. Both creatine and NSAIDs are widely used and available over the counter. Thus, we sought to determine how creatine and NSAIDs would together modulate ASICs. Although ASICs and the kidney are usually not the focus of research, NSAIDs and creatine may act at ASICs with unknown consequences.

We sought to understand the interaction of creatine with rASIC3, and its effect on the proton sensitivity of the channel. We observed that, creatine modulation of rASIC3 depends on extracellular Ca^{2+} concentrations. Also, creatine was found to reduce the inhibitory effect of NSAIDs on rASIC3. These observed effects indicate the importance of determining the dietary supplement and over the counter medication interactions, which would further help in understanding ASIC3 modulation.

3.3 MATERIALS & METHODS:

3.3.1 Cell line selection and rASIC3 expression: The Chinese Hamster Ovarian (CHO-K1) cells were used to heterologously express rASIC3-pNEH with n-terminal GFP tag (Gift from Dr. Eric Guoaux, Vollum Institute, Portland, OR). CHO-K1 cells do not express ASICs; hence form the ideal cell line for recording heterologously expressed channels. The cells were cultured in Ham's F-12 medium (Life technologies) supplemented with 10% fetal bovine serum and 5% pen-strep and kept in an incubator at 37^0C with 5% CO_2. The CHO-K1 cells were plated at 200,000 cells/ml in 35 mm dish containing cover-slips. Twenty four hours after plating, cells were transfected with Lipofectamine LTX and pNGFP-rASIC3-pNEH cDNA. The green fluorescent cells expressing rASIC3 channels were selected for recording using whole-cell patch-clamp electrophysiology. The recordings were performed 24-48 hours after transfection.

3.3.2 Chemicals: Creatine monohydrate was obtained from Sigma-Aldrich. Creatine test solutions were prepared fresh on the day of recording. The pH and osmolarity of all test solutions was adjusted using N-methyl D-gluconate (NMDG) and sucrose solution, respectively. Diclofenac Sodium and Aspirin were obtained from Sigma-Aldrich.

3.3.3 External and internal (pipette) solutions:

The extracellular solution used for recording consisted of (in mM): NaCl (150), KCl (5), HEPES (5), and MES (5). The $CaCl_2$ (1 mM) was added to extracellular solution on the day of recording. The internal (pipette) solution consisted of (in mM): KCl (100), $MgCl_2$ (5), EGTA (10), HEPES (40), NaCl (5) buffered to pH 7.4. N-methyl D-glucamine and HCl were used to adjust the pH of recording solutions.

3.3.4 Whole-cell patch-clamp electrophysiology: For electrophysiology recordings patch pipettes were pulled from borosilicate glass capillary tubes (Sutter Instruments P97 brown filament puller) and were fire polished to 3-10 MΩ resistance. Patch-clamp recording was performed on an inverted microscope with a computer driven pinch-valve array of perpendicular capillary tubes using an Axopatch 200B amplifier and pCLAMP10 data acquisition and analysis software (Molecular Devices), filtered and sampled at 5 and 10 kHz, respectively. All recordings were performed at room temperature and at a holding potential of -70 mV. Data are presented and analyzed using OriginLab 8.0.

The activation profiles of rASIC3 were generated in 1mM Ca^{2+} (Fig. 1) and the nominal Ca^{2+} environment (Fig. 2). Cells plated on coverslips were placed in an external solution (pH 8.0) and test solution (pH 5.5, 7.0, 6.75, 6.5, 6.25, 6.0 for 1mM Ca^{2+}) and (pH 5.5, 7.8, 7.0, 6.75, 6.5, 6.25, 6.0 for nominal Ca^{2+}) in the absence and presence of creatine (1, 5 and, 10 mM) were applied for 5 seconds with a washout period of one minute between exposures to generate a rASIC3 activation pH-response profile while being normalized to pH 5.5. Each pH-response profile was generated with exposure to control followed by exposures from high pH to low pH. The responding low pH mediated current was normalized to the response observed at pH 5.5. The concentration-dependent effect of diclofenac (1, 10, 100, 300, 500, 1000 µM, Fig. 4) and aspirin (1, 10, 100, 300, 500, 1000 µM, Fig. 5) was recorded at condioning pH 8.0 and activation pH 5.5 with increasing concentrations of NSAIDs. The effect of diclofenac and aspirin in the absence of creatine was assessed in rASIC3 by exposing patch-clamped cells to pH 4.5 at conditioning pH of 8.0 followed by pH 4.5 test solution containing 500 µM diclofenac (Fig. 6) or 500 µM aspirin (Fig. 7) at 1 minute intervals. The washout current was obtained with pH 4.5 solution.The 5 mM

creatine was added in the test solution with 500 µM diclofenac or 500 µM aspirin to determine the creatine's effect.

3.3.5 Data Analysis: Data was analyzed using GraphPad Prism6 and OriginLab 8.0 software. The current elicited in the absence and presence of creatine at test pH was normalized to the maximum peak current amplitude observed with their respective pH solution controls. Two groups were analyzed using the unpaired student t test. Statistical significance was determined for a minimum of four individual cells and is presented as the mean ± SEM.

3.4 RESULTS:

3.4.1 Creatine does not shift activation pH dependence of rASIC3 in the presence of 1 mM Ca^{2+}.

To determine the effect of creatine on the proton dependence of rASIC3 in the presence of 1mM calcium we performed an activation experiment. The reducing pH solutions were applied to patched CHO-K1 cells expressing rASIC3 and conditioning pH of 8.0 was used. A rapid reduction from alkaline conditioning pH solution to activation pH, produces transient inward current. The peak current amplitude of rASIC3 increased with decrease in pH (Fig.1a). Data obtained was normalized to the current generated by application of control pH of 5.5 (Fig.1b). The rASIC3 half-maximal value of activation (activation pH_{50}) was 6.62±0.04 with a Hill coefficient of 1.33±0.21. The effect of 3, 5 and, 10 mM creatine on the pH dependence of rASIC3 was measured. Creatine did not alter the activation pH_{50} and Hill coefficient of rASIC3 significantly. The pH_{50} and Hill coefficient values are summarized in Table 1.

3.4.2 Creatine influences the pH dependence of rASIC3 in the nominal Ca^{2+} environment.

The ASIC activity depends greatly on extracellular Ca^{2+} ion concentration and it is tightly regulated by Ca^{2+}. Hence we sought to determine the effect of creatine in the nominal calcium. In the nominal calcium environment, reducing pH solutions were applied to patched CHO-K1 cells expressing rASIC3 and conditioning pH of 8.0 was used. The reduction in extracellular Ca^{2+} greatly increases the rASIC3 response by shifting the pH dependence of the channel (Fig.2a). The reduced Ca^{2+} increases rASIC3 proton sensitivity evident by shift in pH_{50} to a determined value of 7.38±0.08 with a Hill coefficient of 0.7±0.1 ($n \geq 4$) (Fig. 2c). We determined the effect of 1, 5 and 10 mM creatine on rASIC3 activation profile in the absence of Ca^{2+}. The 5 mM creatine

significantly altered the rASIC3 proton sensitivity (Fig. 2b) and shifted the pH50 to 7.0±0.11 ($n \geq 4$, $p=0.0314$, compared to the control) with a Hill coeffcient of 1.4±0.32 (Fig. 2c) suggesting that 5 mM creatine reduces rASIC3 proton sensitivity in nominal calcium conditions. The 1 and 10 mM did not alter the proton sensitivity of rASIC3 in nominal calcium environment. The pH_{50} and Hill coefficient values are summarized in Table 2. Fig.3 represents the rASIC3 activation pH_{50} changes in extracellular calcium and relative pH_{50} in presence of creatine.

3.4.3 Diclofenac and aspirin inhibit rASIC3 steady state current in concentration-dependent manner.

After we determined the effect of creatine on rASIC3 pH dependence, we sought to determine the effect of diclofenac and aspirin on rASIC3 at conditioning pH 8.0 and activation pH 5.5. The diclofenac concentrations (1, 10, 100, 300, 500, and 1000 µM) and aspirin concentration (1, 10, 100, 300, and 1000 µM) were used to determine concentration dependent effect. Diclofenac (Fig. 4a, 4b) and aspirin (Fig. 5a, 5b) both inhibited steady-state current of rASIC3 in a dose dependent manner. The diclofenac and aspirin are poorly soluble in water and hence the complete inhibition of steady-state ASIC currents was not observed. Since ASIC steady-state currents are more evident at pH 4.5, we performed further experiments with activation pH 4.5.

3.4.4 Diclofenac at 500 µM and activation pH 4.5 inhibits steady-state currents of rASIC3, and 5 mM creatine reduces this effect of diclofenac

After determining the effect of NSAIDs on rASIC3 steady-state current, we sought to determine if 5 mM creatine would increase the inhibitory effect of 500 µM diclofenac. In our previous experiments we observed the concentration-dependent inhibition of steady-state current of

rASIC3 by diclofenac. Hence, we chose a 500 µM concentration of diclofenac to determine the combinatorial effect with 5 mM creatine. We used pH 4.5 solution, since steady-state current elicited by rASIC3 is distinctly observed at this pH. The diclofenac at 500 µM inhibited steady-state current of rASIC3 by about 40% which was significantly different from control ($p = 0.006$) but didn't have any effect on peak current amplitude of the channel (Fig. 6a, 6b.) The 5 mM creatine along with 500 µM diclofenac reduced the inhibitory effect of diclonac but only 9% inhibition was observed which was not significantly different than control ($p = 0.33$) (Fig. 6c, 6d). This result indicated that creatine antagonizes diclofenac's inhibitory effect on rASIC3 steady-state current.

3.4.5 Aspirin at 500 µM inhibits steady-state currents of rASIC3 produced by an activation pH 4.5, and 5 mM creatine reduces this effect of aspirin.

After determining the effect of creatine and diclofenac together, we wanted to determine the effect of aspirin and creatine on rASIC3 steady-state current. The control pH of 4.5 was used. The aspirin at 500 µM inhibited steady-state current of rASIC3 by 45%, which was significantly different than control ($p = 0.0117$) (Fig. 7a, 7b) but didn't have any effect on peak current amplitude of the channel. The 5 mM creatine along with 500 µM aspirin reduced inhibitory effect of aspirin and 23% inhibition was observed, but it was not as robust as we observed with diclofenac. Also, the inhibitory effect of aspirin + 5 mM creatine was significantly different from control ($p = 0.0312$) (Fig. 7c, 7d). This showed that creatine antagonizes aspirin's inhibitory effect on rASIC3steady-state current but not as robustly as diclofenac's inhibitory effect.

Table 1. Summary of rASIC3 activation pH_{50} and Hill coefficients in the presence and absence of creatine at 1mM calcium concentration. Creatine was present in the activating pH test solutions (**Activation**). *Italics* indicate significance.

Activation (1 mM Ca^{2+})

	pH_{50}	**P value**	**Hill, *n***	**P value**
Control	6.62 ± 0.04	-	1.33 ± 0.21	-
Creatine				
+ 1 mM	6.7 ± 0.1	0.4857	1.3 ± 0.3	0.9374
+ 5 mM	6.7 ± 0.1	0.4857	1.51 ± 0.5	0.7512
+ 10 mM	6.74 ± 0.04	0.0781	2.8 ± 0.8	0.1258

Table 2. Summary of rASIC3 activation pH_{50} and Hill coefficients in the presence and absence of creatine in nominal calcium concentration. Creatine was present in the activating pH test solutions (**Activation**). *Italics* indicate significance.

Activation (Nominal Ca^{2+})

	pH_{50}	**P value**	**Hill, *n***	**P value**
Control	7.38 ± 0.08	-	0.7 ± 0.1	-
Creatine				
+ 1 mM	7.57 ± 0.06	0.1062	0.7 ± 0.1	1.0
+ 5 mM	*7.0 ± 0.11**	0.0314	0.64 ± 0.11	0.7005
+ 10 mM	7.28 ± 0.1	0.4646	1.4 ± 0.32	0.0818

*, $p<0.05$

3.5 DISCUSSION:

The purpose of this study was to determine if creatine modulates rASIC3 and the effect of combination of creatine and NSAIDs on rASIC3. We determined the activity of creatine on rASIC3 in the presence of Ca^{2+} and nominal Ca^{2+} environment. Our data suggest that creatine reduces rASIC3 proton sensitivity in the nominal Ca^{2+} environment, but has no effect in the presence of Ca^{2+}. Furthermore, our results indicate that creatine diminishes the inhibitory effects of NSAIDs on rASIC3 sustained current.

Creatine is a guanidinium compound which is similar to synthetic and endogenous ASIC3 modulators such as GMQ, agamtine and arcaine[13,18,19]. Other than guanidinium compounds, NSAIDs like diclofenac and aspirin inhibit sustained component of rASIC3 and act as antinociceptives[30,31]. ASIC3 plays an important role in pathophysiology of pain and inflammation[32-42]. It is primarily expressed in the DRG neurons in the peripheral nervous system and has been shown to be involved in perception of pain[13,43]. Creatine has been shown to be beneficial in mitigating pain associated with fibromyalgia, osteoarthritis and muscular dystrophy[21-23,25,26,44]. Hence it was important to determine the effect of creatine on rASIC3.

ASIC3 current is biphasic with a fast transient inward current and sustained current which is non-desensitizing and persists until the acidic pH is removed[45,46]. The sustained current is important in persistent pain sensation[45-47]. The ASIC3 subtype is also tightly regulated by Ca^{2+}, and Ca^{2+} is required to keep the channel in the closed state[17,48,49].

Since the presence of calcium plays an important role in ASIC3 currents we first wanted to analyze the effect of creatine on rASIC3 activation profile in the presence and absence of Ca^{2+}. Our activation profile studies showed that in the presence of $Ca2^{+}$, creatine failed to affect the pH dependence of rASIC3 at 1, 5, and 10 mM concentrations (Figure 1). This observation

suggested that in presence of $Ca2^{+}$, rASIC3 conformation is not favorable for creatine binding and thus creatine failed to modulate rASIC3 proton sensitivity.

We further determined the rASIC3 activation profile in the nominal Ca^{2+} environment. In ischemia, ASICs cause influx of Ca^{2+} ions and extracellular Ca^{2+} concentration reduces[50]. Furthermore, in inflammatory and ischemic conditions, lactate produced due to anaerobic glycolysis, chelates extracellular Ca^{2+}[17,51], activating rASIC3, leading to pain sensation. In the nominal Ca^{2+} environment, rASIC3 activation profile shifted to alkaline pH value of 7.38±0.08 which is very close to physiological pH (Figure 2 and 3). This observation indicates that, in the nominal Ca^{2+} conditions, channel will conduct even at physiological pH possibly producing pain. In nominal Ca^{2+} conditions, the 5 mM creatine shifted the pH dependence of rASIC3 to acidic pH values indicating the modulatory effect of creatine on rASIC3 proton sensitivity in the absence of $Ca2^{+}$. This observation suggests that, in the absence of Ca^{2+} due to change in channel conformation, creatine is able to influence the channel. Hence, we speculated that creatine might stabilize the closed state of the channel.

Next we analyzed the effect of NSAIDs on rASIC3 currents. Consistent with previous findings, our data indicate that diclofenac and aspirin inhibit rASIC3 sustained currents in a dose dependent manner (Figure 4 and 5). Since creatine has been shown to mitigate the pain associated with various diseased conditions, we investigated whether creatine can potentiate the inhibitory effects of NSAIDs on rASIC3 sustained currents. We analyzed the inhibitory ability of NSAIDs at 500µM concentration. Consistent with our previous results both diclofenac and aspirin inhibited rASIC3 sustained currents. We observed that creatine abolished the inhibitory effects of NSAIDs on sustained currents of rASIC3. These findings were contradictory to our hypothesis. These results indicate that, creatine binds to rASIC3 channel and allosterically

modulates it, which further hinders in the binding of NSAIDs. Hence we speculate that, though creatine doesn't have a direct effect in the presence of calcium, it does modulate the channel allosterically which further changes the sensitivity of rASIC3 to ligands like NSAIDs.

Furthermore, previous studies have shown that in absence of Ca^{2+}, diclofenac shows reduced inhibition of rASIC3 sustained currents. In presence of Ca^{2+} diclofenac also shifts the SSD profile of ASICs to a more alkaline pH, indicating that it stabilizes desensitized sate of the channel[31]. Our results suggest that creatine stabilized the closed conformation of the channels. These observations indicate that the NSAIDs reduced inhibition in the presence of creatine could be due to stabilization of two distinct channel conformations by each of them.

To summarize, the results of this study reveal that modulatory effects of creatine on rASIC3 proton sensitivity depends on extracellular Ca^{2+} concentration and it abolishes the inhibitory effects of NSAIDs possibly because of allosteric modulation of the rASIC3 channel.

3.6 FIGURES AND LEGENDS:

Figure 1. Creatine failed to influence proton sensitivity of rASIC3 in the presence of 1 mM Ca^{2+}.

(a) Representative whole-cell patch-clamp recording current for rASIC3 activation in the presence of 1mM Ca^{2+}. **(b)** Summary of activation profiles of heterologously expressed rASIC3 in CHO-K1cells in the presence of 1mM Ca^{2+}. Switching from conditioning pH 8.0 to increasingly acidic test solutions generated the rASIC3 pH activation profiles. The rASIC3 pH-response profiles for control (black square) had a calculated pH_{50} value of 6.62 ± 0.04 with a Hill coefficient of 1.33 ± 0.21, + 1 mM creatine (green star) had a calculated pH_{50} value of 6.7 ± 0.1 and Hill coefficient of 1.3 ± 0.3, + 5 mM creatine (red circle) had a calculated pH_{50} value of 6.7 ± 0.1 and Hill coefficient of 1.51 ± 0.5, and +10 mM creatine (blue triangle) had a calculated pH_{50} value of 6.74 ± 0.04 with a Hill coefficient of 2.8 ± 0.8. The pH_{50} and Hill coefficient values are summarized in Table 1. Data represented as mean ± SEM ($n \geq 4$).

(a)

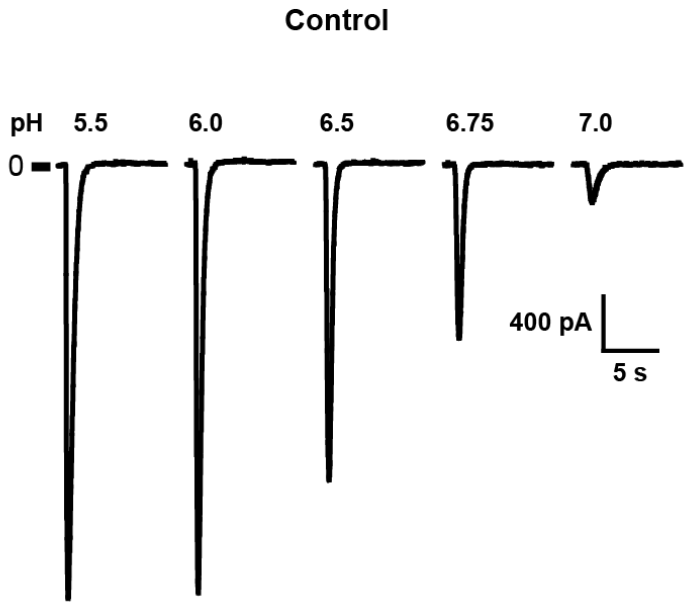
Control
pH 5.5 6.0 6.5 6.75 7.0
0
400 pA
5 s

(b)

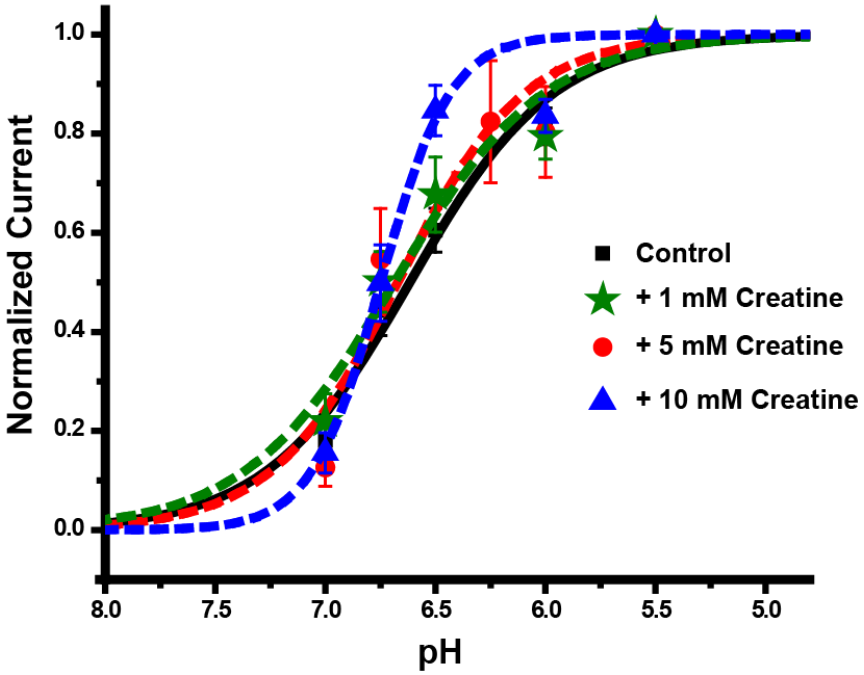
Normalized Current
1.0
0.8
0.6
0.4
0.2
0.0
8.0 7.5 7.0 6.5 6.0 5.5 5.0
pH
Control
+ 1 mM Creatine
+ 5 mM Creatine
+ 10 mM Creatine

Figure 2. Creatine reverses the effects of nominal calcium environment on rASIC3.

(a) Control, **(b)** +5 mM creatine represent whole-cell patch-clamp recording current for rASIC3 activation in nominal Ca^{2+} environment. **(c)** Summary of activation profiles of heterologously expressed rASIC3 in CHO-K1cells in nominal Ca^{2+}. Switching from conditioning pH 8.0 to increasingly acidic test solutions generated the rASIC3 pH activation profiles. The rASIC3 pH-response profiles for control (black square) had a calculated pH_{50} value of 7.38 ± 0.08 with a Hill coefficient of 0.7 ± 0.1, + 1 mM creatine (green star) had a calculated pH_{50} value of 7.57 ± 0.11 and Hill coefficient of 0.7 ± 0.1, + 5 mM creatine (red circle) had a calculated pH_{50} value of 7.0 ± 0.11 ($p = 0.0314$) and Hill coefficient of 0.64 ± 0.11, and +10 mM creatine (blue triangle) had a calculated pH_{50} value of 7.28 ± 0.10 with a Hill coefficient of 1.4 ± 0.32. The pH_{50} and Hill coefficient values are summarized in Table 2. Data represented as mean ± SEM ($n \geq 4$).

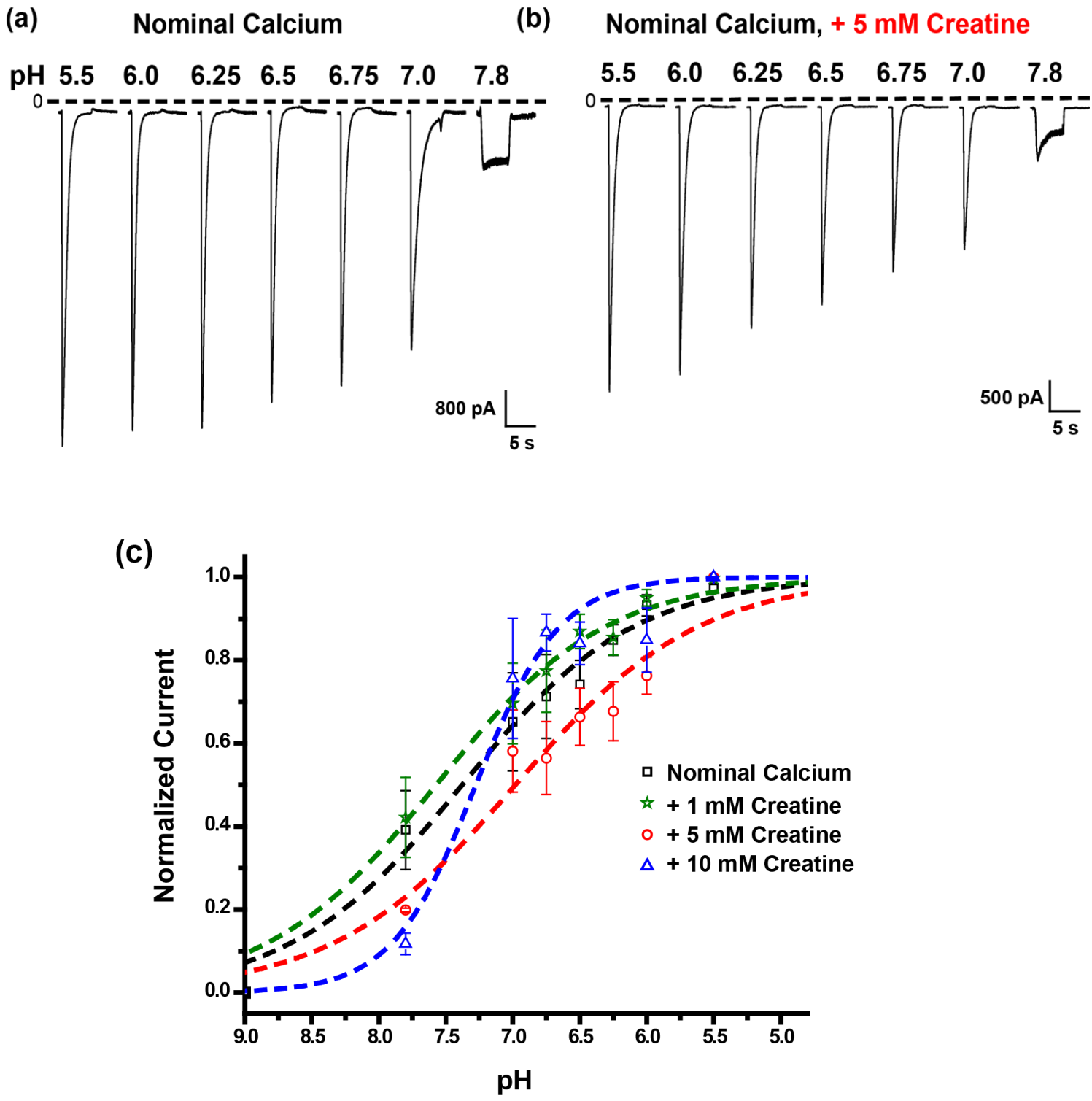
(a)
Nominal Calcium
pH 5.5 6.0 6.25 6.5 6.75 7.0 7.8
0
800 pA
5 s
(b)
Nominal Calcium, + 5 mM Creatine
5.5 6.0 6.25 6.5 6.75 7.0 7.8
0
500 pA
5 s
(c)
Normalized Current
1.0
0.8
0.6
0.4
0.2
0.0
9.0 8.5 8.0 7.5 7.0 6.5 6.0 5.5 5.0
pH
Nominal Calcium
+ 1 mM Creatine
+ 5 mM Creatine
+ 10 mM Creatine

Figure 3. Comparison of rASIC3 activation pH in the absence of calcium.

The calculated rASIC3 pH_{50} values were generated in the absence of calcium for control, 1 mM creatine, 5 mM creatine and 10 mM creatine. Activation pH_{50} were determined in the presence of increasing concentrations of pH (data in Figure 2). The 5 mM creatine significantly reduced the pH_{50} of rASIC3 in nominal Ca^{2+} ($p = 0.0314$). Data represented as mean ± SEM ($n \geq 4$,*$P < 0.05$). For reference, the rASIC3 pH_{50} in the presence of 1 mM calcium is shown (dashed line).

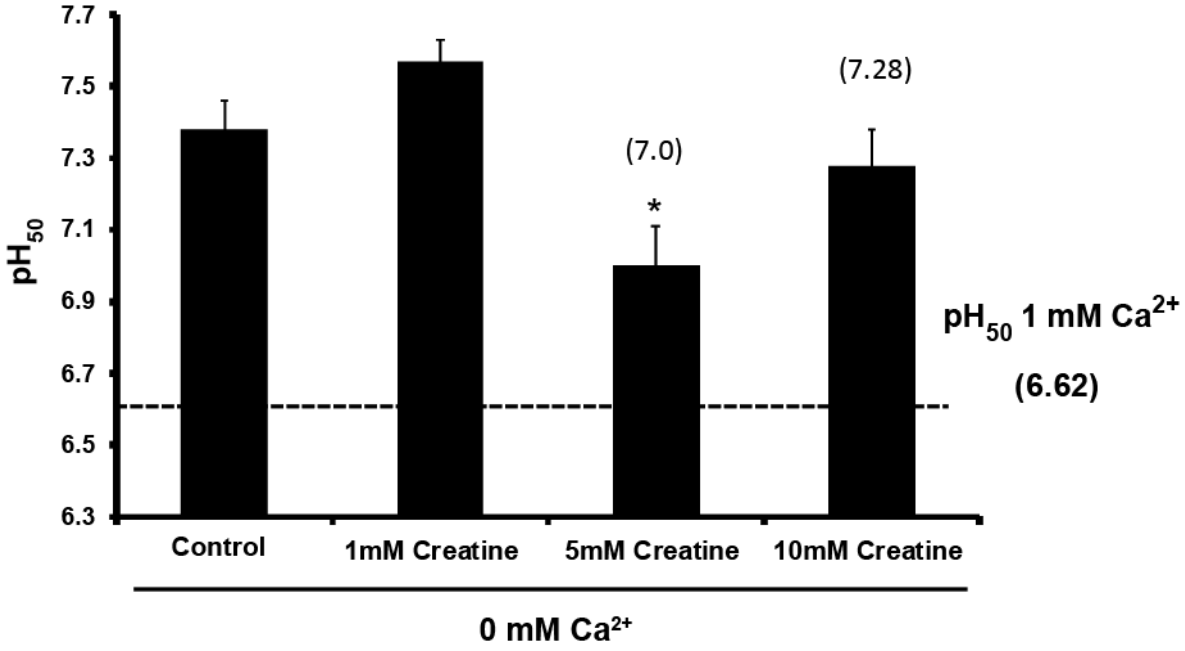
7.7
7.5
7.3
7.1
6.9
6.7
6.5
6.3
pH50
(7.0)
*
(7.28)
pH50 1 mM Ca2+
(6.62)
Control
1mM Creatine
5mM Creatine
10mM Creatine
0 mM Ca2+

Figure 4. Diclofenac inhibits rASIC3 steady-state current in a concentration-dependent manner at activation pH 5.5.

(a) Increasing concentrations of diclofenac were applied to patched rASIC3 expressing cells along with activation pH 5.5. The graph of the percentage response vs Log of concentration was plotted. (b) Represents whole-cell patch-clamp recording current for rASIC3 indicating inhibition of steady-state by increasing diclofenac concentrations.

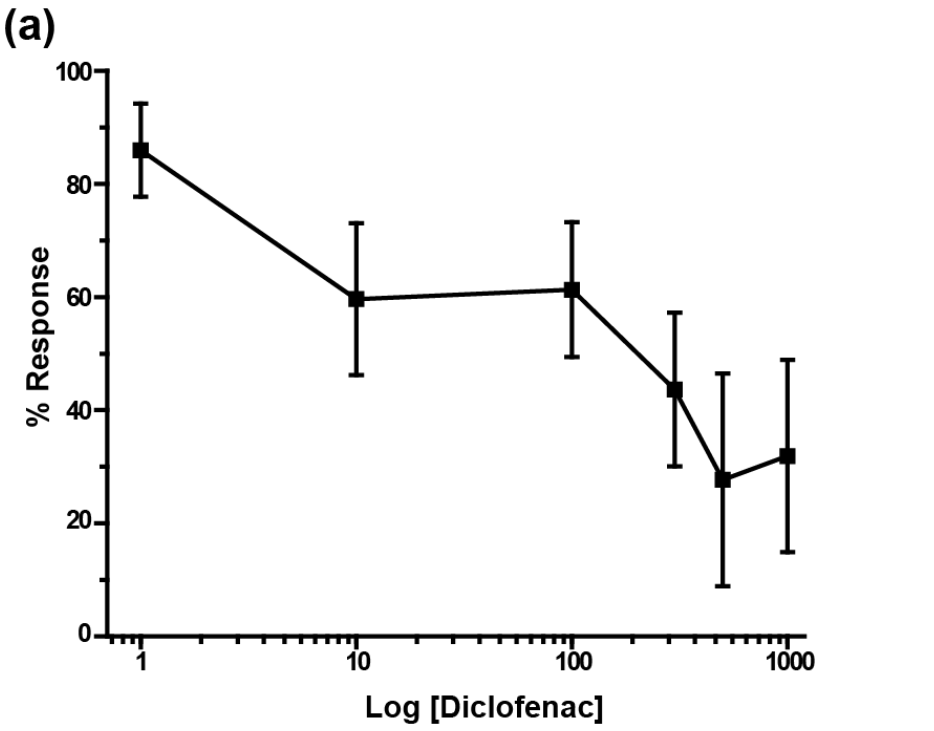
(a)
100
80
60
40
20
0
% Response
1
10
100
1000
Log [Diclofenac]

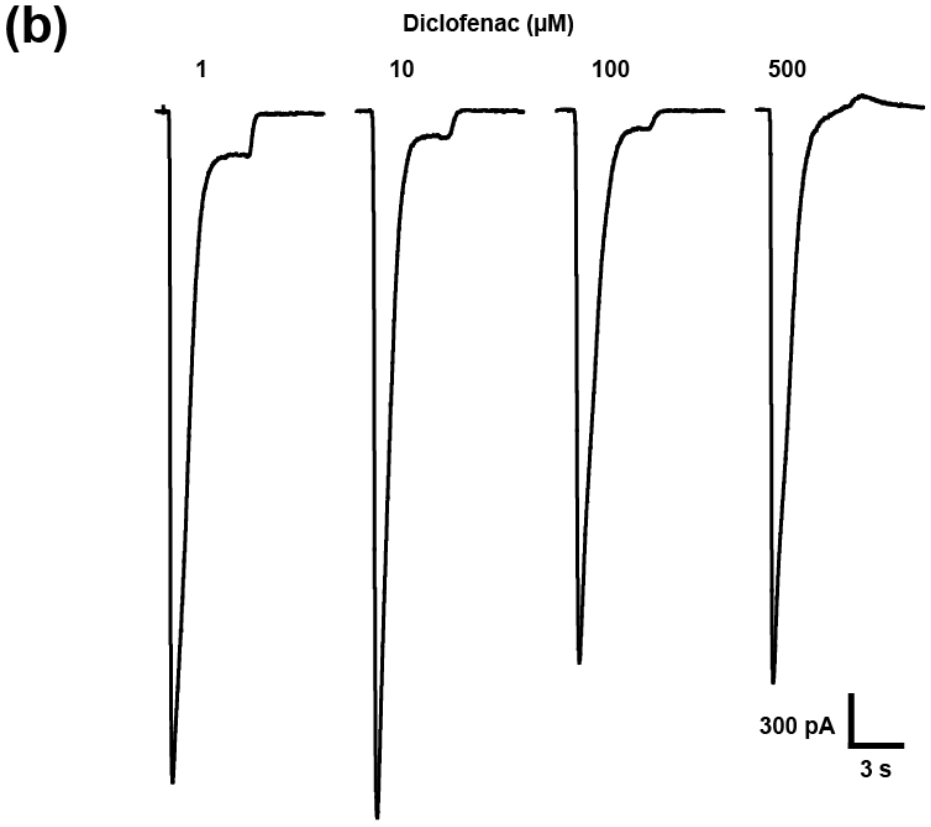
(b)
Diclofenac (μM)
1
10
100
500
300 pA
3 s

Figure 5. Aspirin inhibits rASIC3 steady-state current in concentration-dependent manner at activation pH 5.5.

(a) Increasing concentrations of aspirin were applied to patched rASIC3 expressing cells along with activation pH 5.5. The graph shows the percentage response on Y axis vs. log of concentration on X axis (b) Represents whole-cell patch-clamp recording current for rASIC3 indicating inhibition of steady-state by increasing aspirin concentrations.

(a)

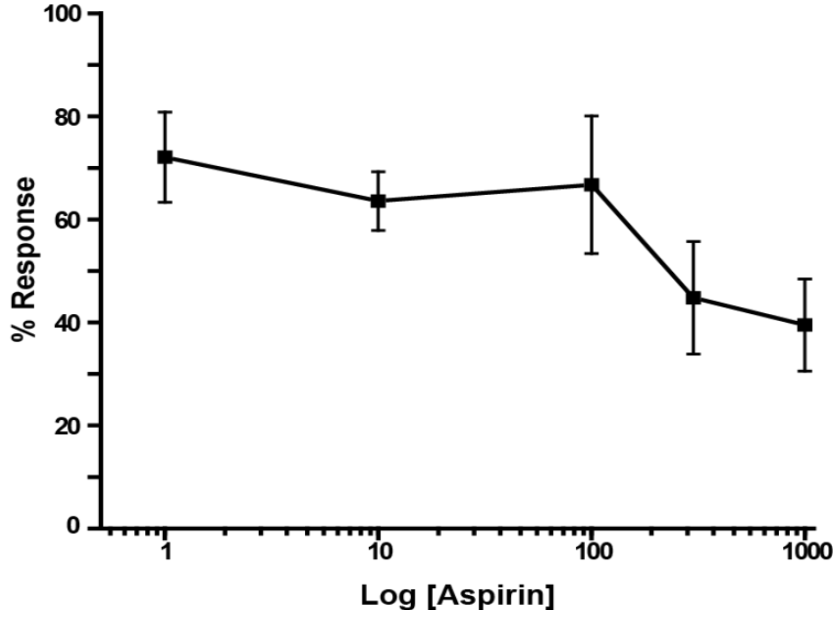
100
80
60
40
20
0
% Response
1
10
100
1000
Log [Aspirin]

(b)

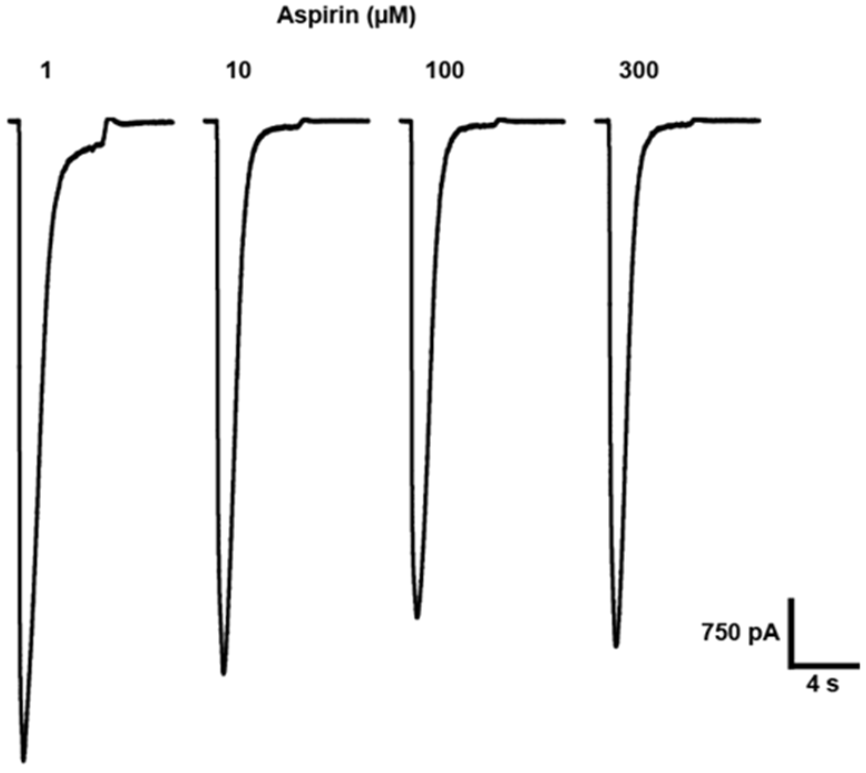
Aspirin (μM)
1
10
100
300
750 pA
4 s

Figure 6. Diclofenac inhibition of rASIC3 steady-state current at activation pH 4.5 in absence and presence of 5 mM creatine

(a) Typical whole-cell patch-clamp recording showing inhibition of rASIC3 steady-state current by 500 µM diclofenac. The 500 µM diclofenac inhibits steady-state current by about 40% (p= 0.006). (**B**) Normalized peak current amplitude of control (pH 4.5), test (pH 4.5 + 500 µM diclofenac), and washout (pH 4.5) with 1 minute between each pulse. Data represented as mean ± SEM (n= ≥ 4, ** p<0.01). **(c)** Typical whole-cell patch-clamp recording showing inhibition of rASIC3 steady-state current by 500 µM diclofenac + 5 mM creatine. The 5 mM creatine reduces steady-state current inhibition by 500 µM diclofenac to about 9% (p = 0.33). (**d**) Normalized peak current amplitude of control (pH 4.5), test (pH 4.5 + 500 µM diclofenac + 5 mM creatine), and washout (pH 4.5) with 1 minute between each pulse. Data represented as mean ± SEM (n= ≥ 4).

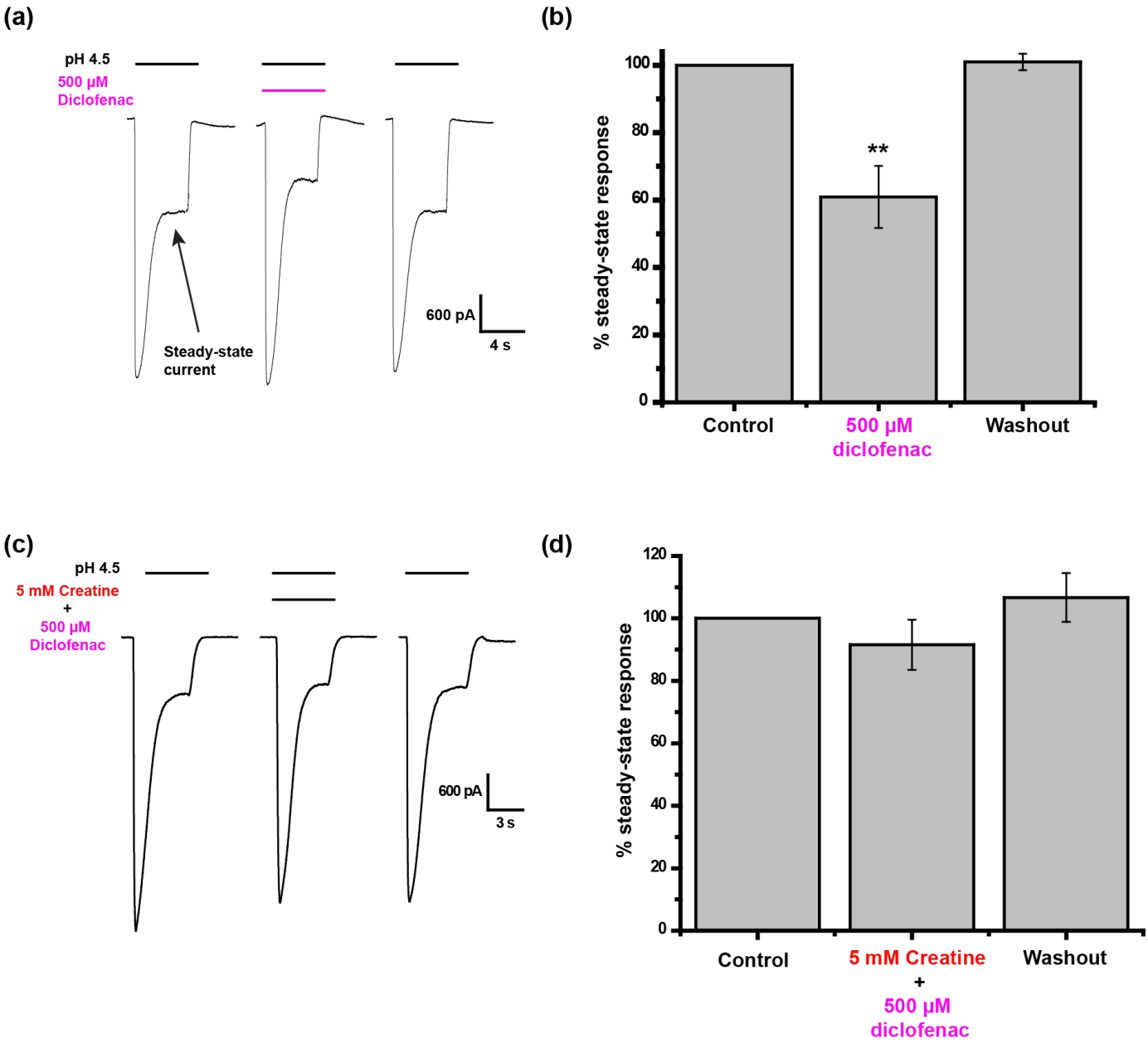
(a)
pH 4.5
500 µM
Diclofenac
Steady-state
current
600 pA
4 s
(b)
% steady-state response
100
80
60
40
20
0
**
Control
500 µM
diclofenac
Washout
(c)
pH 4.5
5 mM Creatine
+
500 µM
Diclofenac
600 pA
3 s
(d)
% steady-state response
120
100
80
60
40
20
0
Control
5 mM Creatine
+
500 µM
diclofenac
Washout

Figure 7. Aspirin inhibition of rASIC3 steady-state current at activation pH 4.5 in absence and presence of 5 mM creatine

(a) Typical whole-cell patch-clamp recording indicating inhibition of rASIC3 steady-state current by 500 µM aspirin. The 500 µM aspirin inhibits steady-state current by about 45% ($p = 0.0117$). (**B**) Normalized peak current amplitude of control (pH 4.5), test (pH 4.5 + 500 µM aspirin), and washout (pH 4.5) with 1 minute between each pulse. Data represented as mean ± SEM ($n = \geq 4$, * $p<0.05$). **(c)** Typical whole-cell patch-clamp recording showing inhibition of rASIC3 steady-state current by 500 µM aspirin + 5 mM creatine. The 5 mM creatine reduces steady-state current inhibition by 500 µM aspirin to about 23% ($p = 0.0312$). **(d)** Normalized peak current amplitude of control (pH 4.5), test (pH 4.5 + 500 µM aspirine + 5 mM creatine), and washout (pH 4.5) with 1 minute between each pulse. Data represented as mean ± SEM ($n = \geq 4$, * $p<0.05$).

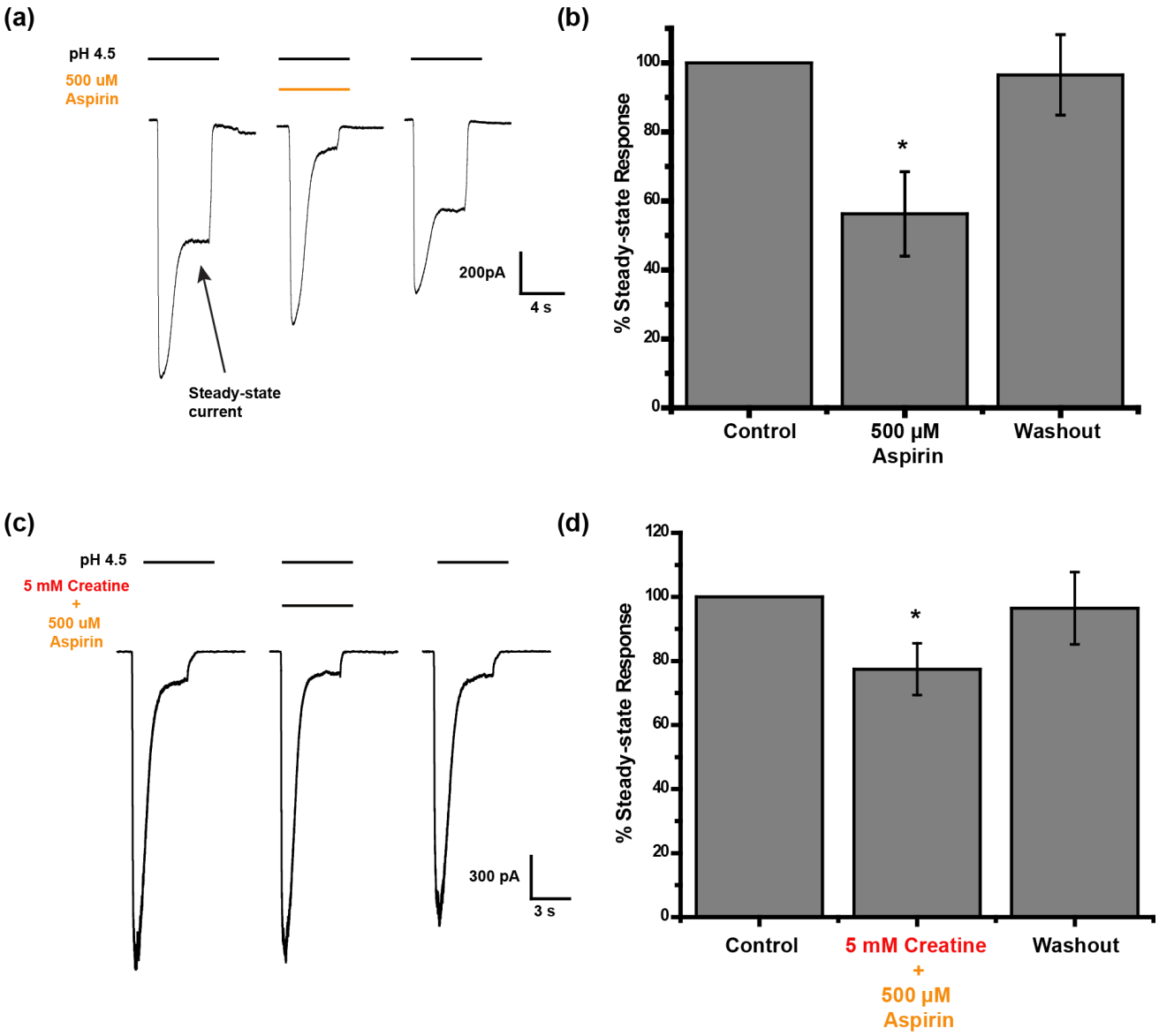
(a)
pH 4.5
500 uM
Aspirin
200pA
4 s
Steady-state
current
(b)
% Steady-state Response
100
80
60
40
20
0
*
Control
500 µM
Aspirin
Washout
(c)
pH 4.5
5 mM Creatine
+
500 uM
Aspirin
300 pA
3 s
(d)
% Steady-state Response
120
100
80
60
40
20
0
*
Control
5 mM Creatine
+
500 µM
Aspirin
Washout

3.7 REFERENCES:

1. Waldmann R, Champigny G, Lingueglia E, De Weille JR, Heurteaux C, Lazdunski M. H(+)-gated cation channels. *Ann N Y Acad Sci*. 1999;868:67-76.

2. Waldmann R, Champigny G, Bassilana F, Heurteaux C, Lazdunski M. A proton-gated cation channel involved in acid-sensing. *Nature*. 1997;386(6621):173-177. doi: 10.1038/386173a0 [doi].

3. Krishtal OA, Pidoplichko VI. A receptor for protons in the membrane of sensory neurons may participate in nociception. *Neuroscience*. 1981;6(12):2599-2601. doi: 0306-4522(81)90105-6 [pii].

4. Kellenberger S, Schild L. Epithelial sodium channel/degenerin family of ion channels: A variety of functions for a shared structure. *Physiol Rev*. 2002;82(3):735-767. doi: 10.1152/physrev.00007.2002 [doi].

5. Boiko N, Kucher V, Wang B, Stockand JD. Restrictive expression of acid-sensing ion channel 5 (asic5) in unipolar brush cells of the vestibulocerebellum. *PLoS One*. 2014;9(3):e91326. doi: 10.1371/journal.pone.0091326 [doi].

6. Sakai H, Lingueglia E, Champigny G, Mattei MG, Lazdunski M. Cloning and functional expression of a novel degenerin-like na+ channel gene in mammals. *J Physiol*. 1999;519 Pt 2:323-333. doi: PHY_9480 [pii].

7. Wiemuth D, Sahin H, Falkenburger BH, Lefevre CM, Wasmuth HE, Grunder S. BASIC--a bile acid-sensitive ion channel highly expressed in bile ducts. *FASEB J*. 2012;26(10):4122-4130. doi: 10.1096/fj.12-207043 [doi].

8. Jasti J, Furukawa H, Gonzales EB, Gouaux E. Structure of acid-sensing ion channel 1 at 1.9 A resolution and low pH. *Nature*. 2007;449(7160):316-323. doi: nature06163 [pii].

9. Gonzales EB, Kawate T, Gouaux E. Pore architecture and ion sites in acid-sensing ion channels and P2X receptors. *Nature*. 2009;460(7255):599-604. doi: 10.1038/nature08218 [doi].

10. Dawson RJ, Benz J, Stohler P, et al. Structure of the acid-sensing ion channel 1 in complex with the gating modifier psalmotoxin 1. *Nat Commun*. 2012;3:936. doi: 10.1038/ncomms1917 [doi].

11. Baconguis I, Bohlen CJ, Goehring A, Julius D, Gouaux E. X-ray structure of acid-sensing ion channel 1-snake toxin complex reveals open state of a na(+)-selective channel. *Cell*. 2014;156(4):717-729. doi: 10.1016/j.cell.2014.01.011 [doi].

12. Deval E, Noel J, Lay N, et al. ASIC3, a sensor of acidic and primary inflammatory pain. *EMBO J*. 2008;27(22):3047-3055. doi: 10.1038/emboj.2008.213 [doi].

13. Li WG, Yu Y, Zhang ZD, Cao H, Xu TL. ASIC3 channels integrate agmatine and multiple inflammatory signals through the nonproton ligand sensing domain. *Mol Pain*. 2010;6:88-8069-6-88. doi: 10.1186/1744-8069-6-88 [doi].

14. Hattori T, Chen J, Harding AM, et al. ASIC2a and ASIC3 heteromultimerize to form pH-sensitive channels in mouse cardiac dorsal root ganglia neurons. *Circ Res*. 2009;105(3):279-286. doi: 10.1161/CIRCRESAHA.109.202036 [doi].

15. Kellenberger S, Schild L. International union of basic and clinical pharmacology. XCI. structure, function, and pharmacology of acid-sensing ion channels and the epithelial na+ channel. *Pharmacol Rev*. 2015;67(1):1-35. doi: 10.1124/pr.114.009225 [doi].

16. Ikeuchi M, Kolker SJ, Burnes LA, Walder RY, Sluka KA. Role of ASIC3 in the primary and secondary hyperalgesia produced by joint inflammation in mice. *Pain*. 2008;137(3):662-669. doi: 10.1016/j.pain.2008.01.020 [doi].

17. Immke DC, McCleskey EW. Lactate enhances the acid-sensing na+ channel on ischemia-sensing neurons. *Nat Neurosci*. 2001;4(9):869-870. doi: 10.1038/nn0901-869 [doi].

18. Yu Y, Chen Z, Li WG, et al. A nonproton ligand sensor in the acid-sensing ion channel. *Neuron*. 2010;68(1):61-72. doi: 10.1016/j.neuron.2010.09.001 [doi].

19. Alijevic O, Kellenberger S. Subtype-specific modulation of acid-sensing ion channel (ASIC) function by 2-guanidine-4-methylquinazoline. *J Biol Chem*. 2012;287(43):36059-36070. doi: 10.1074/jbc.M112.360487 [doi].

20. Walker JB. Creatine: Biosynthesis, regulation, and function. *Adv Enzymol Relat Areas Mol Biol*. 1979;50:177-242.

21. Neves M,Jr, Gualano B, Roschel H, et al. Beneficial effect of creatine supplementation in knee osteoarthritis. *Med Sci Sports Exerc*. 2011;43(8):1538-1543. doi: 10.1249/MSS.0b013e3182118592 [doi].

22. Nabuurs CI, Choe CU, Veltien A, et al. Disturbed energy metabolism and muscular dystrophy caused by pure creatine deficiency are reversible by creatine intake. *J Physiol*. 2013;591(Pt 2):571-592. doi: 10.1113/jphysiol.2012.241760 [doi].

23. Banerjee B, Sharma U, Balasubramanian K, Kalaivani M, Kalra V, Jagannathan NR. Effect of creatine monohydrate in improving cellular energetics and muscle strength in ambulatory duchenne muscular dystrophy patients: A randomized, placebo-controlled 31P MRS study. *Magn Reson Imaging*. 2010;28(5):698-707. doi: 10.1016/j.mri.2010.03.008 [doi].

24. Tarnopolsky MA, Mahoney DJ, Vajsar J, et al. Creatine monohydrate enhances strength and body composition in duchenne muscular dystrophy. *Neurology*. 2004;62(10):1771-1777.

25. Leader A, Amital D, Rubinow A, Amital H. An open-label study adding creatine monohydrate to ongoing medical regimens in patients with the fibromyalgia syndrome. *Ann N Y Acad Sci*. 2009;1173:829-836. doi: 10.1111/j.1749-6632.2009.04811.x [doi].

26. Alves CR, Santiago BM, Lima FR, et al. Creatine supplementation in fibromyalgia: A randomized, double-blind, placebo-controlled trial. *Arthritis Care Res (Hoboken)*. 2013;65(9):1449-1459. doi: 10.1002/acr.22020 [doi].

27. Adhihetty PJ, Beal MF. Creatine and its potential therapeutic value for targeting cellular energy impairment in neurodegenerative diseases. *Neuromolecular Med*. 2008;10(4):275-290. doi: 10.1007/s12017-008-8053-y [doi].

28. Wallimann T, Wyss M, Brdiczka D, Nicolay K, Eppenberger HM. Intracellular compartmentation, structure and function of creatine kinase isoenzymes in tissues with high and fluctuating energy demands: The 'phosphocreatine circuit' for cellular energy homeostasis. *Biochem J*. 1992;281 (Pt 1)(Pt 1):21-40.

29. Brewer GJ, Wallimann TW. Protective effect of the energy precursor creatine against toxicity of glutamate and beta-amyloid in rat hippocampal neurons. *J Neurochem*. 2000;74(5):1968-1978.

30. Voilley N, de Weille J, Mamet J, Lazdunski M. Nonsteroid anti-inflammatory drugs inhibit both the activity and the inflammation-induced expression of acid-sensing ion channels in nociceptors. *J Neurosci*. 2001;21(20):8026-8033. doi: 21/20/8026 [pii].

31. Dorofeeva NA, Barygin OI, Staruschenko A, Bolshakov KV, Magazanik LG. Mechanisms of non-steroid anti-inflammatory drugs action on ASICs expressed in hippocampal interneurons. *J Neurochem*. 2008;106(1):429-441. doi: 10.1111/j.1471-4159.2008.05412.x [doi].

32. Duan B, Wang YZ, Yang T, et al. Extracellular spermine exacerbates ischemic neuronal injury through sensitization of ASIC1a channels to extracellular acidosis. *J Neurosci*. 2011;31(6):2101-2112. doi: 10.1523/JNEUROSCI.4351-10.2011 [doi].

33. Yang ZJ, Ni X, Carter EL, Kibler K, Martin LJ, Koehler RC. Neuroprotective effect of acid-sensing ion channel inhibitor psalmotoxin-1 after hypoxia-ischemia in newborn piglet striatum. *Neurobiol Dis*. 2011;43(2):446-454. doi: 10.1016/j.nbd.2011.04.018 [doi].

34. Xiong ZG, Zhu XM, Chu XP, et al. Neuroprotection in ischemia: Blocking calcium-permeable acid-sensing ion channels. *Cell*. 2004;118(6):687-698. doi: 10.1016/j.cell.2004.08.026 [doi].

35. Sherwood TW, Askwith CC. Dynorphin opioid peptides enhance acid-sensing ion channel 1a activity and acidosis-induced neuronal death. *J Neurosci*. 2009;29(45):14371-14380. doi: 10.1523/JNEUROSCI.2186-09.2009 [doi].

36. Sluka KA, Gregory NS. The dichotomized role for acid sensing ion channels in musculoskeletal pain and inflammation. *Neuropharmacology*. 2015;94:58-63. doi: 10.1016/j.neuropharm.2014.12.013 [doi].

37. Wemmie JA, Taugher RJ, Kreple CJ. Acid-sensing ion channels in pain and disease. *Nat Rev Neurosci*. 2013;14(7):461-471. doi: 10.1038/nrn3529 [doi].

38. Izumi M, Ikeuchi M, Ji Q, Tani T. Local ASIC3 modulates pain and disease progression in a rat model of osteoarthritis. *J Biomed Sci*. 2012;19:77-0127-19-77. doi: 10.1186/1423-0127-19-77 [doi].

39. Diochot S, Baron A, Salinas M, et al. Black mamba venom peptides target acid-sensing ion channels to abolish pain. *Nature*. 2012;490(7421):552-555. doi: 10.1038/nature11494 [doi].

40. Bohlen CJ, Chesler AT, Sharif-Naeini R, et al. A heteromeric texas coral snake toxin targets acid-sensing ion channels to produce pain. *Nature*. 2011;479(7373):410-414. doi: 10.1038/nature10607 [doi].

41. Baron A, Lingueglia E. Pharmacology of acid-sensing ion channels - physiological and therapeutical perspectives. *Neuropharmacology*. 2015;94:19-35. doi: 10.1016/j.neuropharm.2015.01.005 [doi].

42. Wu H, Wang C, Liu B, et al. Altered expression pattern of acid-sensing ion channel isoforms in piriform cortex after seizures. *Mol Neurobiol*. 2015. doi: 10.1007/s12035-015-9130-5 [doi].

43. Li WG, Xu TL. ASIC3 channels in multimodal sensory perception. *ACS Chem Neurosci*. 2011;2(1):26-37. doi: 10.1021/cn100094b [doi].

44. Becque MD, Lochmann JD, Melrose DR. Effects of oral creatine supplementation on muscular strength and body composition. *Med Sci Sports Exerc*. 2000;32(3):654-658.

45. Yagi J, Wenk HN, Naves LA, McCleskey EW. Sustained currents through ASIC3 ion channels at the modest pH changes that occur during myocardial ischemia. *Circ Res*. 2006;99(5):501-509. doi: 01.RES.0000238388.79295.4c [pii].

46. Salinas M, Lazdunski M, Lingueglia E. Structural elements for the generation of sustained currents by the acid pain sensor ASIC3. *J Biol Chem*. 2009;284(46):31851-31859. doi: 10.1074/jbc.M109.043984 [doi].

47. de Weille JR, Bassilana F, Lazdunski M, Waldmann R. Identification, functional expression and chromosomal localisation of a sustained human proton-gated cation channel. *FEBS Lett*. 1998;433(3):257-260. doi: S0014-5793(98)00916-8 [pii].

48. Immke DC, McCleskey EW. Protons open acid-sensing ion channels by catalyzing relief of Ca2+ blockade. *Neuron*. 2003;37(1):75-84. doi: S0896627302011303 [pii].

49. Zhang P, Sigworth FJ, Canessa CM. Gating of acid-sensitive ion channel-1: Release of Ca2+ block vs. allosteric mechanism. *J Gen Physiol*. 2006;127(2):109-117. doi: jgp.200509396 [pii].

50. Yermolaieva O, Leonard AS, Schnizler MK, Abboud FM, Welsh MJ. Extracellular acidosis increases neuronal cell calcium by activating acid-sensing ion channel 1a. *Proc Natl Acad Sci U S A*. 2004;101(17):6752-6757. doi: 10.1073/pnas.0308636100 [doi].

51. Andersen LW, Mackenhauer J, Roberts JC, Berg KM, Cocchi MN, Donnino MW. Etiology and therapeutic approach to elevated lactate. *Mayo Clin Proc*. 2013;88(10):1127-1140. doi: 10.1016/j.mayocp.2013.06.012 [doi].

CHAPTER 4

General Discussion

Dietary supplements, or nutraceuticals are over the counter products that are available to supplement the diet. They include vitamins, minerals, amino acids, fish oil and a variety of synthetic and natural products[1]. Creatine is an endogenous compound and a dietary supplement. Along with muscle building, it has also been shown to be beneficial as a prophylactic *in vivo* model of ischemic stroke and has been shown to protect from excitotoxicity *in vitro*[2-5]. Creatine is generally considered as safe dietary supplement. The ASIC1a subtype previously has been shown to worsen the symptoms of ischemic stroke by allowing the influx of Na^+ and Ca^{2+} ions[6,7]. A variety of ligands have been shown to modulate ASIC1a activity. The ASIC1a inhibitor psalmotoxin-1 reduces the damage in ischemia due to hypoxia[7]. Spermine, which is a polyamine, that activates ASIC1a, has been shown to worsen ischemic stroke[8]. Pharmacological inhibition of ASIC1a or knockdown of ASIC1a expression has been shown to protect from ischemic stroke.Our results indicate that creatine modulates ASIC1a activity by affecting channel desensitization and proton sensitivity.

The ASIC3 subtype is involved in a perception of pain sensation and is expressed in DRG neurons in PNS[9-11]. It primarily senses acidic and inflammatory pain[10]. Inflammatory mediators can also modulate ASICs and contribute to pain sensation[12,1314,15]. The exact mechanism of creatine's effects on ASIC3 has not been characterized. The canonical NSAIDs inhibit cyclooxygenase enzyme along with ASICs to lessen the pain sensation[14,15]. Creatine has been shown to mitigate the pain and inflammation associated with various disorders[16-19]. Whether this action is mediated through ASIC3 remains unknown. There is a possibility that a significant amount of the population takes creatine and NSAIDs together since both are available over-the counter. NSAIDs may contribute to kidney issues as well as creatine can worsen the kidney damage. Combined use of both NSAIDs and creatine may be problematic, but hypothesis-driven research has not been done to confirm anecdotal concerns. Thus, combined use of these two compounds leading to a loss in kidney function is speculative at best. Though this interaction is not ASIC mediated, NSAIDs and creatine may modulate ASIC3 with unknown consequences. The findings of our study reveal that creatine alters the proton sensitivity of rASIC3 under nominal Ca^{2+} conditions and reduces the inhibitory effects of NSAIDs suggesting that, there might be a potential interaction between NSAIDs and creatine which needs to be investigated further.

Modulation of ASIC1a by creatine

The first part of the present study investigated the interaction of creatine with hASIC1a to determine if creatine could modulate the channel. Because of creatine's neuroprotective effects, we hypothesized that creatine inhibits hASIC1a channel by reducing the proton sensitivity of hASIC1a. The conditioning pH of 8.0 was used for all experiments, so that all ASIC channels

were in closed state. The activation profile analysis suggested that, creatine at 5 and 10 mM shifts the pH dependence of hASIC1a to lower pH values and thus reduces proton sensitivity of hASIC1a when desensitization is not introduced in the channel (Chapter 2, Fig.2). This denotes that, in the presence of creatine, a reduction in hASIC1a current will be observed and lower pH will be required to activate the channels thus indicating reduction in their proton sensitivity. This could play some role in ischemic stroke when the reduction in external pH leads to activation of ASICs causing Na^+ and Ca^{2+} influx.

Along with the effect on activation of channels, creatine at higher concentration of 10 mM shifted the pH dependence of steady-state desensitization (SSD) of hASIC1a to lower pH values (Chapter 2, Fig.3) . But we did not observe any effect on SSD at 5 mM creatine. The SSD gives the number of channels that are available for opening after exposure to acidic pH. The shift in SSD to lower pH values suggests that creatine increases the availability of channels for opening and recovers hASIC1a from desensitization. The observed recovery could be due to the increase in the number of closed channels. We speculate that creatine may have an affinity for the desensitized state of the hASIC1a channels and shifts them to closed state, thus making them available for opening. Creatine at 10 mM shifted the SSD profile of hASIC1a to acidic pH values indicating that, at higher concentration of creatine, more number of ASIC1a will be available for opening. However, creatine at 5 mM did not alter the SSD profile of ASICs. Hence monitoring the use of dietary supplements is important. This argument can be supported by a study which showed that prophylactic creatine supplementation was neuroprotective in a mouse model of ischemic stroke but creatine administered after stroke failed to show neuroprotection[20]. From these results we can speculate that, clinically, creatine might be effective as a prophylactic agent in ischemic stroke when brain pH is neutral. After ischemic events, brain pH is lowered, and

most of the ASIC1a are in desensitized state. Creatine administered post ischemic stroke can increase the activation from desensitization and in turn the ASIC1a availability for opening leading to higher influx of Na^+ and Ca^{2+} ions.

Previously, it has been shown that GMQ shifts the pH dependence of ASIC1a to more acidic value and GMQ binding site in hASIC1a might be accessible in desensitized state and thus, GMQ is able to bind the desensitized channel[21]. Similarly, creatine may have an affinity for the desensitized channel and is able to stabilize the channels to a closed state, making them available for further acid stimulation. The peptides like RF-amide, FMRF-amide, and dynorphins have been shown to modulate ASIC1a desensitization by shifting the ASIC1a desensitization curve to lower pH values and in turn increase the recovery from desensitization[21-25]. The β sheets 11-12 linker of ASIC1a in palm domain is important in desensitization and modulation of ASICs by peptides[26]. Similarly, we show that creatine has an affnity for desensitized channel and stabilizes closed conformation of hASIC1a.

The effect of creatine on hASIC1a efficacy was also studied where test pulse was bracketed with control activation pH 5.0 to compensate for desensitization. The 5 mM creatine did not increase efficacy of hASIC1a but 10 mM creatine increased hASIC1a efficacy by about 40% (Chapter 2, Fig.4) . This suggested that 10 mM creatine is able to recover desensitized channels. Hence clinically, in case of persistent acidification, creatine at higher concentration is able to rescue the channels from desensitization. This phenomenon is important in ischemic state where constant low pH can desensitize the channels and presence of creatine can rescue them worsening the damage. Thus we speculate that, at higher concentrations, creatine can have deleterious consequences in ischemic diseased state.

The other aspect we looked at is the open-state desensitization of hASIC1a. The 5 and 10 mM creatine applied along with a pH 6.0 lead to difference in channel desensitization kinetics. Creatine slowed down the open-state desensitization kinetics of hASIC1a (Chapter 2, Fig.5). Hence, creatine reduces the number of channels in desensitized state and further contributes to the modulation of desensitization and proton sensitivity of hASIC1a. This indicates that, at higher concentration, creatine can have serious side effects. This effect is similar to one observed with spermine. Spermine delays the open-state desensitization and contributes to neuronal damage after ischemia[8,25]. The diarylamides significantly facilitate the ASIC1a open-state desensitization, which indicates their potential use as neuroprotectives[27].

The desensitization of hASIC1a causes tachyphylaxis that is indicated by a reduction in current after repeated exposure to low pH solution. The Cl^- ions have been shown to facilitate tachyphylaxis of hASIC1a[28]. Ligands like spermine and dynorphins shift steady-state desensitization curve to acidic pH and reduce desensitization at acidic conditioning pH of 7.2 and, in turn, increase neuronal injury after ischemia[8,25]. Hence, we determined the effect of creatine on desensitization at varying conditioning pH of 8.0, 7.4 and 7.2. At conditioning pH 8.0, creatine at 5 and 10 mM didn't have any effect on hASIC1a desensitization. But at conditioning pH of 7.4 and 7.2, creatine reduced desensitization (Chapter 2, Fig. 6). At conditioning pH 7.4 and 7.2, most channels are in desensitized state. When activated with low pH solution with creatine, we speculate that creatine binds to the desensitized channels and it pushes the channels to the closed state by stabilizing the closed conformation. This makes more channels available for opening after repeated exposure to low pH solution and attenuates desensitization. The conditioning pH 7.4 and 7.2 also mimic the physiological state in case of diseased states like ischemia where local pH is reduced[6]. The tachyphylaxis reversal effect of

creatine was observed at 5 and 10 mM creatine concentration at conditioning pH 7.2. According to Chen and Grunder, tachyphylaxis depends on the binding of protons to the channel[29] .The hASIC1a channel can have short lived or long lived desensitized state depending on how much protons bind[30]. Creatine may have an effect on proton binding of the channel and hence reverses tachyphylaxis.

The hASIC1a subtype, when activated, undergoes two desensitization states, short-lived (τ = 0.5 s) and long lived (τ = 229 s)[30]. These states can influence the recovery of channels for further stimulation by acid. Ideally, the compound for neuroprotection should increase the channels in the long-lived desensitized state so that fewer number of channels will be available for opening after acid stimulation. The ASIC1a ligand PcTx-1 has more affinity for the open and desensitized states of the channel and shifts the SSD curve of ASIC1a to a more alkaline pH to increase its proton sensitivity and thus contributing to neuroprotection[7,31,32].

From our results, it is clear that, creatine has an affinity for the desensitized state of hASIC1a and stabilizes the closed conformation (Chapter 4, Fig. 1). This increases number of hASIC1a channels in closed state that can be opened by the low pH solution. Thus, we speculate that, clinically, creatine may have some beneficial effects when administered as a prophylactic. If creatine is given post ischemic stroke (where brain pH decreases significantly), we anticipate that it may reactivate desensitized ASICs and increase influx of N^{a+} and Ca^{2+} ions further leading to neuronal death.

Modulation of ASIC3 by creatine

Once we tested the effect of hASIC1a, we sought to determine its effect on rASIC3. The ASIC3 subtype is primarily expressed in the PNS and is expressed in Aβ fibers in sensory nerve

endings that innervate the skin, heart and visceral organs[33-37]. ASIC3 has been shown to play an important role in acidic and inflammatory pain[10]. rASIC3 is modulated by Ca^{2+} and extracellular concentration of Ca^{2+} plays an important role in maintaining ASIC3 in the closed conformational state[38-41]. Also, inflammation reduces the extracellular Ca^{2+} concentration that can activate ASICs. Hence we wanted to determine the effect of creatine in the nominal Ca^{2+} environment to mimic physiological conditions.

Our results indicated that creatine, while in the presence of Ca^{2+}, did not shift the pH dependence of rASIC3 at 1, 5, and 10 mM concentrations (Chapter 3 , Fig.1). In nominal Ca^{2+} , the activation profile of rASIC3 shifted to higher pH values, suggesting that in low Ca^{2+} environment channels are open even at physiological pH (Chapter 3 , Fig.2). At 5 mM concentration, creatine shifted the rASIC3 activation profile to acidic pH values, and influences the proton sensitivity of the channel in the absence of Ca^{2+} (Chapter 3 , Fig.2). The increase in Ca^{2+} ions extracellularly shifts the activation profile ASICs to acidic pH values indicating that Ca^{2+} stabilizes the closed state of the channel[42]. Hence we speculated that creatine may stabilize the closed state of the rASIC3 channel.

NSAIDs including aspirin and diclofenac, are known to inhibit the cyclooxygenase enzyme[14,15]. Also, they have been shown to inhibit ASIC3 sustained current. Our results were consistent with previous findings that, diclofenac and aspirin inhibit the rASIC3 sustained current (Chapter 3 , Fig.4 and Fig. 5). Since, both NSAIDs and creatine mitigate pain and inflammation[16-19], we investigated their combined effect on rASIC3. Creatine (5 mM) reduced the inhibitory effect of diclofenac and aspirin on rASIC3 sustained current (Chapter 3 , Fig.6 and Fig.7). This observation suggests that creatine antagonized the NSAIDs effect. Creatine may bind to ASICs and cause conformational changes which can further modulate NSAIDs activity.

Since we didn't see the effect of creatine on proton sensitivity in the presence of Ca^{2+} , we speculate that creatine reduction of the inhibitory effect NSAIDs could be due to allosteric modulation of channel.

Diclofenac has been shown to inhibit ASICs non-competitively by inhibitng the open channel[15]. Diclofenac also shifted the SSD curve for ASICs to higher pH values, suggesting that diclofenac favors the desensitized state and shifts channels to the desensitized conformation[15].The diclofenac inhibitory effect was reducd in low Ca^{2+} conditions. Our activation curve data in the nominal Ca^{2+} suggest that creatine may stabilize the closed conformation. Also, it is known that Ca^{2+} stabilizes the closed state of the ASIC3 channel[39,40]. Thus we speculated that, inhibition of diclofenac effect by creatine could be due to stabilization of possibly two different states. Since the binding sites for NSAIDs and creatine are not known the exact mechanism still remains elusive. Determination of the combinatorial effect would be an important finding since both creatine and NSAIDs are available over the counter and significant amount of the population may consume these drugs and supplement concomitantly. The National Center for Complimentary and Integrative Health has described the drug-supplement interactions along with reduced or increased effectiveness, side effect of drugs[43]. Thus, it is important to let a healthcare provider know about the dietary supplements being consumed to avoid unwanted effects.

Taken together, our results indicate that creatine alters the hASIC1a and rASIC3 desensitization and proton sensitivity, respectively. While the effect of creatine on hASIC1a is concentration dependent, its effect on rASIC3 is influenced by the presence of Ca^{2+}. Furthermore, (a) creatine increases the efficacy of hASIC1a and (b) reduces the efficacy of NSAIDs on rASIC3. Thus, in conclusion, if we consider the role of ASICs in ischemic stroke

and pain, the use of creatine as a dietary supplement should be monitored in these diseased states and when used in combination with other over the counter medications.

4.1 Future directions

The findings of this study have revealed aspects of ASIC modulation by the dietary supplement creatine. In the future, the experiments could be performed on neuronal cell line to determine the effects of creatine on endegenously expressed ASICs and ASIC heteromers. Furthermore, this study would reveal the effects of these channels on the overall activity of neurons (e.g., action potential generation and the resting membrane potential). The experiments can be performed in an *in vivo* ischemic model to determine the effect of creatine.

It has been found that the extracellular Ca^{2+} concentration reduces from 1.2 mM to 0.1 mM in focal ischemia due to Ca^{2+} influx into the cell[44]. Since Ca^{2+} is the key factor in ASIC modulation, as well as in many of the diseased states, further experiments should be done to explore creatine's effects in variable Ca^{2+} concentrations.

We showed that creatine primarily modulates desensitization of hASIC1a. Mutating the conserved residues in ASICs that regulate channel desensitization[45] will further delineate creatine's effect.

Since the binding sites for creatine and NSAIDs are not known, determining the binding site would predict their possible interactions. To further understand the effects of creatine on ASICs, determining the effect of creatine in ASIC3 knockout mice and understanding the effectiveness of NSAIDs in presence of creatine *in vivo* would further delineate the ASIC and creatine interactions.

Figures and Legends

Fig. 1. Proposed mechanism of hASIC1a modulation by creatine.

(a) Creatine stabilizes the closed conformation of hASIC1a and reduces the steady-state desensitization. **(b)** Increased availability of hASIC1a in closed state leads to the proton mediated opening of channels. **(C)** Creatine slows-down the open-state desensitization.

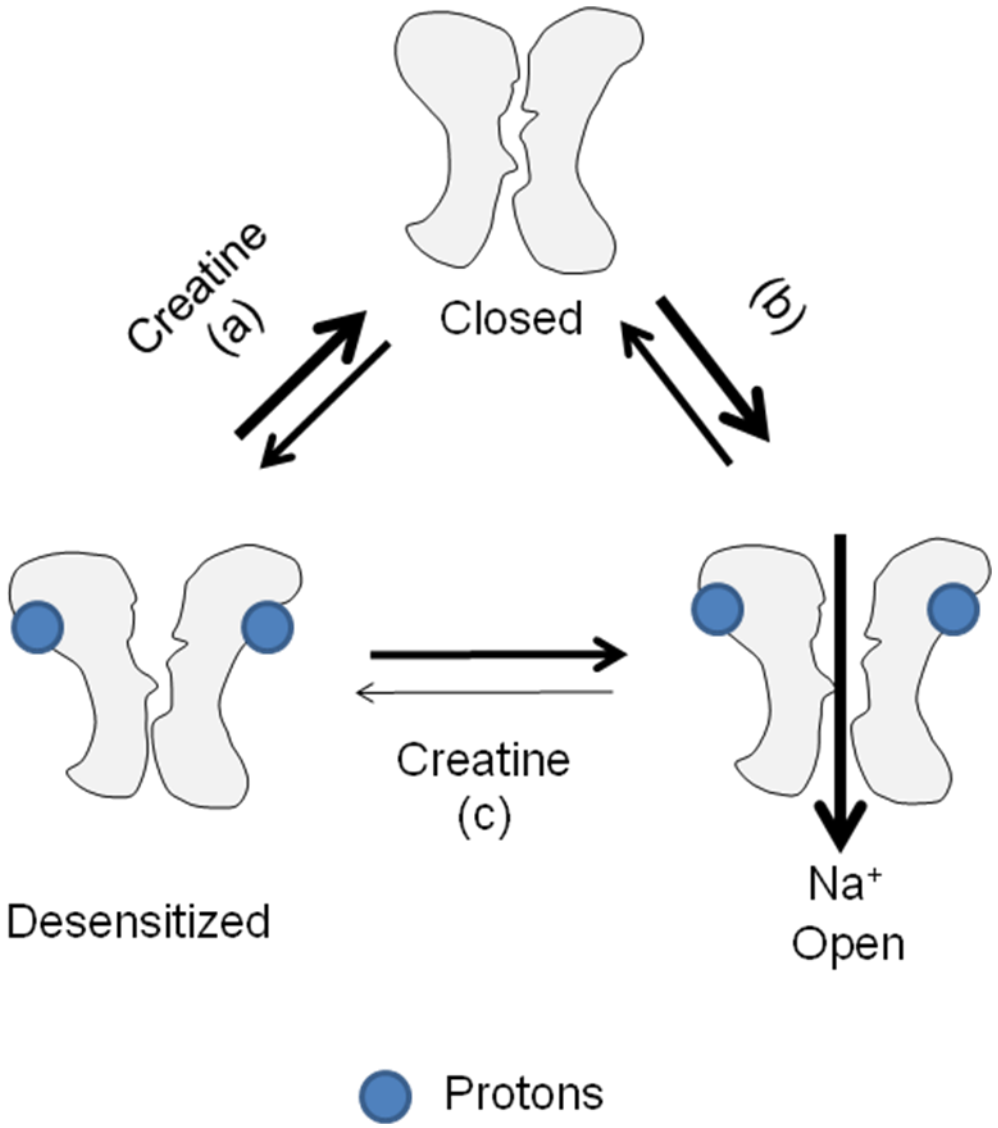
Creatine
(a)
Closed
(b)
Creatine
(c)
Desensitized
Na+
Open
Protons

4.2 References

1. National Center for Complementary and Integrative Health (NCCIH). Using dietary supplements wisely. https://nccih.nih.gov/health/supplements/wiseuse.htm. Updated July, 08 2015.

2. Zhu S, Li M, Figueroa BE, et al. Prophylactic creatine administration mediates neuroprotection in cerebral ischemia in mice. *J Neurosci*. 2004;24(26):5909-5912. doi: 10.1523/JNEUROSCI.1278-04.2004 [doi].

3. Otellin VA, Korzhevskii DE, Kostkin VB, Balestrino M, Lensman MV, Polenov SA. The neuroprotective effect of creatine in rats with cerebral ischemia. *Dokl Biol Sci*. 2003;390:197-199.

4. Adcock KH, Nedelcu J, Loenneker T, Martin E, Wallimann T, Wagner BP. Neuroprotection of creatine supplementation in neonatal rats with transient cerebral hypoxia-ischemia. *Dev Neurosci*. 2002;24(5):382-388. doi: 69043 [doi].

5. Genius J, Geiger J, Bender A, Moller HJ, Klopstock T, Rujescu D. Creatine protects against excitoxicity in an in vitro model of neurodegeneration. *PLoS One*. 2012;7(2):e30554. doi: 10.1371/journal.pone.0030554 [doi].

6. Xiong ZG, Zhu XM, Chu XP, et al. Neuroprotection in ischemia: Blocking calcium-permeable acid-sensing ion channels. *Cell*. 2004;118(6):687-698. doi: 10.1016/j.cell.2004.08.026 [doi].

7. Yang ZJ, Ni X, Carter EL, Kibler K, Martin LJ, Koehler RC. Neuroprotective effect of acid-sensing ion channel inhibitor psalmotoxin-1 after hypoxia-ischemia in newborn piglet striatum. *Neurobiol Dis*. 2011;43(2):446-454. doi: 10.1016/j.nbd.2011.04.018 [doi].

8. Duan B, Wang YZ, Yang T, et al. Extracellular spermine exacerbates ischemic neuronal injury through sensitization of ASIC1a channels to extracellular acidosis. *J Neurosci*. 2011;31(6):2101-2112. doi: 10.1523/JNEUROSCI.4351-10.2011 [doi].

9. Lingueglia E, de Weille JR, Bassilana F, et al. A modulatory subunit of acid sensing ion channels in brain and dorsal root ganglion cells. *J Biol Chem*. 1997;272(47):29778-29783.

10. Deval E, Noel J, Lay N, et al. ASIC3, a sensor of acidic and primary inflammatory pain. *EMBO J*. 2008;27(22):3047-3055. doi: 10.1038/emboj.2008.213 [doi].

11. Yagi J, Wenk HN, Naves LA, McCleskey EW. Sustained currents through ASIC3 ion channels at the modest pH changes that occur during myocardial ischemia. *Circ Res*. 2006;99(5):501-509. doi: 01.RES.0000238388.79295.4c [pii].

12. Li WG, Yu Y, Zhang ZD, Cao H, Xu TL. ASIC3 channels integrate agmatine and multiple inflammatory signals through the nonproton ligand sensing domain. *Mol Pain*. 2010;6:88-8069-6-88. doi: 10.1186/1744-8069-6-88 [doi].

13. Duan B, Wu LJ, Yu YQ, et al. Upregulation of acid-sensing ion channel ASIC1a in spinal dorsal horn neurons contributes to inflammatory pain hypersensitivity. *J Neurosci*. 2007;27(41):11139-11148. doi: 27/41/11139 [pii].

14. Voilley N, de Weille J, Mamet J, Lazdunski M. Nonsteroid anti-inflammatory drugs inhibit both the activity and the inflammation-induced expression of acid-sensing ion channels in nociceptors. *J Neurosci*. 2001;21(20):8026-8033. doi: 21/20/8026 [pii].

15. Dorofeeva NA, Barygin OI, Staruschenko A, Bolshakov KV, Magazanik LG. Mechanisms of non-steroid anti-inflammatory drugs action on ASICs expressed in hippocampal interneurons. *J Neurochem*. 2008;106(1):429-441. doi: 10.1111/j.1471-4159.2008.05412.x [doi].

16. Leader A, Amital D, Rubinow A, Amital H. An open-label study adding creatine monohydrate to ongoing medical regimens in patients with the fibromyalgia syndrome. *Ann N Y Acad Sci*. 2009;1173:829-836. doi: 10.1111/j.1749-6632.2009.04811.x [doi].

17. Neves M,Jr, Gualano B, Roschel H, et al. Beneficial effect of creatine supplementation in knee osteoarthritis. *Med Sci Sports Exerc*. 2011;43(8):1538-1543. doi: 10.1249/MSS.0b013e3182118592 [doi].

18. Alves CR, Santiago BM, Lima FR, et al. Creatine supplementation in fibromyalgia: A randomized, double-blind, placebo-controlled trial. *Arthritis Care Res (Hoboken)*. 2013;65(9):1449-1459. doi: 10.1002/acr.22020 [doi].

19. Nomura A, Zhang M, Sakamoto T, et al. Anti-inflammatory activity of creatine supplementation in endothelial cells in vitro. *Br J Pharmacol*. 2003;139(4):715-720. doi: 10.1038/sj.bjp.0705316 [doi].

20. Prass K, Royl G, Lindauer U, et al. Improved reperfusion and neuroprotection by creatine in a mouse model of stroke. *J Cereb Blood Flow Metab*. 2007;27(3):452-459. doi: 9600351 [pii].

21. Alijevic O, Kellenberger S. Subtype-specific modulation of acid-sensing ion channel (ASIC) function by 2-guanidine-4-methylquinazoline. *J Biol Chem*. 2012;287(43):36059-36070. doi: 10.1074/jbc.M112.360487 [doi].

22. Askwith CC, Cheng C, Ikuma M, Benson C, Price MP, Welsh MJ. Neuropeptide FF and FMRFamide potentiate acid-evoked currents from sensory neurons and proton-gated DEG/ENaC channels. *Neuron*. 2000;26(1):133-141. doi: S0896-6273(00)81144-7 [pii].

23. Sherwood TW, Askwith CC. Endogenous arginine-phenylalanine-amide-related peptides alter steady-state desensitization of ASIC1a. *J Biol Chem*. 2008;283(4):1818-1830. doi: M705118200 [pii].

24. Vick JS, Askwith CC. ASICs and neuropeptides. *Neuropharmacology*. 2015;94:36-41. doi: 10.1016/j.neuropharm.2014.12.012 [doi].

25. Sherwood TW, Askwith CC. Dynorphin opioid peptides enhance acid-sensing ion channel 1a activity and acidosis-induced neuronal death. *J Neurosci*. 2009;29(45):14371-14380. doi: 10.1523/JNEUROSCI.2186-09.2009 [doi].

26. Frey EN, Pavlovicz RE, Wegman CJ, Li C, Askwith CC. Conformational changes in the lower palm domain of ASIC1a contribute to desensitization and RFamide modulation. *PLoS One*. 2013;8(8):e71733. doi: 10.1371/journal.pone.0071733 [doi].

27. Chen X, Qiu L, Li M, et al. Diarylamidines: High potency inhibitors of acid-sensing ion channels. *Neuropharmacology*. 2010;58(7):1045-1053. doi: 10.1016/j.neuropharm.2010.01.011 [doi].

28. Kusama N, Harding AM, Benson CJ. Extracellular chloride modulates the desensitization kinetics of acid-sensing ion channel 1a (ASIC1a). *J Biol Chem*. 2010;285(23):17425-17431. doi: 10.1074/jbc.M109.091561 [doi].

29. Chen X, Grunder S. Permeating protons contribute to tachyphylaxis of the acid-sensing ion channel (ASIC) 1a. *J Physiol*. 2007;579(Pt 3):657-670. doi: jphysiol.2006.120733 [pii].

30. Li T, Yang Y, Canessa CM. Impact of recovery from desensitization on acid-sensing ion channel-1a (ASIC1a) current and response to high frequency stimulation. *J Biol Chem*. 2012;287(48):40680-40689. doi: M112.418400 [pii].

31. Chen X, Kalbacher H, Grunder S. Interaction of acid-sensing ion channel (ASIC) 1 with the tarantula toxin psalmotoxin 1 is state dependent. *J Gen Physiol*. 2006;127(3):267-276. doi: jgp.200509409 [pii].

32. Chen X, Kalbacher H, Grunder S. The tarantula toxin psalmotoxin 1 inhibits acid-sensing ion channel (ASIC) 1a by increasing its apparent H+ affinity. *J Gen Physiol*. 2005;126(1):71-79. doi: jgp.200509303 [pii].

33. Price MP, McIlwrath SL, Xie J, et al. The DRASIC cation channel contributes to the detection of cutaneous touch and acid stimuli in mice. *Neuron*. 2001;32(6):1071-1083. doi: S0896-6273(01)00547-5 [pii].

34. Hattori T, Chen J, Harding AM, et al. ASIC2a and ASIC3 heteromultimerize to form pH-sensitive channels in mouse cardiac dorsal root ganglia neurons. *Circ Res*. 2009;105(3):279-286. doi: 10.1161/CIRCRESAHA.109.202036 [doi].

35. Sutherland SP, Benson CJ, Adelman JP, McCleskey EW. Acid-sensing ion channel 3 matches the acid-gated current in cardiac ischemia-sensing neurons. *Proc Natl Acad Sci U S A*. 2001;98(2):711-716. doi: 10.1073/pnas.011404498 [doi].

36. Holzer P. Acid-sensing ion channels in gastrointestinal function. *Neuropharmacology*. 2015;94:72-79. doi: 10.1016/j.neuropharm.2014.12.009 [doi].

37. Sluka KA, Price MP, Breese NM, Stucky CL, Wemmie JA, Welsh MJ. Chronic hyperalgesia induced by repeated acid injections in muscle is abolished by the loss of ASIC3, but not ASIC1. *Pain*. 2003;106(3):229-239. doi: S0304395903002690 [pii].

38. Waldmann R, Champigny G, Bassilana F, Heurteaux C, Lazdunski M. A proton-gated cation channel involved in acid-sensing. *Nature*. 1997;386(6621):173-177. doi: 10.1038/386173a0 [doi].

39. Immke DC, McCleskey EW. Protons open acid-sensing ion channels by catalyzing relief of Ca2+ blockade. *Neuron*. 2003;37(1):75-84. doi: S0896627302011303 [pii].

40. Zhang P, Sigworth FJ, Canessa CM. Gating of acid-sensitive ion channel-1: Release of Ca2+ block vs. allosteric mechanism. *J Gen Physiol*. 2006;127(2):109-117. doi: jgp.200509396 [pii].

41. Berdiev BK, Mapstone TB, Markert JM, et al. pH alterations "reset" Ca2+ sensitivity of brain na+ channel 2, a degenerin/epithelial na+ ion channel, in planar lipid bilayers. *J Biol Chem*. 2001;276(42):38755-38761. doi: 10.1074/jbc.M107266200 [doi].

42. Babini E, Paukert M, Geisler HS, Grunder S. Alternative splicing and interaction with di- and polyvalent cations control the dynamic range of acid-sensing ion channel 1 (ASIC1). *J Biol Chem*. 2002;277(44):41597-41603. doi: 10.1074/jbc.M205877200 [doi].

43. National Center for Complementary and Integrative Health (NCCIH). Understanding drug-supplement interactions. https://nccih.nih.gov/health/herbs/understanding-interactions. Updated March 09, 2015.

44. Kristian T, Gido G, Kuroda S, Schutz A, Siesjo BK. Calcium metabolism of focal and penumbral tissues in rats subjected to transient middle cerebral artery occlusion. *Exp Brain Res*. 1998;120(4):503-509.

45. Cushman KA, Marsh-Haffner J, Adelman JP, McCleskey EW. A conformation change in the extracellular domain that accompanies desensitization of acid-sensing ion channel (ASIC) 3. *J Gen Physiol*. 2007;129(4):345-350. doi: jgp.200709757 [pii].

Appendix A:

Detergent screening of the human voltage-gated ion channel (Hv1) using fluorescence-detection size exclusion chromatography.

Amruta Agharkar[1], Jennifer Rzadkowolski[2], Mandy McBroom[1], Eric B. Gonzales[1,3,4*]

Affiliations
[1]Department of Pharmacology & Neuroscience, UNT Health Science Center, Fort Worth, Texas, United States
[2]Texas College of Osteopathic Medicine, UNT Health Science Center, Fort Worth, Texas, United States
[3]Institute for Aging and Alzheimer's Disease Research, UNT Health Science Center, Fort Worth, Texas, United States
[4]Cardiovascular Research Institute, UNT Health Science Center, Fort Worth, Texas, United States

Agharkar A, Rzadkowolski J, McBroom M, Gonzales EB. Detergent screening of the human voltage-gated proton channel using fluorescence-detection size-exclusion chromatography.

Protein Sci. 2014;23(8):1136-1147. doi: 10.1002/pro.2492 [doi]. PMID: 24863684

*Corresponding Author:
Eric B. Gonzales, Ph.D.
Assistant Professor
Department of Pharmacology & Neuroscience
UNT Health Science Center
3500 Camp Bowie Blvd.
Fort Worth, TX 76107
Email: eric.b.gonzales@unthsc.edu
Phone: 817-735-2755
Fax: 817-735-0408

Funding:
UNT Health Science Center Intramural Seed Grant Program
American Heart Association (12BGIA8820001)
Welch Foundation (BK-1736).

Abstract

The human voltage-gated proton channel (Hv1) is a membrane protein consisting of four transmembrane domains and internal amino- and carboxy-termini. The protein is activated by membrane depolarization, similar to other voltage-sensitive proteins. However, the Hv1 proton channel lacks a traditional ion pore. The human Hv1 proton channel has been implicated in mediating sperm capacitance, stroke, and most recently as a biomarker/mediator of cancer metastasis. Recently, the three-dimensional structures for homologues of this voltage-gated proton channel were reported. However, it is not clear what artificial environment is needed to facilitate the isolation and purification of the human Hv1 proton channel for structural study. In the present study, we generated a chimeric protein that placed an enhanced green fluorescent protein (EGFP) to the amino-terminus of the human Hv1 proton channel (termed EGFP-Hv1). The chimeric protein was expressed in a baculovirus expression system using Sf9 cells and subjected to detergent screening using fluorescence-detection size exclusion chromatography (FSEC). The EGFP-Hv1 proton channel can be solubilized in the zwitterionic detergent Anzergent 3-12 and the nonionic n-dodecyl-β-D-maltoside (DDM) with little protein aggregation and a prominent monomeric protein peak at 48 hours post infection. Furthermore, we demonstrate that the chimeric protein exhibits a monomeric protein peak, which is distinguishable from protein aggregates, at the final size exclusion chromatography purification step. Taken together, we can conclude that solubilization in DDM will provide a useable final product for further structural characterization of the full-length human Hv1 proton channel.

Keywords:

Voltage-gated proton channel, detergent screen, electrophysiology, fluorescent-detection size exclusion chromatography

Abbreviations and Symbols:

Hv1, human voltage-gated proton channel; mVSOP, mouse voltage-sensor domain-only protein; DDM, n-dodecyl-β-D-maltoside; β-OG, n-octyl-β-D-glucoside; DM, n-decyl-β-D-maltoside; LDAO, n-Dodecyl-N,N-Dimethyl-3-Ammonio-1-Propanesulfonate/N,N-Dimethyl-1-N-(3-Sulfopropyl)-1-Dodecanaminium Hydroxide, Inner Salt; FSEC, fluorescence detection size exclusion chromatography;

Introduction

Membrane proteins make up nearly 40% of pharmaceutical targets[1] and make up to 30% of the human-genome[2]. Determining the three-dimensional crystal structure of membrane proteins provides a map of the protein's architecture and a template for designing drugs that can selectively target these proteins. X-ray crystallography has assisted these efforts by providing the structure of membrane proteins [3,4]. To achieve this goal, a membrane protein must be purified, maintained in its native conformation, and form well-ordered protein lattices to yield meaningful diffraction data. Complicating this endeavor is the realization that not all membrane proteins, in their wild-type configuration, are suitable for protein crystallization studies. Thus, the need for precrystallization screening of protein constructs is crucial before undertaking large-scale studies to solve a membrane protein's structure. One technique that has utilized small cell culture volumes (2 ml) coupled with fluorescently labeling of the protein is the fluorescence-detection size exclusion chromatography method, FSEC [5-7]. The use of FSEC in a variety of protein expression systems (e.g. human embryonic kidney cells, *Saccharomyces cerevisae*, *Spongidoptera frugiperda* cells) has led to a variety of membrane protein structures. Thus, this assessment of protein stability is well suited for novel membrane proteins where the three dimensional structure has evaded resolution.

The human voltage-gated proton channel is a member of the voltage-sensing proteins (VSPs), which include voltage-gated ion channels and the voltage-gated phosphatases [8]. Proton currents generated by membrane depolarization were first observed in marine dinoflagelates [9], snails [10], and in isolated microglia from neonatal brain cell culture [11]. The voltage-gated proton current in microglia was sensitive to divalent cations, such as zinc, and tetraelthylammonium

(TEA) [12]. In 2006, the mammalian genes encoding the mouse voltage-sensor domain-only protein (mVSOP) gene [13] and the human homologue (Hv1) [14] were cloned. All voltage-gated proton channels consist of four transmembrane domains, with the voltage sensor residing in the 4th membrane-spanning segment, that facilitates the efflux of protons from the acidic cell interior [14]. Furthermore, these proton channels are functional as monomers but can form dimers [15]. There are homologous voltage-gated proton channels throughout the evolutionary chain. Unlike other voltage-gated ion channels, the Hv1 proton channel lacks the typical re-entrant pore loop domain or the transmembrane segments S5 and S6.

The Hv1 proton channel plays an important role in normal function and pathologies. The channel plays an important role in male fertility by alkalinizing sperm cytoplasm, leading to sperm capacitation within the female reproductive tract [16]. The production of reactive oxygen species following stroke is enhanced by the presence of the Hv1 proton channel on microglia through balancing the net cellular loss of negative charge with protons[17]. Furthermore, the Hv1 proton channel helps phagocytes generate superoxides required for the clearance of pathogens[18]. Recently, it was discovered that the Hv1 proton channel is overexpressed in metastatic breast cancer cells and helps in cancer cell proliferation, migration, and may serve as a cancer biomarker for the severity of cancer progression [19,20].

One barrier to obtaining the structure of a complete Hv1 proton channel is identifying a suitable environment for purifying properly folded protein. The fluid mosaic architecture of plasma membrane provides the optimal environment for membrane protein stability. However, maintaining this environment may not be possible while purifying sufficient quantities for crystallographic study. Detergents are a common means to isolate membrane proteins. However,

detergents are inherently destructive to that same membrane and alter protein folding. Non-ionic detergents, such as maltosides, mimic the cellular membrane hydrophilic-lipophilic environment suited for stabilizing the protein in a functional state. Many non-ionic detergents have been screened for membrane protein isolation. The choice of detergent depends on its physico-chemical properties such as polarity of head group, length of side chain and critical micelle concentration[21]. Previous studies have indicated that alkyl maltosides are preferred over a similar chemical class of alkyl glucosides for the determination of □-helical-rich membrane proteins [22]. With respect to channel proteins, these integral membrane proteins find stability within octyl-glucosides more frequently than other classes of detergents [23], but there are exceptions that may be more related to the types of proteins studied. The voltage-sensing domain (Ci-VSD) of the voltage-sensing phosphatase of *Ciona intestinalis* (Ci-VSP) was stable in the detergent Anzergent 3-14, which differs from dodecyl maltoside [24], and the wild-type Hv1 proton channel was stable in a combination of maltosides [15]. Although these detergent classes are most successful as far as membrane proteins are concerned, their utility in the purification of the Hv1 proton channel for structural studies is unclear.

Recently the crystal structures of two voltage-sensing proteins were reported that provide the first glimpse of these unique protein's architecture. The isolated Ci-VSD was solved using a combination of detergents along with protein crystallography to reveal the structure of the protein to 2.5 Å resolution [25]. The other voltage-sensor protein structure that was solved utilized an engineered chimeric receptor of the mouse mVSOP. A functional chimeric mouse mVSOP was generated consisting of removal of the first 74 N-terminal residues, the replacement of the C-terminal coiled-coiled □-helices with the leucine zipper protein GCN4, and the replacement of a amino acids spanning the middle of second transmembrane domain to the middle of third

transmembrane domain[26]. This chimeric mVSOP protein structure was solved to 3.45 Å resolution using a single detergent in the buffer solution used for crystallography. Despite these recent advances, the full-length Hv1 proton channel crystal structure remains elusive.

Here we assessed the stability of a full-length human voltage-gated proton channel (Hv1) with an N-terminal enhanced green fluorescent protein, termed EGFP-Hv1, expressed in the baculovirus expression system of *Spongidoptera frugiperda* cells (Sf9 cells) in non-ionic and zwitterionic detergents. We used fluorescence-detection size- exclusion chromatography (FSEC) to assess the time-dependent stability and monodispersity of the EGFP-Hv1 in several detergents. The chimeric EGFP-Hv1 proton channel was observed to be ideally isolated at 48 hours post infection, as the protein is susceptible to non-specific protein cleavage that separates the fluorescent tag from the proton channel. Our data show that solubilization and purification of EGFP-Hv1 protein was most stable using dodecyl maltoside, as shown in our FSEC and SEC analysis. Our results suggest that this frequently used detergent should be the focus of protein solubilization and stability protocols for the human Hv1 proton channel.

Results:

1. Chimeric EGFP-Hv1 proton channel is functional when expressed in CHO-K1 cells.

We initiated our studies by first assessing the function of a chimeric EGFP-Hv1 proton channel where the green fluorescent protein is located at the amino terminus of the channel. The Hv1 proton channel has been subjected to both amino- and carboxy-termini deletion as well as tagging with fluorescent proteins [27]. Incorporation of the amino-terminal EGFP protein to the Hv1 proton channel could alter the channel's activity. Thus, we assessed the chimeric channel's functionality using whole-cell patch clamp electrophysiology. The acquired Hv1 proton channel cDNA was subcloned into the mammalian expression vector pNGFP-EU [5] using PCR to engineer XhoI and BamHI restriction sites at the 5' and 3' end of the Hv1 proton channel cDNA. The resulting vector, pNGFP-Hv1, was used to transfect CHO-K1 cells. Chimeric channel expression was observed after 24 hours using fluorescent microscopy (Figure 1A). However, we were unable to determine if the EGFP-Hv1 proton channels were located in the plasma membrane. Using intracellular and extracellular solutions with pH values of 5.5 and 7.0, respectively, we observed outward Hv1 proton channel current using depolarizing voltage-steps (-60 mV to +130 mV) (Figure 2B). Voltage steps from -60 mV up to 0 mV failed to yield measurable current. Although the EGFP-Hv1 proton channel yielded voltage-dependent proton current when expressed in CHO cells, this does not rule out that the Sf9 expression system generated properly folded and functional protein.

2. EGFP-Hv1 protein is most stable 48 hours after infection and n-dodecyl-β-D-maltoside stabilizes protein at 24 hours.

After establishing that the chimeric EGFP-Hv1 proton channel was a functional protein construct, we initiated studies to determine solution conditions that would stabilize solubilized human Hv1 proton channel protein when expressed in a baculovirus expression system. We conducted a time course to establish the optimal time for chimeric EGFP-Hv1 protein production. To focus on these time points, we chose the commonly used n-dodecyl-β-D-maltoside (DDM) to solubilize the harvested and isolated aliquots of infected Sf9 cells. This non-ionic detergent, DDM, has a critical micelle concentration of 0.12 mM and is one of the most frequently used detergent in membrane protein crystallography [22]. Aliquots of the EGFP-Hv1 proton channel culture were taken at four time points following infection: 24, 48, 72, and 96 hours. At 24 hours, a single, monodisperse peak of EGFP-Hv1 chimeric protein was observed and corresponds to the molecular weight of EGFP-Hv1 monomer with the elution volume of 16.83 ml (Figure 1A). The protein void peak, indicative of non-specific protein aggregation, was negligible in comparison to the EGFP-Hv1 proton peak. We used a purified polyhistidine tagged EGFP as our control, which is similar to the EGFP used in our chimeric EGFP protein construct.

At 48 hours, a single monodisperse peak of EGFP-Hv1 chimeric protein was observed at 16.79 ml elution volume with the emergence of free EGFP when solubilized in a DDM solubilization buffer (Figure 1B). The free EGFP peak's appearance suggests that there is cleavage and separation of EGFP and the Hv1 proton channel by the time aliquots of the protein culture are taken. Compared to solubilization of the 24 hour EGFP-Hv1 infected cell culture, there was an increase in protein aggregation as seen by the robust protein void peak. The FSEC analysis after 72 hours of infection indicates that there is partial degradation of EGFP-Hv1 chimeric protein because two protein peaks are observed at 15.34 ml and 16.73 ml elution

volume respectively (Figure 1C). A diffuse protein peak emerged at 12.59 ml elution volume that was absent at the earlier time points.

At the 96 hour time point, there was near complete reduction of the EGFP-Hv1 protein peaks at 15.46 and 16.67 ml elution volume seen in Figure 1C. Furthermore, the higher molecular weight protein peak was increased (12.61 ml eluton volume). The major protein peak in the 96 hour protein sample is the free EGFP peak, suggesting that at this time most of the protein that is detecteable is cleaved EGFP as a result of nonspecfici protein degradation. (Figure 1D). Furthermore, the increase in free EGFP at 72 and 96 hours of culture suggested that these time points would yield low quantities of intact EGFP-Hv1 proteins as the polyhistidine affinity tage is on the amino-terminus of EGFP. Thus, the chimeric EGFP-Hv1 proton channel was stable with minimal nonspecific protein cleavage of the chimeric receptor at 48 hours after Sf9 cell infection. Although our initial study used a detergent that is frequently used for both solubilization and crystallization experiments, n-dodecyl-β-D-maltoside may not yield or generate well-ordered protein crystals. Hence, we screened additional non-ionic and zwitterionic detergents for the maintenance of monodisperse chimeric EGFP-Hv1 proton channel protein at 24 and 48 hours of infected Sf9 cell culture.

3. β-Octylglucoside fails to maintain the monodispersity of protein.

Another common detergent used in the crystallization of membrane proteins is a group consisting of the octyl-glucosides, which include the detergent n-octyl-β-D-glucoside (β-OG). This non-ionic glucoside has a critical micelle concentration of 23.4 mM [28] and has been used to determine the crystal structure of a variety of membrane proteins. As the detergent consists of a glucose head group and shorter alkyl chain than DDM, we solubilized the EGFP-Hv1 chimeric

protein to assess the protein's stability in this second most frequently used detergent. Based on the time-course study using DDM, we focused on aliquots of infected Sf9 cells that were harvested at 24 and 48 hour time points.

The FSEC analysis of the EGFP-Hv1 chimeric protein showed that the protein was eluted at 16.75 and 16.87 ml elution volumes in β-OG detergent at 24 and 48 hours, respectively (Figure 2A and 2B). At both time points, we observed EGFP-Hv1 proton channel protein peaks that lacked monodispersity, characterized by increases in chromatographic "shoulders" around the protein peak. The protein void peak differed between the two time points. At 24 hours, the EGFP-Hv1 proton channel chimeric protein peak was the same amplitude as the protein void peak. The ratio of protein void peak to chimeric protein, however, increased at the 48 hour mark. This suggests that the EGFP-Hv1 chimeric receptor is not stable if solubilized in n-octyl-β-D-glucoside and formed protein aggregates once removed from the plasma membrane.

4. LDAO fails to maintain the monodispersity of protein at 48 hours

We continued to explore other detergents, based on their physicochemical properties. The next detergent used was the zwitterionic detergent n-dodecyl-N,N-dimethylamine-N-oxide (LDAO). At the time of their review, Newstead and colleagues determined that LDAO accounted for nine membrane protein structures [22]. The detergent consists of a 12 carbon alkyl chain and a electrical neutral head group consisting of a zwitterionic amine oxide. We observed that the EGFP-Hv1 chimeric protein was stable at 24 hours when solubilized in LDAO solubilization solution. The resulting chromatogram showed a symmetrical peak that eluted at 16.49 ml and had a small protein void peak (Figure 3A). Solubilization of the 48 hour aliquot resulted in a main protein peak that eluted at 16.47 ml elution volume (Figure 3B). Although the

elution volumes between the 24 and 48 hour aliquots were similar, the protein void peaks were not. The ratio of protein void versus EGFP-Hv1 proton channel chimeric protein was increased, suggesting that when more protein is present there was a corresponding increase in protein aggregation. Although the protein quantity will be reduced if pursued, our data suggests that LDAO may be a candidate for large-scale protein purification of the EGFP-Hv1 proton channel chimeric protein when harvested at 24 hours.

5. Anzergent 3-12 stabilizes the EGFP-Hv1 chimeric protein at 24 and 48 hours.

In a recent report, the voltage-sensing domain (VSD) of the *Ciona intestinalis* voltage-dependent phosphatase (Ci-VSP) expressed in *E.* coli[24] was purified and used to form diffraction quality protein crystals for structure determination[25]. In those reports, a variety of detergents were used to solubilize and purify the voltage sensor domain. Of the 14 detergents used, two showed the most promise, with resulting purified protein exhibiting homogeneity and monodispersity. These were Anzergent 3-12 and 3-14, which have alkyl chains of 12 and 14 carbons, respectively. They provide a different chemical backbone than the other detergents used and are zwitterionic (where the charges remain in the headgroup and not in the carbon chain). Both Anzergents demonstrated utility for solubilization and reconstitution of the Ci-VSD. However, these detergents have not been assessed for stabilizing the intact Hv1 proton channel. Thus, we sought to characterize the stability of the chimeric EGFP-Hv1 proton channel using Anzergent 3-12. The FSEC profiles of the chimeric EGFP-Hv1 proton channel protein provide evidence to suggest that Anzergent 3-12 has potential for stabilizing the solubilized chimeric protein (Figure 4A and 4B). A single, monodisperse peak was observed at 16.73 ml when the 24 hour aliquot was analyzed (Figure 2A). There was a protein void peak using Anzergent 3-12,

which differs from DDM and LDAO at the same time point. There was no discernable free EGFP in the solubilized sample.

At 48 hours, EGP-Hv1 chimeric protein was eluted at 16.53 ml as a single peak (Figure 4B). The EGFP-Hv1 protein peak differed at the 48 hour mark when solubilized in Anzergent 3-12, as the symmetry of the peak was reduced with the emergence of a low-molecule weight shoulder. Furthermore, the protein void was more robust than the chimeric EGFP-Hv1 proton channel peak. These results indicated that Anzergent 3-12 was suitable for solubilizing the EGFP-Hv1 containing cells at 24 hours, but may also be vulnerable to protein aggregation and reduced protein stability if solubilized using samples isolated at time points greater than 24 hours.

6. Large-scale purification of chimeric EGFP-Hv1 proton channel is stabilized by n-dodecyl-β-D-maltoside.

Based on our data, the small-scale assessment of the chimeric EGFP-Hv1 proton channel showed that n-dodecyl-□-D-maltoside provided sufficient stability to warrant large-scale study. Next, we considered if a large-scale of infect Sf9 cells culture (2 liters) would generate sufficient protein and retain stability when isolating the chimeric EGFP-Hv1 proton channel. we generated and purified the chimeric EGFP-Hv1 proton channel from 4 liters of Sf9 cell culture at 48 hours. The isolation of the EGFP-Hv1 proton channel was performed with cobalt metal affinity resin (Figure 6A). We utilized a 20 mM imidazole wash buffer that resulted in a protein peak with 200 mAU absorbance. The EGFP-Hv1 proton channel was eluted with 250 mM imidazole solution and resulted in a robust protein peak (~600 mAU). The resulting protein was retained using 3 ml fractions. Five fractions that made up the resulting EGFP-Hv1 proton channel peak were

collected, combined, and analyzed using size exclusion chromatography using a Superose 6 100/300 column. The resulting chromatogram gave no indication of a protein void peak, which suggests that larger quantities of the protein, while in DDM solution, should remain stable and not form significant protein aggregates (Figure 6B).

Protein began to elute from the after the 8 ml elution volume mark and increased steadily. The first peak was observed at 14.46 ml elution volume. This peak lacked monodispersity. The major peak eluted at 16.99 ml elution volume and represents the major peak. Despite using the same SEC protein column, the resulting EGFP-Hv1 proton channel protein eluted at a higher elution volume than the protein in the FSEC studies. The discrepancy is due to the difference in tubing lengths separating the column from the fluorescence detectors on the FSEC (HPLC) and SEC (FPLC) instruments.

Discussion:

The human Hv1 proton channel though belongs to voltage-gated ion channel family but it differs from typical voltage-gated ion channels. We sought to characterize the Hv1 proton channel's expression and monodispersity when solubilized in commonly used detergents using the fluorescence-detection size exclusion chromatography assay. To express the chimeric EGFP-Hv1 proton channel, we used a baculovirus/insect expression system. The Hv1 proton channel studies have used other expression systems to produce the protein. *E. coli*, *Picchia pastoris*, and mammalian cells have been used to express either Hv1 proton channel, the Hv1 truncated C-terminal domain, Ci-VSP [24,29].The Ci-VSD protein was overexpressed in E-coli X-10 gold cells [25]. Similar to our chimeric EGFP-Hv1 proton channel, the recent mVSOP protein structure was generated using the baculovirus expression system [26]. The insect expression system provides an environment with lipid composition that most closely mimics the plasma membrane environment in mammalian cells, with similar post-translational modifications [30]. Furthermore, we observed that despite the variety of detergents used, the most commonly used class, the maltosides, provided the most stable environment for the purified protein.

In preparing the chimeric EGFP-Hv1 proton channel for expression in CHO-K1 cells, we subcloned the chimeric protein gene into a mammalian expression system for functional assessment. Based on our electrophysiological studies, the chimeric EGFP-Hv1 proton channel is functionally similar to the human Hv1 proton channel activity in previous reports. Our greatest concern for studying the channel's function was how well the Hv1 proton channel would tolerate a fluorescent protein at the protein's N-terminus and whether the chimeric receptor would target to the plasma membrane. Previous reports have shown that the full length Hv1 proton channel

can be transiently expressed in HeLa cells and the protein is localized to intracellular compartments [27]. Removal of the N-terminus had no effect on receptor localization. However, the removal of the C-terminus led to the more global localization of the Hv1 proton channel [27]. In our study, we focused solely on the N-terminally tagged Hv1 proton channel. With our fluorescent microscopy, we can confirm that the chimeric receptor was expressed throughout the CHO-K1 cells at 24 hours after transfection. Furthermore, our whole-cell patch-clamp experiments suggested that the chimeric EGFP-Hv1 proton channel reaches the plasma membrane to mediate outgoing proton current, as observed with current following membrane depolarization. Since we did not modify the C-terminus of the protein, this outcome was expected.

Although the EGFP-Hv1 proton channel generated voltage-dependent proton current when expressed in CHO cells, this does not rule out that protein expressed in the Sf9 expression system is properly folded and functional. There is a possibility that the expressed EGFP-Hv1 proton channel protein, when expressed in Sf9 cells, is non-functional even if present in the plasma membrane. Consideration and caution should be taken when performing structural experiments where the protein expression system differs from the expression system used for functional studies. In the case of the recently solved chimeric mVSOP protein structure, the investigators utilized the baculovirus expression system (Sf9 cells) for protein generation. Furthermore, two functional assays were used to test protein function: whole-cell patch clamp electrophysiology using HEK293t cells; and proton flux studies by reconstituting the purified protein in liposomes [26]. As a measure of retained function following generating chimeric protein, coupling FSEC and whole-cell patch clamp electrophysiology is a powerful screening protocol to focus on the protein constructs, especially those modified to enhance protein stability and crystal

formation that is stable and functional. As the protein structure is pursued, the use of FSEC, coupled with electrophysiology (either in-house or via collaboration/contract research organization) should be used in the pursuit of the full-length Hv1 proton channel's three-dimensional structure.

The mVSOP/Hv1 proton channels have been the focus of structural studies with protein crystallographic success coming from the structure determination of the Hv1 proton channel C-terminus and the recent Ci-VSD and chimeric mVSOP structures. The Hv1 proton channel C-terminal domain (residue 221-273) was expressed in *E. coli* and yielded a protein crystal with x-ray diffraction to 2.5 Å resolution[31] and was improved in subsequent studies [32,33]. This provided a glimpse of the how the Hv1 proton channel may form dimers while in the plasma membrane. The recently determined structure of Ci-VSD in the active and resting state provided coordinates of the structural changes that occur within these voltage sensing transition states. The crystal structure of the chimeric mVSOP showed the proton channel in its resting state at resolution of 3.45 Å and shows that the chimeric channel was observed to be a dimer when expressed in HEK293T cells for electrophysiology. However, the chimeric protein forms trimers upon crystallization, which might be due to the leucine-zipper motif of the transcriptional activator GCN4 protein added to the construct at protein's C-terminus [26]. Despite this surprise, the chimeric mVSOP protein had the fundamental characteristics of the voltage-gated proton channel.

The Hv1 proton channel C-terminal domain has been implicated in affecting the channel's sensitivity to temperature [32]. However, what is clear in our studies is that the human voltage-gated proton channel is not a stable dimer once extracted from the plasma membrane. Of the three reports mentioned[15,31,32], the resulting Hv1 proton channel, once purified, was present

as a monomer, instead of a dimer, when in the absence of cross-linker reactions. With exposures to cross-linking reagents with increasing concentrations, each of these studies shows that the Hv1 proton channel can dimerize. Thus, the dimeric form of the Hv1 proton channel may be stable while in the plasma membrane, but loses this stability once removed from the lipid environment. Such is the case when membrane proteins are solubilized in detergent, a less than ideal substitute for the plasma membrane. We observed evidence of a mixed population of monomeric and dimeric protein in our final size exclusion chromatography purification (Figure 6). While a more robust peak is observed at the corresponding elution volume for monomeric EGFP-Hv1 proton channel, we observed a peak that corresponds to a dimer of the EGFP-Hv1 proton channel. However, this peak was not as robust as the monomeric EGFP-Hv1 proton channel peak. With the trimerization of the chimeric mVSOP, there remains the possibility that the monomeric Hv1 proton channel could still multimerize during crystallization.

Based on our FSEC assessment of the chimeric EGFP-Hv1 proton channel stability, we observed that Anzergent 3-12 (zwitterionic) and dodecyl maltoside (nonionic) detergents provided the most promising chromatographic profiles at 48 hours. With protein expression and purification, there is a balancing act between robust protein expression and minimal protein aggregation. In our time course experiments, we observed that the void peak increased at each 24-hour interval. Although there was no void peak at 24 hours, there was the least amount of protein expressed. Considerably more protein is produced by 48 hours, with a void peak similar to the protein peak. Harvesting protein at the 24 hour time point would reduce the amount of protein lost to aggregation, but would require more culture and greater cost to obtain sufficient protein for subsequent structural studies. Once taken to larger cell culture, we observed a

significant and robust monomeric EGFP-Hv1 proton channel peak. The isolation and purification of the chimeric protein was done in the presence of the nonionic detergent dodecyl maltoside.

The stability of the human voltage-gated proton channel in either Anzergent 3-12 or dodecyl maltoside is not surprising. Previous reports suggested that these two detergents, or similar detergents, provide a stable environment for the protein. Full-length human Hv1 proton channel was purified and reconstituted following solubilization and purification from *Pichia pastoris* using a combination of maltosides [29]. For solubilization, dodecyl maltoside was used to extract the protein from the plasma membrane and a working concentration of 1 mM of DDM was used for affinity resin conjugation and elution. At the final size exclusion chromatography step, a shorter maltoside, decyl maltoside (DM), was used. From this final purification, subsequent reconstitution of the protein was performed and the protein remained functional. The recent structures of the Ci-VSD and the chimeric mVSOP are examples of the complexity involved in stabilizing a protein outside of the plasma membrane and for forming diffracting protein crystals. Li and colleagues used different combinations of detergents to solubilize the protein, to complex the protein with a monoclonal antibody, and to grow protein crystals. The protein crystals that would reveal the active state of the protein, Ci-VSD R217E in complex with antibody, were obtained using the detergent LDAO. The essentially wild type protein was purified using a combination of LDAO and decyl maltoside [25]. The chimeric mVSOP protein was solubilized in DDM, with purification and crystallization being performed in CYMAL-5 detergent [26]. The reports for the Ci-VSD and chimeric mVSOP proteins suggests that maltosides are best used for solubilization and that crystallization may require additional detergents to generate diffraction quality protein crystals. Our metal affinity chromatography and SEC purification utilized DDM and yielded a robust monomeric EGFP-Hv1 proton channel peak.

Thus, our findings are consistent with previous reports regarding the voltage-sensing protein/proton channel stability up to the size exclusion chromatography step. The protein crystallization studies will most likely require the use of multiple detergents that facilitate crystal formation.

The utility of Anzergent 3-12 in stabilizing the EGFP-Hv1 proton channel is similar to what was observed for a homolog of the Hv1 proton channel protein and the corresponding crystal structures. Li et al. in 2012 truncated a voltage-sensing phosphatase, thus removing the phosphatase domain and focusing on the voltage-sensor domain [24]. Fourteen detergents were screened to isolate the voltage-sensing domain and five of those detergents provided the greatest solubilization of the Ci-VSP domain, which included Anzergents 3-12 and 3-14. For this truncated construct, the solubilized Ci-VSP protein was monodisperse, homogeneous, and was stable a week after concentration. Our detergent screen was not focused on the EGFP-Hv1 proton channel stability after the final size exclusion chromatography purification. However, we did observe similar higher molecular weight protein products after concentration and SEC analysis [24]. In the Ci-VSP purification, dodecyl maltoside yielded not only the monomeric protein, but also higher molecular weight products closer to the void. In our assessment using the detergent, we did not observe a protein void, but did see a higher molecular weight product near the monomeric EGFP-Hv1 proton channel peak. We did not observe this peak in our initial FSEC screen at 48 hours post infection. One possible explanation may be that when the EGFP-Hv1 proton construct is concentrated prior to SEC analysis, there is opportunity for the protein to aggregate or dimerize. This aggregation/dimerization could be managed in future studies by molecular modification of the protein construct. This includes minimizing disulfide formation from free cysteines by reaction with iodoacetamide [34], site directed mutagenesis, or further

modification of the elution buffer by addition of reducing agents dithiothreitol (DTT) or β-mercaptoethanol.

In conclusion our study demonstrates the feasibility of expressing a functional chimeric EGFP-Hv1 proton channel in a baculovirus expression system and confirms that both dodecyl maltoside and Anzergent 3-12 could be used for purification of this full-length proton channel. Future studies will focus on improving the protein's monodispersity and the generation of Hv1 proton channel protein crystals for structural determination. The identification of novel ligands may also enhance the stability of these fascinating membrane proteins and lead to the determination of the human Hv1 proton channel's crystal structure.

Materials and Methods:

Subcloning of Hv1 proton channel gene and generation of Hv1 baculoviral expression system. The full-length human voltage-gated proton channel (Yuriy Kirichock, University of California San Francisco, via Addgene) was subcloned into a modified pFastBac1 vector (Life Technolgies, Grand Island, NY, USA) containing an amino terminal enhanced green fluorescent protein and polyhistidine tag (Eric Gouaux, Vollum Institute, Portland OR). DH10Bac supercompetent cells (Life Technologies) were transformed with the pFB-GFPHv1 plasmid DNA according to manufacturer's protocol to generate bacmid DNA. The resulting EGFP-Hv1 bacmid DNA was then used to transfect *Spongidoptera frugiperda* (SF9) insect cells using Cellfectin transfection reagent (Life Technologies). After 96-hour incubation at 27º C, EGFP-Hv1 P1 bacuovirus was isolated and passed through a 0.22 μm filter. The isolated P1 virus was stored at 4º C until used. P2 baculovirus was obtained by inoculating Sf9 cell culture (1.0×10^6 cells/ml) with 150-200 μl P1 virus and harvested using filtration at 96 hours post infection.

Solubilization Buffer. Protein solubilization buffer consisted of 150 mM NaCl, 20 mM Tris-Cl, and 20 mM detergent. Elution buffers for HPLC assessment were similar to solubilization buffer, but with 1 mM detergent in most cases. Four detergents were identified for the solubilization and stability screen. These include n-dodecyl-β-D-maltoside (C12M), n-Octyl-β-D-glucopyranoside (β-OG), n-Dodecyl-N,N-Dimethylamine-N-Oxide (LDAO), and n-Dodecyl-N,N-Dimethyl-3-Ammonio-1-Propanesulfonate/N,N-Dimethyl-1-N-(3-Sulfopropyl)-1-Dodecanaminium Hydroxide, Inner Salt (Anzergent 3-12). All detergents were obtained from Anatrace/Affymetrix. The protease inhibitor phenylmethylsulfonyl fluoride (PMSF) was supplemented to each solubilization buffer and filtered using a 0.22 μm filter, aliquoted, and

stored at -20º C. The frozen solubilization buffers were thawed prior to use and any remaining buffer was discarded.

Fluorescence Detection Size Exclusion Chromatography (FSEC) assay. Sf9 cell culture (100 ml at $1x10^6$ cells/ml) were infected with P2 baculovirus and 1 ml aliquots of infected cells were collected at four time points using centrifugation: 24, 48, 72, and 96 hours. The supernatant was removed and cells were stored at -80º C for subsequent FSEC analysis. To solublize the isolated cells, the cells were thawed and resuspended in solubilization buffer and placed on a rotisserie rotator for 1 hour at 4º C. Crude solubilized samples were subjected to centrifugation prior to column injection to remove any insoluble or aggregated material. The supernatant was transferred to a clean, capless, microcentrifuge tube and placed in an automated sample injector of a Shimadzu HPLC equipped with a fluorescence detector and UV absorbance detector. Solubilized protein samples were passed through a Superose 6/10-300 GL size exclusion chromatography column (GE Biosciences). The FSEC apparatus was was equilibrated with elution buffer for 2 hours using a flow rate of 0.5 ml/min. Aliquots of the solubilized samples (75 □l) were injected onto the sizing column using an autosampler. Column eluants were analyzed using the fluorescence detector (Shimadzu) with excitation/emission wavelength parameters of 487/507 nm, respectively [5,35]. Under these parameters, only the enhanced green fluorescent protein is observed, which can be attributed to intact chimeric protein or cleaved EGFP. Chromatograms were plotted using OriginLab 8.0 for further assessment.

Transfection of CHO cells with Hv1-pNGFP-EU construct: The full length Hv1 proton channel gene was subcloned into pNGFP-EU vector at the EcoRI and BamHI sites at the 5' and 3' ends, respectively [5]. Chinese Hamster Ovarian cells (CHO-K1, Eton Biosciences) were plated at a cell confluency of 200,000 cells/ml in a 35 mm tissue culture dish and were allowed

to adhere to glass coverslips (overnight) prior to transfection. Cells were transfected using 1 μg pNEGFP-Hv1 cDNA using Lipofectamine LTX according to manufacturer's instructions. Transfected cells expressing the chimeric EGFP-Hv1 proton channel were imaged using an EVOS fluorescent microscope (Life Technologies) and assessed for function 24-48 hours after transfection.

Metal affinity and size exclusion chromatography: A 2-liter Sf9 cell culture was infected with 20 ml of the chimeric EGFP-Hv1 proton channel P2 virus and incubated at 37°C with shaking at 125 rpm for 48 hours. Cells were isolated using centrifugation. Collected cells were sonicated and membranes were isolated using ultracentrifugation. Isolated membranes were homogenized using a Dounce homogenizer in a sonication buffer consisting of (mM): NaCl (150), Tris-Cl (20) at pH 8.0, and DDM (40). Homogenized membranes and buffer were mixed further at 4°C for 1 hour. Insoluble material was separated from the membrane solubilized supernatant using ultracentrifugation. Cobalt metal affinity chromatography resin was equilibrated with equilibration buffer consisting of (in mM): NaCl (150), Tris-Cl (20) at pH 8.0, and DDM (20). Once equilibrated, the cobalt resin was added to membrane supernatant and allowed to rotate for 1 hour at 4°C. Chimeric EGFP-Hv1 proton channel protein bound resin was washed with wash buffer (equilibration buffer supplemented with 20 mM imidazole). Final elution of the chimeric EGFP-Hv1 proton channel protein was achieved using elution buffer (equilibration buffer supplemented with 250 mM imidazole). Eluting protein fractions (3 ml) were collected during the wash and elution steps. Desired fractions were collected from affinity chromatography and concentrated prior to loading onto a FPLC for size exclusion chromatography using a Superose 6/10-300 GL (GE) column at an elution rate of 0.5 ml/min.

Electrophysiology: Whole-cell patch clamp electrophysiology was used to determine the functionality of Hv1 proton channel construct. Patch pipettes were pulled from borosilicate glass using flaming brown pipette puller (Sutter Instruments P97 brown filament puller) and were fire polished to a resistance ranging from 16-22 MΩ in the described extracellular and internal solutions. Extracellular solution consisted of (in mM): HEPES (100), $MgCl_2$ (1), $CaCl_2$ (1), 75mM N-methyl-D-glucamine, or NMDG (75) buffered to pH 7.0. The internal (pipette) solution consisted of (in mM) NMDG (75), $MgCl_2$ (1), EGTA (1), and MES (100) buffered to pH 5.5[36]. The recording was performed using pCLAMP data acquisition and analysis software, filtered and samples at 5 and 10 kHz, respectively. Patched cells were subjected to whole-cell capacitance and 95% series resistance compensation. All the recordings were done at room temperature and holding potential of cells was set to -60 mV. The recording protocol consisted of an initial holding potential of -60 mV and proton currents were observed as voltage steps were applied from -60 mV to +130 mV in 10 mV increments. Data is presented and analyzed using OriginLab 8.0 software.

Figure and Legends

Figure 1. Expression and functional analysis of chimeric EGFP-Hv1 Hv1 proton channel transiently expressed in Chinese hamster ovary (CHO) cells. (**A**) Cells expressing the EGFP-Hv1 proton channel 24 hours post transfection as seen through a fluorescent microsope (FITC filter cube). (**B**) Typical whole-cell patch clamp recordings of expressed chimeric EGFP-Hv1 proton channel. Whole cell patch clamp recording were performed 24 hours post transfection. The EGFP-Hv1 proton channels were clamped at an initial Vh of -60 mV, and subjected to +10 mV voltage steps (500 ms duration) to +130 mV. The voltage step to +80 mV and corresponding response is highlighted in red. Scale bars are in milliseconds (ms) and pico-Amperes (pA), respectively.

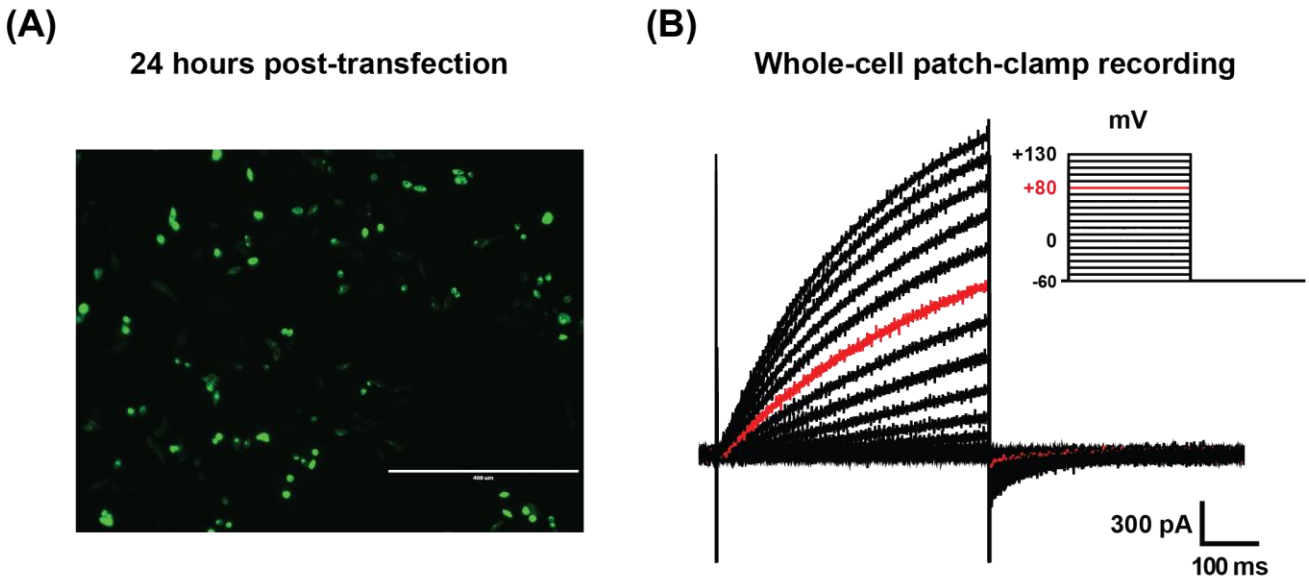
(A)
24 hours post-transfection
(B)
Whole-cell patch-clamp recording
mV
+130
+80
0
-60
300 pA
100 ms

Figure 1

Figure 2. Fluorescence-detection size exclusion chromatography time course analysis of chimeric EGFP-Hv1 proton channel solubilized in dodecyl maltoside. Crude supernatant of EGFP-Hv1 proton channel containing plasma membranes from Sf9 cells were analyzed at **(A)** 24 hours**,** (**B**) 48 hours, (**C**) 72 hours, and (**D**) 96 hours. Chromatogram peaks associated with protein void (Void), chimeric protein (EGP-Hv1), and free monomeric EGFP (EGFP) are shown. Chimeric protein (black) and free monomeric EGFP (green) are scaled for comparison. Elution volume (ml) and Fluourescence are shown. a.u.= arbitrary units.

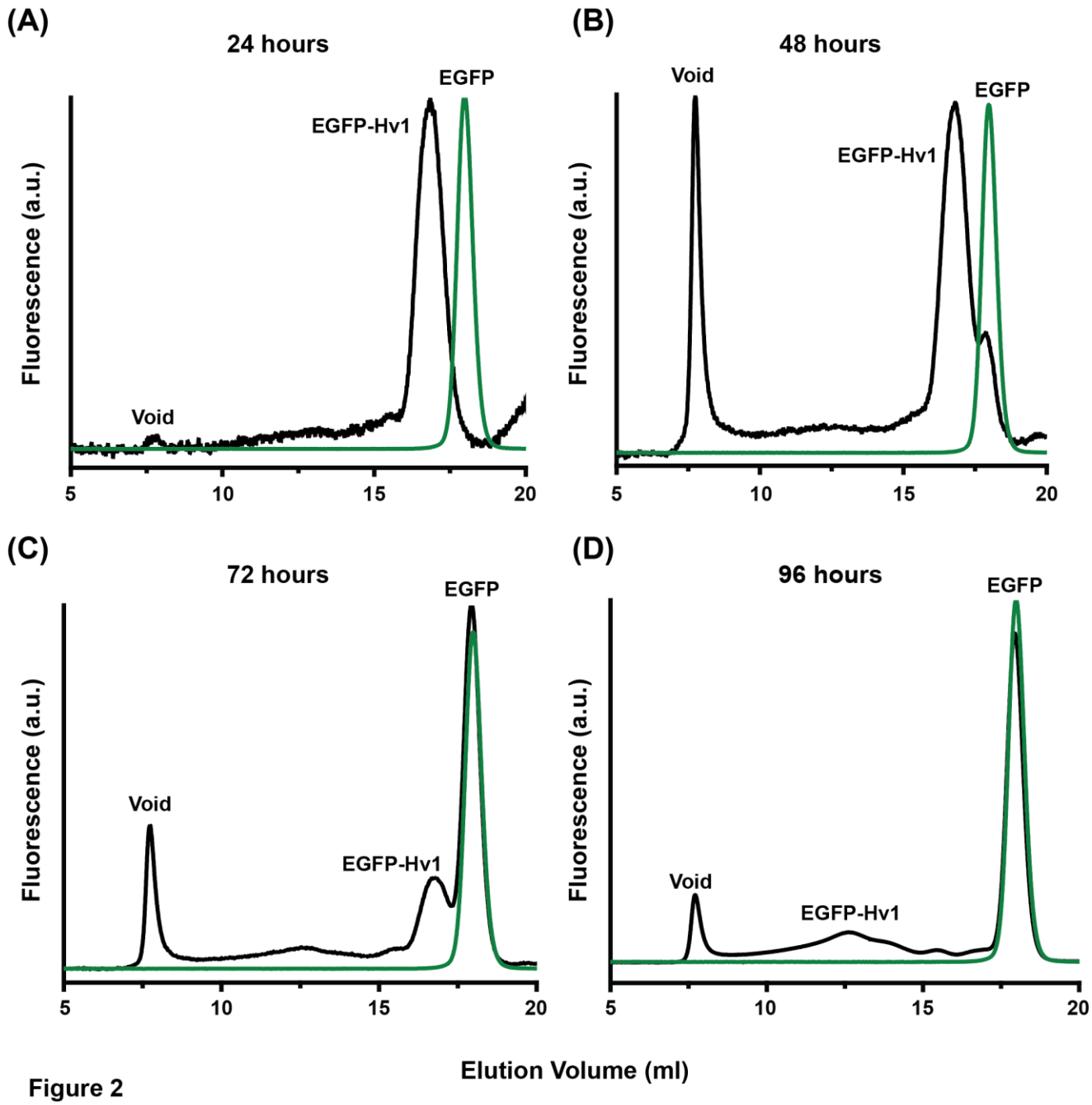
(A)
24 hours
EGFP
EGFP-Hv1
Void
Fluorescence (a.u.)
5
10
15
20
(B)
48 hours
Void
EGFP
EGFP-Hv1
Fluorescence (a.u.)
5
10
15
20
(C)
72 hours
EGFP
Void
EGFP-Hv1
Fluorescence (a.u.)
5
10
15
20
(D)
96 hours
EGFP
Void
EGFP-Hv1
Fluorescence (a.u.)
5
10
15
20
Elution Volume (ml)

Figure 2

Figure 3. FSEC analysis of Hv1 channel protein solubilized in βOG detergent. (**A**) 24 hours and (**B**) 48 hours after infection in SF9 cells. Chromatogram peaks associated with protein void (Void), chimeric protein (EGP-Hv1), and free monomeric EGFP (EGFP) are shown. Chimeric protein (blue) and free monomeric EGFP (green) are scaled for comparison. Chromatogram profiles are scaled for comparison. Elution volume (ml) and Fluorescence are shown. a.u.= arbitrary units.

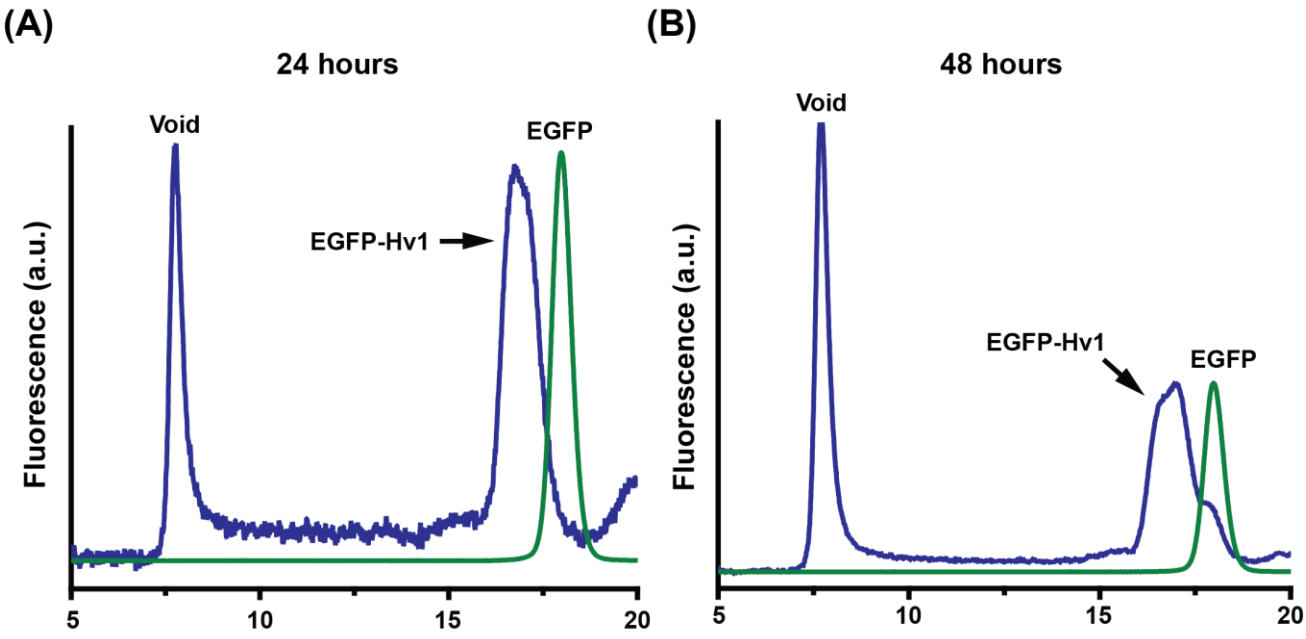
(A)
24 hours
Void
EGFP
EGFP-Hv1
Fluorescence (a.u.)
5
10
15
20
(B)
48 hours
Void
EGFP-Hv1
EGFP
Fluorescence (a.u.)
5
10
15
20
Elution Volume (ml)

Figure 3

Figure 4. FSEC analysis of Hv1 channel protein solubilized in LDAO detergent. (**A**) 24 hours and (**B**) 48 hours after infection in SF9 cells. Chimeric protein (orange) and free monomeric EGFP (green) are scaled for comparison. Chromatogram profiles are scaled for comparison. Elution volume (ml) and Fluourescence are shown. a.u.= arbitrary units.

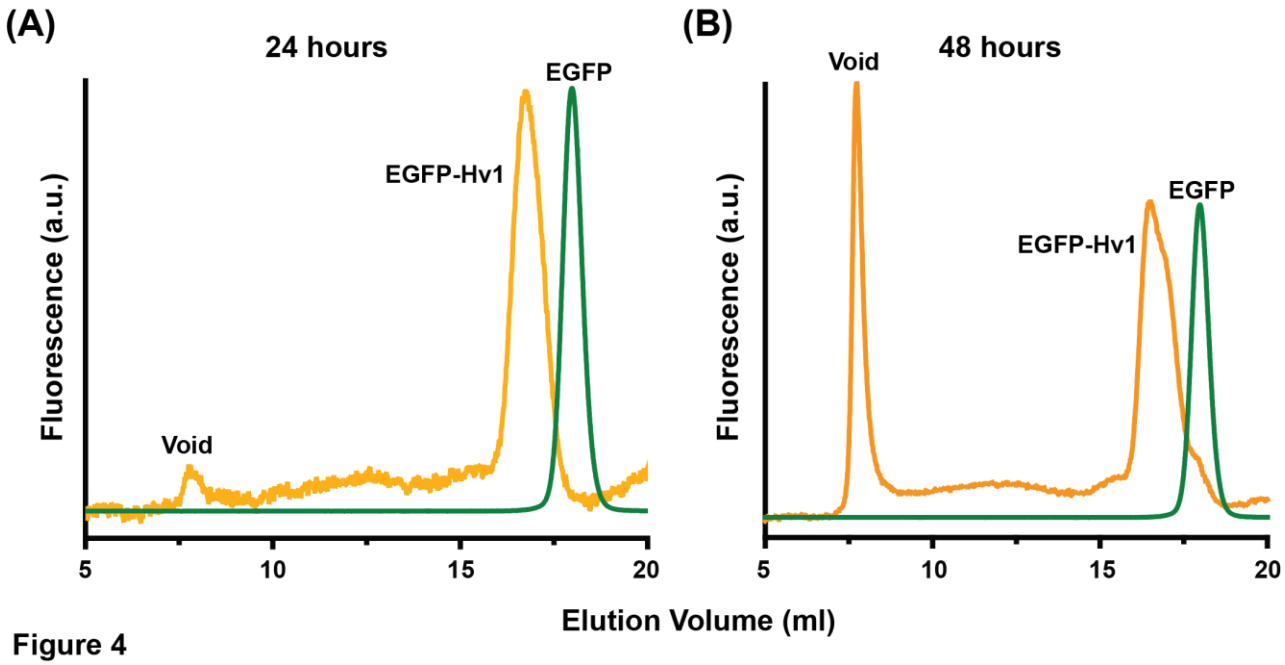
(A)
24 hours
EGFP
EGFP-Hv1
Void
Fluorescence (a.u.)
5
10
15
20
(B)
48 hours
Void
EGFP
EGFP-Hv1
Fluorescence (a.u.)
5
10
15
20
Elution Volume (ml)

Figure 4

Figure 5. FSEC analysis of Hv1 channel protein solubilized in Anzergent detergent. (**A**) 24 hours and (**B**) 48 hours after infection in SF9 cells. Chromatogram peaks associated with protein void (Void), chimeric protein (EGP-Hv1), and free monomeric EGFP (EGFP) are shown. Chimeric protein (purple) and free monomeric EGFP (green) are scaled for comparison. Chromatogram profiles are scaled for comparison. Elution volume (ml) and Fluorescence are shown. a.u.= arbitrary units.

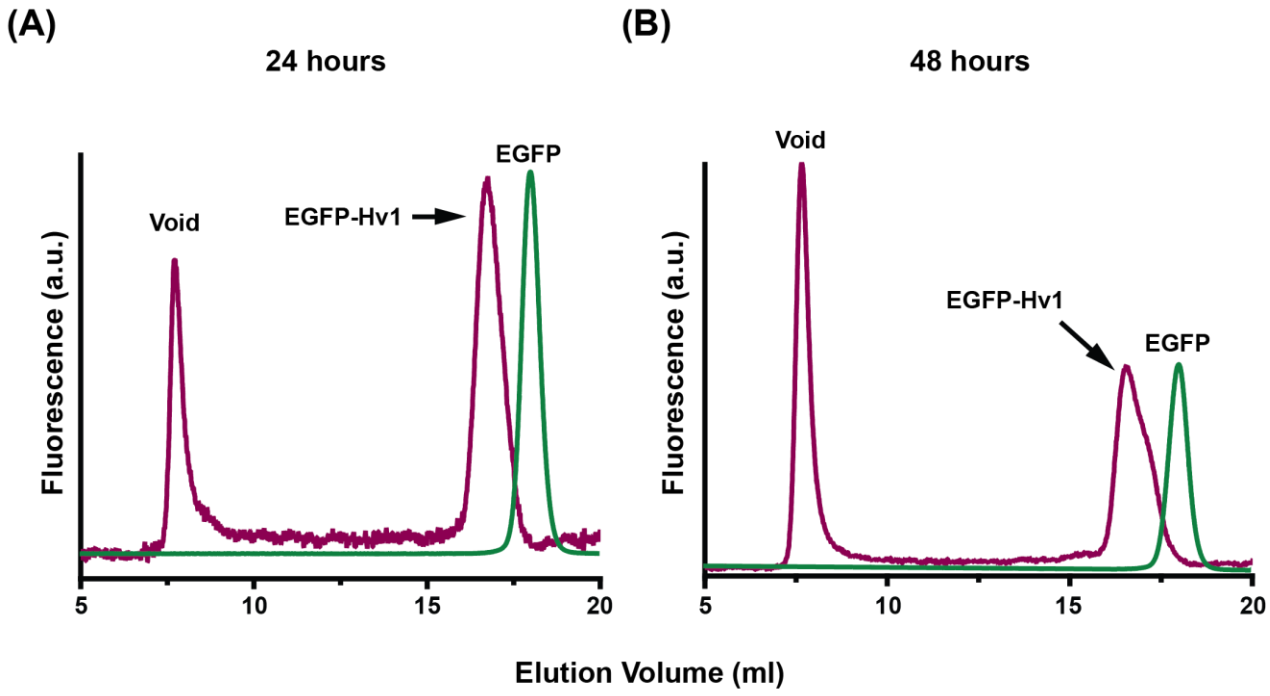
(A)
24 hours
(B)
48 hours
Void
EGFP-Hv1
EGFP
Fluorescence (a.u.)
5
10
15
20
Elution Volume (ml)

Figure 5

Figure 6. Isolation and purification of the chimeric EGFP-Hv1 proton channel. (A) Cobalt metal affinity chromatography elution profile of isolated EGFP-Hv1 proton channel is shown. Axes of the chromatography profile are labeled Elution volume (ml) and Absorbance at 280 nm (mAu), respectively. Equilibration, wash, and elution with increasing concentrations of imidazole are depicted (dashed line). Small grey vertical marks along the x-axis represent protein 3 ml protein fractions. (**B**) Size exclusion chromatography profile of chimeric EGFP-Hv2 protein is shown. Chromatography axes are the same as panel A. Chimeric monomeric EGFP-Hv1 proton channels is labeled. Small grey vertical marks along x-axis indicate the 0.3 ml protein fractions obtained using a Superose 6/10-300 GL (GE) column.

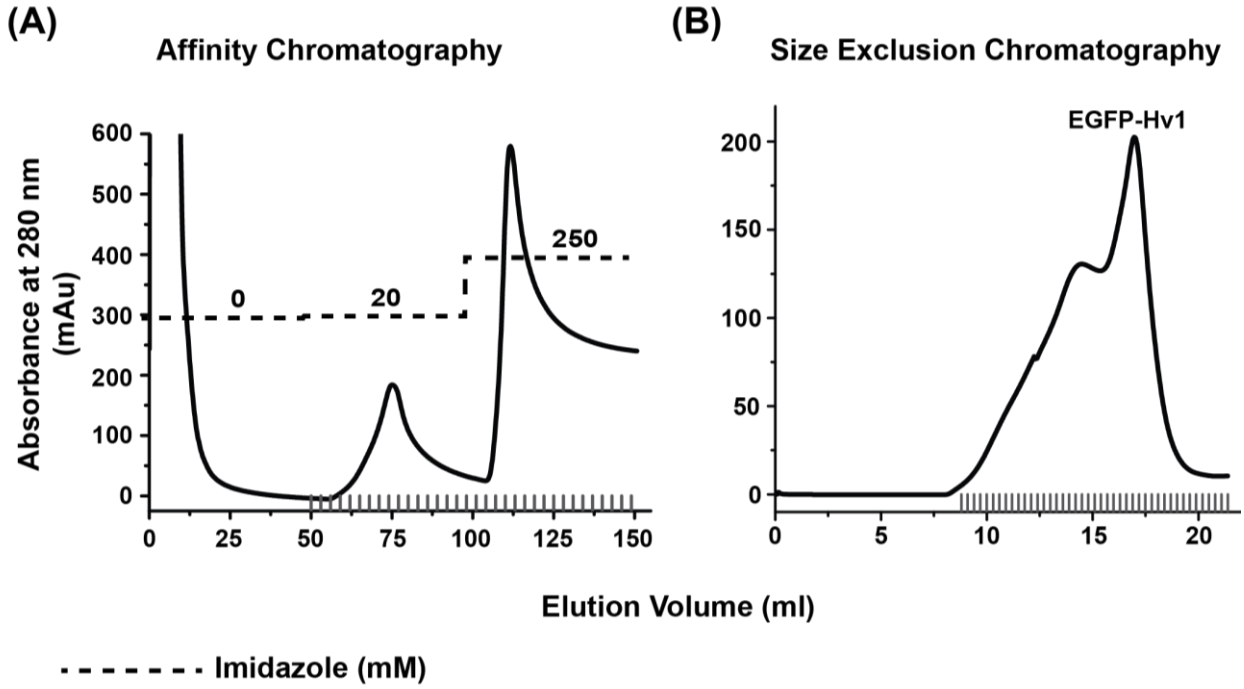
(A)
Affinity Chromatography
Absorbance at 280 nm (mAu)
600
500
400
300
200
100
0
0
25
50
75
100
125
150
0
20
250
(B)
Size Exclusion Chromatography
EGFP-Hv1
200
150
100
50
0
0
5
10
15
20
Elution Volume (ml)
Imidazole (mM)

Figure 6

References

1. Overington JP, Al-Lazikani B, Hopkins AL. How many drug targets are there? Nat Rev Drug Discov 2006;5(12):993-6.
2. Krogh A, Larsson B, von Heijne G, Sonnhammer EL. Predicting transmembrane protein topology with a hidden Markov model: application to complete genomes. J Mol Biol 2001;305(3):567-80.
3. Tate CG. Overexpression of mammalian integral membrane proteins for structural studies. FEBS Lett 2001;504(3):94-8.
4. Bolla JR, Su CC, Yu EW. Biomolecular membrane protein crystallization. Philos Mag (Abingdon) 2012;92(19-21):2648-2661.
5. Kawate T, Gouaux E. Fluorescence-detection size-exclusion chromatography for precrystallization screening of integral membrane proteins. Structure 2006;14(4):673-81.
6. Drew D, Newstead S, Sonoda Y, Kim H, von Heijne G, Iwata S. GFP-based optimization scheme for the overexpression and purification of eukaryotic membrane proteins in Saccharomyces cerevisiae. Nat Protoc 2008;3(5):784-98.
7. Drew D, Kim H. Screening for high-yielding Saccharomyces cerevisiae clones: using a green fluorescent protein fusion strategy in the production of membrane proteins. Methods Mol Biol 2012;866:75-86.
8. DeCoursey TE, Hosler J. Philosophy of voltage-gated proton channels. J R Soc Interface 2014;11(92):20130799.
9. Nawata T, Sibaoka F. Coupling between action potentials and bioluminescence in Noctiluca: effects of inorganic ions and pH in vacuolar sap. Journal of Comparative Physiology 1979;134:137-149.
10. Thomas RC, Meech RW. Hydrogen ion currents and intracellular pH in depolarized voltage-clamped snail neurones. Nature 1982;299(5886):826-8.
11. Eder C, Fischer HG, Hadding U, Heinemann U. Properties of voltage-gated potassium currents of microglia differentiated with granulocyte/macrophage colony-stimulating factor. J Membr Biol 1995;147(2):137-46.
12. Eder C, Fischer HG, Hadding U, Heinemann U. Properties of voltage-gated currents of microglia developed using macrophage colony-stimulating factor. Pflugers Arch 1995;430(4):526-33.
13. Sasaki M, Takagi M, Okamura Y. A voltage sensor-domain protein is a voltage-gated proton channel. Science 2006;312(5773):589-92.
14. Ramsey IS, Moran MM, Chong JA, Clapham DE. A voltage-gated proton-selective channel lacking the pore domain. Nature 2006;440(7088):1213-6.
15. Lee SY, Letts JA, Mackinnon R. Dimeric subunit stoichiometry of the human voltage-dependent proton channel Hv1. Proc Natl Acad Sci U S A 2008;105(22):7692-5.
16. Lishko PV, Botchkina IL, Fedorenko A, Kirichok Y. Acid extrusion from human spermatozoa is mediated by flagellar voltage-gated proton channel. Cell 2010;140(3):327-37.
17. Wu LJ, Wu G, Akhavan Sharif MR, Baker A, Jia Y, Fahey FH, Luo HR, Feener EP, Clapham DE. The voltage-gated proton channel Hv1 enhances brain damage from ischemic stroke. Nat Neurosci 2012;15(4):565-73.

18. Ramsey IS, Ruchti E, Kaczmarek JS, Clapham DE. Hv1 proton channels are required for high-level NADPH oxidase-dependent superoxide production during the phagocyte respiratory burst. Proc Natl Acad Sci U S A 2009;106(18):7642-7.
19. Wang Y, Li SJ, Pan J, Che Y, Yin J, Zhao Q. Specific expression of the human voltage-gated proton channel Hv1 in highly metastatic breast cancer cells, promotes tumor progression and metastasis. Biochem Biophys Res Commun 2011;412(2):353-9.
20. Wang Y, Li SJ, Wu X, Che Y, Li Q. Clinicopathological and biological significance of human voltage-gated proton channel Hv1 protein overexpression in breast cancer. J Biol Chem 2012;287(17):13877-88.
21. Prive GG. Detergents for the stabilization and crystallization of membrane proteins. Methods 2007;41(4):388-97.
22. Newstead S, Ferrandon S, Iwata S. Rationalizing alpha-helical membrane protein crystallization. Protein Sci 2008;17(3):466-72.
23. Newstead S, Kim H, von Heijne G, Iwata S, Drew D. High-throughput fluorescent-based optimization of eukaryotic membrane protein overexpression and purification in Saccharomyces cerevisiae. Proc Natl Acad Sci U S A 2007;104(35):13936-41.
24. Li Q, Jogini V, Wanderling S, Cortes DM, Perozo E. Expression, purification, and reconstitution of the voltage-sensing domain from Ci-VSP. Biochemistry 2012;51(41):8132-42.
25. Li Q, Wanderling S, Paduch M, Medovoy D, Singharoy A, McGreevy R, Villalba-Galea CA, Hulse RE, Roux B, Schulten K and others. Structural mechanism of voltage-dependent gating in an isolated voltage-sensing domain. Nat Struct Mol Biol 2014;21(3):244-52.
26. Takeshita K, Sakata S, Yamashita E, Fujiwara Y, Kawanabe A, Kurokawa T, Okochi Y, Matsuda M, Narita H, Okamura Y and others. X-ray crystal structure of voltage-gated proton channel. Nat Struct Mol Biol 2014;21(4):352-7.
27. Li SJ, Zhao Q, Zhou Q, Unno H, Zhai Y, Sun F. The role and structure of the carboxyl-terminal domain of the human voltage-gated proton channel Hv1. J Biol Chem 2010;285(16):12047-54.
28. Chattopadhyay A, London E. Fluorimetric determination of critical micelle concentration avoiding interference from detergent charge. Anal Biochem 1984;139(2):408-12.
29. Lee SY, Letts JA, MacKinnon R. Functional reconstitution of purified human Hv1 H+ channels. J Mol Biol 2009;387(5):1055-60.
30. Midgett CR, Madden DR. Breaking the bottleneck: eukaryotic membrane protein expression for high-resolution structural studies. J Struct Biol 2007;160(3):265-74.
31. Li SJ, Zhao Q, Zhou Q, Zhai Y. Expression, purification, crystallization and preliminary crystallographic study of the carboxyl-terminal domain of the human voltage-gated proton channel Hv1. Acta Crystallogr Sect F Struct Biol Cryst Commun 2009;65(Pt 3):279-81.
32. Fujiwara Y, Kurokawa T, Takeshita K, Kobayashi M, Okochi Y, Nakagawa A, Okamura Y. The cytoplasmic coiled-coil mediates cooperative gating temperature sensitivity in the voltage-gated H(+) channel Hv1. Nat Commun 2012;3:816.
33. Fujiwara Y, Takeshita K, Nakagawa A, Okamura Y. Structural characteristics of the redox-sensing coiled coil in the voltage-gated H+ channel. J Biol Chem 2013;288(25):17968-75.

34. Kruse AC, Hu J, Pan AC, Arlow DH, Rosenbaum DM, Rosemond E, Green HF, Liu T, Chae PS, Dror RO and others. Structure and dynamics of the M3 muscarinic acetylcholine receptor. Nature 2012;482(7386):552-6.
35. Gonzales EB, Kawate T, Gouaux E. Pore architecture and ion sites in acid-sensing ion channels and P2X receptors. Nature 2009;460(7255):599-604.
36. Sakata S, Kurokawa T, Norholm MH, Takagi M, Okochi Y, von Heijne G, Okamura Y. Functionality of the voltage-gated proton channel truncated in S4. Proc Natl Acad Sci U S A 2010;107(5):2313-8.